ECOHYDROLOGY OF THE CAATINGA TROPICAL DRY FOREST

A Dissertation

by

CYNTHIA LOUISE WRIGHT

Submitted to the Office of Graduate and Professional Studies of
Texas A&M University
in partial fulfillment of the requirements for the degree of

DOCTOR OF PHILOSOPHY

Chair of Committee,	Bradford Wilcox
Co-Chair of Committee,	Jason West
Committee Members,	X. Ben Wu
	Cristine Morgan
Head of Department,	Cliff Lamb

May 2020

Major Subject: Ecosystem Science and Management

ABSTRACT

The overarching goal of this study is to improve our understanding of ecohydrological process in tropical dry forests. Tropical dry forests provide ideal natural settings for ecohydrology research because of their distinct rainfall seasonality and high diversity of tree species and morphologies. This study takes place in the largest contiguous tropical dry forests of the Americas, the Caatinga biome of northeast Brazil. The objective of Chapter II was to determine if woody vegetation alters the temporal structure of soil water. I used a continuous wavelet transform examine soil water variability across different soil depths and time scales. Results indicate that soil water in the forested Caatinga more variable (high frequency changes) at short times and less variable at long time scales (low frequency changes) compared to the pasture site, due to differences in vegetation cover and soil properties. The objective of Chapter III was to use plant functional types to better understand plant water-use and conservation strategies. Field data included pre-dawn and mid-day leaf water potential, leaf thickness, specific leaf area, leaf $\delta^{13}C$, and stable water isotopes, δD and $\delta^{18}O$, of stem water and soil water. Results show that the plant functional type defined for the Caatinga dry forest are appropriate for understanding general differences in plant response to water stress. The objective of Chapter IV was to better understand the rate of water use for tree species of high vs. low wood density as a response to water availability, i.e. soil moisture, and demand, i.e. vapor pressure deficit. Results indicate that high vs. low wood density species are differentially sensitive to water availability and demand. The results of this dissertation have important implications for

understanding how dry forests might respond to anthropogenic influences, such as land use change and climate change.

DEDICATION

To my parents Charles and Mirna Wright. Los quiero.

ACKNOWLEDGEMENTS

Firstly, I would like to express my sincere appreciation to my advisors Brad Wilcox and Jason West for believing in me through this winding path. I first met Brad as a junior undergraduate at Texas A&M. Since then, Brad has continually advised me no matter my affiliation with A&M. He has been invested in my professional and personal development. I have great gratitude for Dr. Jason West. His support and belief in me have been monumental, especially during the final stages of research. I am also thankful to my committee members Ben Wu and Cristine Morgan, both who supported me through their teaching and research excellence since my undergraduate days at Texas A&M.

Next, I would like to say how indebted I am to the educators who first inspired me. These teachers include Ms. Julia West, Mrs. Theresa Chambers, Mr. Ebrahim Zakizadeh, Mr. Jared, Mrs. Rebecca Manriquez Fuentes, Mrs. Christine Manriquez, Mr. Marcos Esparza, Coach David Borden, and my environmental science teacher Mrs. Patt Sims. These educators from my small school in Presidio, TX, inspired me to write, to ask questions, and to strive for knowledge, excellence, and integrity. I would also like to thank my first boss, Amy Borde, of the Pacific Northwest National Lab in Sequim, WA. Leading fieldwork in Brazil made me realize how much I relied on the field skills I developed while working for Amy as a Post Bachelors Research Associate. I would also like to thank my master's advisor, Dr. Michael McClain of the IHE Delft Institute for Water Education for his continued support beyond my time in the Netherlands.

I am thankful to the countless colleagues and professors at Texas A&M, Universidade Federal Rural de Pernambuco, Unidade Acadêmica de Serra Talhada

(UAST), Universidade Federal Rural de Pernambuco (UFRPE), Recife, and Universidade Federal de Pernambuco (UFPE), Recife that have shared their time and wisdom with me. From Texas A&M, these include: Dr. Binayak Mohanty and Dr. Nandita Gaur for introducing me to the wavelet transform method; Dr. Georgianne Moore for helping me through my prelims, with my sap flux data, and for her sincere support as Associate Department Head for Graduate Programs; and Dr. Ayumi Hyodo for streamlining all my work at the Stable Isotopes for Biosphere Science laboratory. I would also like to fellow ESSM graduate students Shishir Basant for talking me through my sap flux sensor construction and installation over the phone. A warm thanks also to Dr. Yong Zhou for his support during my prelims and his invaluable friendship.

In Serra Talhada, I would like to thank my mentor Dr. Eduardo Soares de Souza, without whom, none of my efforts in the Caatinga would have been possible. I would also like to thank Dr. André Luiz Alves de Lima for sharing his knowledge of Caatinga trees and helping me in the field; Dr. Rodolfo Souza and his family for welcoming me; and Dr. Luiz Guilherme for sharing tapiocas, coffees and rides with me and for helping me transport my samples once I was back in Texas. I am also thankful to all the colleagues and friends I shared an office space with during my year at UAST. I am indebted to the students at Serra Talhada who spent countless hours in the field with me, and who were so willing to share their knowledge, experiences, and culture with me. These include Erison Martins, Cléa Medeiros, Fernando Isaias, Hugo Felipe da Silva, Lypson Simões, and the chemistry lab managers at UAST. I am also thankful to Dr. José Romualdo de Sousa Lima of the Universidade Federal Rural de Pernambuco, Unidade Acadêmica de Garanhuns, for equipment support. I would like to thank the university drivers João Batista and others for

driving our team to the field at 4 am twice a month for six months. I am also thankful to my friends Abinair Bernardes, Elanuza Sá, João Araújo, Cléber Ataíde, and others for helping me survive the inevitable solitude of living in the Sertão. I would like countless others who provided support during the many bus trips between Serra Talhada and Recife.

In Recife, I am thankful to Dr. António C.D. Antonino at UFPE for his support through the TAMU-CAPES collaboration. I am thankful to Dr. Maria Betânia at UFRPE for helping me import sample material and for putting me in touch with other Brazilian students during the 21st World Congress of Soil Science in Rio de Janeiro. At this conference, I was lucky to have met people like Amanda de Lima and Larissa Fernandes, both colleagues who became great friends that would help me navigate the bureaucracy and language barriers to obtaining Brazilian plant export permits. Thank you to my friends Eduardo Damasceno, Alan Silva, Andreia de Lima, and the Lima family who would adopt me during the last months of my stay in Brazil as I tried to figure out a logistics to export my samples from Recife to Texas A&M.

I am thankful to my great friends from all around the world. I would like to thank Dr. Luana Cruz of UNICAMP for her making Brazil feel small and less intimidating. Also, a heartfelt thanks to Kelly Fouchy for traveling halfway across the world from France to the middle-of-nowhere Brazil to encourage me in the field, and for her support during my final sprint in dissertation writing. I thank colleague and friend Dr. María Poca of CONICET, San Luis, Argentina for her support, and Dr. Javier Gyenge and Maria Elena Fernandez of INTA, Tandil, Argentina for teaching me about thermal-dissipation sap flux sensors.

I am also grateful to my family. To my siblings, Charles and Courtney, and to my grandmother, Mary Wright, for keeping my spirits high and understanding when I couldn't be home. I am also thankful to my family in Ojinaga, Chihuahua, Mexico. Last but not least, I am most grateful to my parents for supporting and encouraging my curiosity, and for raising me in an amazing and unique community with direct access to the beauty of Big Bend country. My parents have been my strong foundation even when everything else was shaking. They trusted me to follow my passions, to leave home to travel the world, and have kept me grounded in God. Thank you for being there for me, especially during those uncertain times that are part of the PhD process and inevitably part of living abroad.

CONTRIBUTORS AND FUNDING SOURCES

Contributors

This work was supervised by a dissertation committee consisting of Dr. Bradford Wilcox (chair), Dr. Jason West (co-chair), and Dr. X. Ben Wu from the Department of Ecosystem Science and Management and Dr. Cristine Morgan from the Department of Soil and Crop Sciences. Fieldwork was made possible with the help undergraduate students at the Federal Rural University of Pernambuco, Academic Unit of Serra Talhada, including Erison Martin, Cléa Medeiros, Fernando Isaias, Hugo Felipe da Silva, Lypson Simoes, among others. Collaborators at the same university include Dr. Eduardo Soares de Souza and Dr. André Luiz Alves de Lima; meteorological data was provided by Dr. Rodolfo Souza as part of the ONDACBC project in Northeast Brazil. I completed all other work for the dissertation independently.

Funding Sources

I would like to acknowledge my funding support, the National Science Foundation Graduate Research Fellowship for three years of financial support; the National Security Education Program Boren Fellowship for funding my year in Brazil, fueling my passion for science and the Portuguese language; and the Franklin F. Wasko Graduate Merit Fellowship for funding my last year at A&M. My doctoral education would not have been possible without this generous financial support. Contents are solely the responsibility of the authors and do not necessarily represent the official views of the funding agencies.

TABLE OF CONTENTS

Page

LIST OF FIGURES

Page

LIST OF TABLES

Page

I INTRODUCTION

Seasonally dry tropical forests (SDTF) are the most threatened tropical forest of the world (Janzen 1988; Miles et al. 2006; Sanchez-Azofeifa et al. 2005). Even in comparison to humid counterparts, SDTF have experienced the highest rates of deforestation (Hansen et al. 2013; Janzen 1988; Salazar et al. 2015) despite being areas of high endemism and biodiversity (Albuquerque et al. 2012; Miles et al., 2006). Threats to SDTF include deforestation and fragmentation from agricultural expansion, grazing, timber harvesting, desertification, and urban expansion (Leal et al. 2005; Mariano et al. 2018; Miles et al. 2006; Portillo-Quintero and Sanchez-Azofeifa 2010; Redo et al. 2013). Fragmented forested patches of various ages are reflective of migration, abandonment, and regrowth/successional patterns (Antongiovanni et al. 2018; Miles et al. 2006; Portillo-Quintero and Sanchez-Azofeifa 2010) and the harsh climate means that cleared land is susceptible to erosion, degradation and desertification (Tomasella et al. 2018). Moreover, less than 4% of the dry tropics are protected (Portillo-Quintero and Sanchez-Azofeifa, 2010).

Seasonally Dry Tropical Forests

Like all tropical systems, STDF are located between 23°28′N and 23°28′S and are found in dry regions, ranging from sub-humid to arid climates, across Latin America, Africa, Asia, and Australia (Figure 1-1). SDTF are defined as forests or shrublands with low and highly seasonal rainfall and by drought-deciduous vegetation.

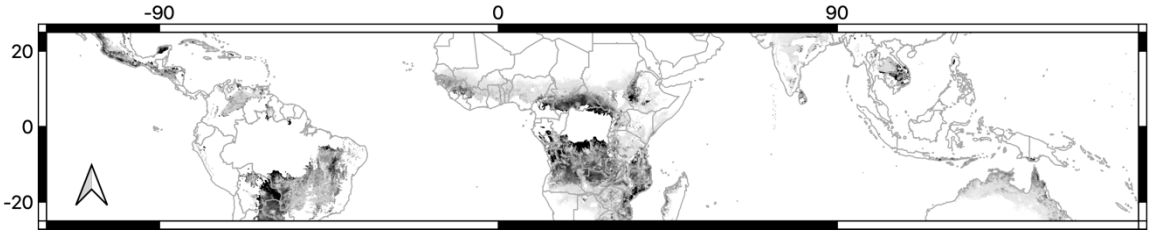

Figure I-1. The distribution of seasonally dry tropical forests. Adapted from Hansen et al. (2003) using QGIS (2019).

Mean annual rainfall is generally less than 1,600 mm but can range from 250 to 2,000 mm and is severely limited for 4 to 7 months (Bullock et al. 1995; Dirzo et al. 2011; Janzen, 1988). This strong seasonality in rainfall means that there is a sudden increase followed by a slow reduction in water and nutrients (Mooney et al. 1995). In addition, inter-annual rainfall variability is also high (Feng et al. 2013; Vico et al. 2015). Variability over time can induce lagged vegetation responses and can potentially alter vegetation structure and function (Allen et al. 2017; Barbosa and Kumar 2016; Erasmi et al. 2014; Pereira et al. 2014). It remains unclear, then, how dry forests will respond under climate change scenarios which predict a decrease in the magnitude of wet season rains, altered dry season length, changes in rainfall timing, and subsequent low rainfall years (Allen et al. 2017; Chadwick et al. 2015; Vico et al. 2015).

It is important to note that the geographic distribution of SDTF is a subject of disagreement. First, these forests are called by several names—deserts and xeric shrublands, dry mesmo-america, shrublands, deciduous broadleaf forests, caatingas, bosques secos, ect… (Sarkinen et al. 2011). Second, there is a limited set of species which occur across most SDTF nuclei—for example, only nine in South America (Sarkinen et al

2011). Even within SDTF biomes, there is large heterogeneity in vegetation structure and composition (Siquiera-Filho et al. 2012). Often, SDTF are associated or even classified as savanna biomes (Linares-Palomino et al. 2012; Prance et al. 2006). This distinction, or lack of, brings up a complex point because of the bistability of forest vs. grass cover associated with savannas (Bueno et al. 2018; Staver et al. 2011). Third, many SDTF occur in small fragmented extents (Antongiovanni et al. 2018; Galicia et al. 2009), or on the margins of humid forests, savannas, and wetlands. These fragmented and / or transitional forests are difficult to detect via remote sensing techniques (Sarkinen et al. 2011) and might be missed if setting a threshold on canopy cover (Hansen et al. 2013). Lastly, dry forests have long been impacted by chronic and acute anthropogenic activity and thus we do not know the true original extent of tropical dry forests (Murphy and Lugo 1986; Ribeiro et al. 2015). The combination of these factors means that it is difficult to delineate SDTF boundaries based on land cover or floristic composition (Sarkinen et al 2011).

Additionally, SDTF in the neotropics are sometimes referred to as succulent biomes because a large portion of the drought-deciduous vegetation is characterized by small-leaved, spinescent, and stem succulent trees which are fire intolerant (Gagnon et al. 2018; Oliveira-Filho et al. 2013; Schrire et al. 2005). By this definition, succulent biomes are not found in Asia nor Australia and do not include savannas, such as the Cerrado, the Pampas nor the Chaco (Schrire et al. 2005; Werneck 2011). Based on this classification, we can thus define neotropical SDTF not only biomes with strong rainfall seasonality and drought-deciduous vegetation, but also as a system that is different from a savanna because of the lack of a fire regime, and the distinct presence of stem succulent trees. Fire regimes are the

distinction between SDTF and savannas (Mooney et al. 2005; Pennington et al. 2000; Werneck 2011).

In terms of hydrology, rainfall seasonality in SDFT drives water fluxes across the landscape. In one of the few reviews of hydrologic research in SDTF, Farrick and Branefireun (2013) suggest that SDTF are more like arid ecosystems because they are dominated by lateral flows, particularly Hortonian overland flow. Yet, these same authors later go on to show that for a SDTF in Mexico, overland flow is likely limited during the wet season and instead, the hydrological behavior of this system is more like that of the humid tropics (Farrick and Branefireun 2014a, 2014b). From a catchment perspective, a comparative study between humid vs. semiarid tropical environment shows that, even though two sub-basins had similar physical and hydrological characteristics, with rainfall on the same order of magnitude, the river-regimes and water-availability were more than an order of magnitude different (Amorim et al. 2009). This suggests that there are important differences in water fluxes. Importantly, quantifying hydrologic fluxes in SDTF remains as a limited area of research. Considering that SDTF are defined by rainfall seasonality, and not mean annual precipitation, understanding the number, timing, and size of precipitation events could provide key insight into hydrological fluxes, as well as corresponding biological responses.

The Caatinga Dry Forest

More than half of the remaining SDTF are located in Latin America, with one of the largest contiguous portions located in northeast Brazil (Miles et al. 2006; Portillo-Quintero and Sanchez-Azofeifa, 2010). This biome, the Caatinga, covers an area of about 6 to 9 × 10^5 km^2 (Sampaio et al. 1995). Like other dry forests, the Caatinga is scientifically

neglected and under-protected, especially when compared to the humid tropical forests or other major Brazilian ecosystems like the Amazon, Atlantic Rainforest, and Cerrado (Portillo-Quintero and Sanchez-Azofeifa 2010; Santos et al. 2011). Like other SDFT, it is also highly deforested, fragmented and degraded (Antongiovanni et al. 2018; Tomasella et al 2018) and includes enclaves of higher elevation, more humid forests (i.e. brejos), short-statured shrublands and cacti. The Caatinga is an important dry tropical forest because, besides being one of the largest dry forests, it also is one of the most populated (Miles et al. 2006).

Annual rainfall in this region ranges from lows of 200 mm in the interior portion of the biome, up to 2000 mm in the eastern regions concentrated in a 3- to 4-month period (Sampaio 1995). Rainfall in erratic and unpredictable because it is not in the direct path of maritime tropical air. Instead, a stable dry air mass originating from the subtropical high in the South Atlantic (Figure I-2) keeps the Caatinga dry for a great part of the year. When rainfall does occur, it is usually because the southeasterly trade winds have been disrupted by one or more of the three competing air masses: a continental convective air from the Amazon, a stable moist air mass likely influenced by the position of the ITCZ in the summer, and the Atlantic polar front. This means that summer, summer-autumn, or autumn-winter rains are possible in any combination (Webb 1974). In Pernambuco state specifically, the Borborema Massif formation has enough of an elevation gradient from the coast moving inland to create an orographic effect.

Seasonality plays an important role in the Caatinga and in Northeast Brazil. Compared to other seasonal regions such as Western and Central Africa and Northern Australia, Northeast Brazil exhibit greater variability. This seasonality likely impacts

hydrological processes and consequently ecological and anthropogenic responses. For example, in an agricultural setting, Machado et al. (2015) found that although drainage into soil occurs during the wet season, correspondingly high ET may ultimately decrease soil water storage.

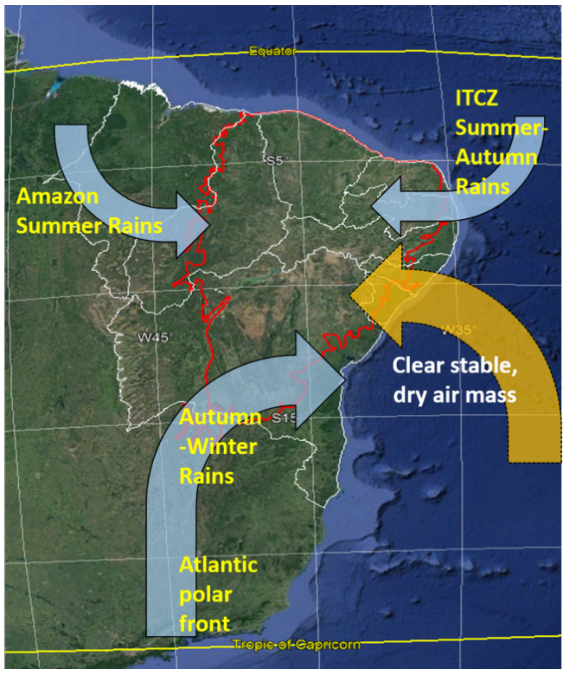

Figure I-2. Competing masses of air which influence rainfall regimes in the Caatinga biome, outlined in red. Background image from Google (2018) and outline from MMA / IBGE (2007).

Vegetation of the Caatinga

Like other SDTFs, the Caatinga is a patchwork of forest and degraded bare soil. Until recently, the Caatinga biome was generally regarded as low in biodiversity and productivity, and not in the same ranks as other SDTF in terms of endemism. Research ultimately revealed that Caatinga has a significant plant species richness and endemism and is a unique floristic province/biome (Albuquerque 2012; Prado and Gibbs, 1993). Since then, the Caatinga is one of the more well-known SDTF, although perhaps still with some trepidation—deforestation, devaluation, and scientific negligence persist.

Perhaps because the Caatinga has been so heavily degraded and the native vegetation is hardly recognizable, or perhaps because of the extreme aridity and the harsh living conditions, this region has long been misunderstood. Nonetheless, indigenous communities have passed down the secretes to surviving in this landscape. This is evident in the common name of native trees, derived from Tupi language. For example, species such as the "umbuzeiro" (*Spondias tuberosa* Arruda) and "imburana de cambão" (*Commiphora leptophloeos* (Mart.) Gillett)—"umbu" means stores water, and "rana" which means "false" umbu (Maia 2012)—describe the substantial water storage capacities of some of the native species. Note that the umbuzeiro appears to store water in large root tuber vessel and the imburana stores water in its large soft trunk. These trees were often a source of water for people and animals during prolonged drought conditions, even after European colonization. The species are discussed in greater detail in Chapters III and IV.

Important phenology work has documented interesting characteristics that might hint at how plants respond or prepare to respond to rainfall; for example, soil and stem water storage (Borchert, 1994), differences in wood density (Lima and Rodal 2010;

Oliveira et al. 2015), leaf shedding (Borchert 1994), pre-rain green-up (Ryan et al. 2017), and partitioning of soil water (Worbes et al. 2013). The work of Oliveira et al. (2015), Lima et al. (2012), and Lima and Rodal (2010), which classify plant functional groups based on phenology and wood density, are foundational to the objectives of this dissertation. Oliveira et al. (2015) describes four functional groups classified according to patterns in vegetative phenophases, including bud break, adult leaves, and leaf shedding, responding to several environmental variables, including photoperiod, rainfall, temperature, air humidity, and soil water. These groups are: 1) deciduous low wood density, 2) late-deciduous high wood density, 3) early deciduous high wood density, and 4) evergreens. While soil water availability was important for the deciduous species of low and high wood densities, the evergreen species were less sensitive and may have alternate water sources, such groundwater. Moreover, the authors suggest that considering multi-year rainfall variability may also affect phenological timing of some of the functional groups. Therefore, analyzing the propagation of rainfall pulses and soil water variability will provide context for understanding functional group adaptations to water stress. For example, the presence of evergreen species might indicate that groundwater is accessible, but it is still unclear what the depth to groundwater is, if tree roots can extend into unconsolidated bedrock, and to what extent this vegetation depends on soil water. Similarly, it is possible that low wood density species decouple from soil water under moderate to high water stress conditions, since these species have a higher stem water storage capacity.

Dissertation Aims

This dissertation focuses on key ecohydrological aspects the Caatinga dry forest related to water availability and plant responses. The over-arching question for each chapter is:

II) Are the soil moisture dynamics different in a deforested vs. forested cover?

III) Can we use plant functional types to categorize plant water use and conservation strategies of different tree species in the Caatinga?

IV) Do woody plant functional types ultimately use available water at different rates? Are low wood density species more aggressive or more conservative water users relative to high wood density species?

References

Aguirre-Gutiérrez, J., Oliveras, I., Rifai, S., Fauset, S., Adu-Bredu, S., Affum-Baffoe, K., … Malhi, Y. (2019). Drier tropical forests are susceptible to functional changes in response to a long-term drought. *Ecology Letters*, *22*(5), 855–865. https://doi.org/10.1111/ele.13243

Albuquerque, U. P. de, de Lima Araújo, E., El-Deir, A. C. A., de Lima, A. L. A., Souto, A., Bezerra, B. M., … Severi, W. (2012). Caatinga Revisited: Ecology and Conservation of an Important Seasonal Dry Forest. *The Scientific World Journal*, *2012*, 1–18. https://doi.org/10.1100/2012/205182

Allen, K., Dupuy, J. M., Gei, M. G., Hulshof, C., Medvigy, D., Pizano, C., … Waring, B. G. (2017). Will seasonally dry tropical forests be sensitive or resistant to future changes in rainfall regimes? *Environmental Research Letters*, *12*(2).

Amorim, I. L. de, Sampaio, E. V. de S. B., & Araújo, E. de L. (2009). Fenologia de espécies lenhosas da caatinga do Seridó, RN. *Revista Arvore*, *33*(3), 491–499. https://doi.org/10.1590/s0100-67622009000300011

Antongiovanni, M., Venticinque, E. M., & Fonseca, C. R. (2018). Fragmentation patterns of the Caatinga drylands. *Landscape Ecology*, *33*(8), 1353–1367. https://doi.org/10.1007/s10980-018-0672-6

Barbosa, H. A., & Kumar, T. V. L. (2016). Influence of rainfall variability on the vegetation dynamics over Northeastern Brazil. *Journal of Arid Environments*, *124*, 377–387. https://doi.org/10.1016/j.jaridenv.2015.08.015

Borchert, R. (1994). Soil and Stem Water Storage Determine Phenology and Distribution of Tropical Dry Forest Trees. *Ecology*, *75*(5), 1437–1449.

Bueno, M. L., Dexter, K. G., Pennington, R. T., Pontara, V., Neves, D. M., Ratter, J. A., & de Oliveira-Filho, A. T. (2018). The environmental triangle of the Cerrado Domain: Ecological factors driving shifts in tree species composition between forests and savannas. *Journal of Ecology*, *106*(5), 2109–2120. https://doi.org/10.1111/1365-2745.12969

Bullock, S. H., Mooney, H. A., & Medina, E. (1995). *Seasonally dry tropical forests*. (S H Bullock, H. A. Mooney, & E. Medina, Eds.), *Seasonally dry tropical forests*.

Chadwick, R., Good, P., Martin, G., & Rowell, D. P. (2016). Large rainfall changes consistently projected over substantial areas of tropical land. *Nature Climate Change*, *6*(2), 177–181. https://doi.org/10.1038/nclimate2805

Dirzo, R., Young, H. S., Mooney, H. A., & Ceballos, G. (2011). *Seasonally dry tropical forests: ecology and conservation*. Island Press.

Erasmi, S., Schucknecht, A., Barbosa, M. P., & Matschullat, J. J. (2014). Vegetation Greenness in Northeastern Brazil and Its Relation to ENSO Warm Events. *Remote Sensing*, *6*(4), 3041–3058. https://doi.org/10.3390/rs6043041

Farrick, K. K., & Branfireun, B. A. (2013). Left high and dry: a call to action for increased hydrological research in tropical dry forests. *Hydrological Processes*, *27*(22), 3254–3262. https://doi.org/10.1002/hyp.9935

Farrick, K. K., & Branfireun, B. A. (2014a). Infiltration and soil water dynamics in a tropical dry forest: it may be dry but definitely not arid. *Hydrological Processes*, *28*(14), 4377–4387. https://doi.org/10.1002/hyp.10177

Farrick, K. K., & Branfireun, B. A. (2014b). Soil water storage, rainfall and runoff relationships in a tropical dry forest catchment. *Water Resources Research*, 7206–7230. https://doi.org/10.1002/2013WR014956.Received

Feng, X., Porporato, A., & Rodriguez-Iturbe, I. (2013). Changes in rainfall seasonality in the tropics. *NATURE CLIMATE CHANGE*, *3*(9), 811–815. https://doi.org/10.1038/NCLIMATE1907

Gagnon, E., Ringelberg, J. J., Bruneau, A., Lewis, G. P., & Hughes, C. E. (2019). Global Succulent Biome phylogenetic conservatism across the pantropical Caesalpinia Group (Leguminosae). *New Phytologist*, *222*(4), 1994–2008. https://doi.org/10.1111/nph.15633

Galicia, L., Zarco-Arista, A. E., Mendoza-Robles, K. I., Palacio-Prieto, J. L., & García-Romero, A. (2008). Land use/cover, landforms and fragmentation patterns in a tropical dry forest in the southern Pacific region of Mexico. *Singapore Journal of Tropical Geography*, *29*(2), 137–154. https://doi.org/10.1111/j.1467-9493.2008.00326.x

Google. (2018). [Northeast Brazil region]. Retrieved October 2018, from Google Earth Pro 7.3. SIO, NOAA, U.S. Navy, NGA, GEBCO. IBCAO. Landsat / Copernicus.

Hansen, M. C., DeFries, R. S., Townshend, J. R. G., Carroll, M., Dimiceli, C., & Sohlberg, R. A. (2003). Global percent tree cover at a spatial resolution of 500 meters: First results of the MODIS vegetation continuous fields algorithm. *Earth Interactions*, *7*(10), 1–15. Map data available at https://glad.geog.umd.edu/projects/gfm/drytropics/data.html

Hansen, M. C., Potapov, P. V, Moore, R., Hancher, M., Turubanova, S. A. A., Tyukavina, A., … others. (2013). High-resolution global maps of 21st-century forest cover change. *Science*, *342*(6160), 850–853.

Janzen, D. H. (1988). Management of Habitat Fragments in a Tropical Dry Forest : Growth. *Annals of the Missouri Botanical Garden*, *75*(1), 105–116. https://doi.org/10.2307/2399468

Leal, I. R., Silva, J. M. C. da, Tabarelli, M., & Lacher, T. E. J. (2005). Changing the Course of Biodiversity Conservation in the Caatinga of Northeastern Brazil, *19*(3), 701–706.

Lima, A. L. A., & Rodal, M. J. N. (2010). Phenology and wood density of plants growing in the semi-arid region of northeastern Brazil. *Journal of Arid Environments*, *74*(11), 1363–1373. https://doi.org/10.1016/j.jaridenv.2010.05.009

Lima, A. L. A., Sampaio, E. V. S. B., de Castro, C. C., Rodal, M. J. N., Antonino, A. C. D., & de Melo, A. L. (2012). Do the phenology and functional stem attributes of woody species allow for the identification of functional groups in the semiarid region of Brazil? *Trees*, *26*(5), 1605–1616. https://doi.org/10.1007/s00468-012-0735-2

Linares-Palomino, R., Oliveira-Filho, A. T., & Pennington, R. T. (2011). Neotropical seasonally dry forests: diversity, endemism, and biogeography of woody plants. In *Seasonally dry tropical forests* (pp. 3–21). Springer.

Machado, C., Lima, J. de S., Antonino, A., Alves, E., Souza, E. de S., Ribeiro, A., & Firmino, F. (2015). Fluxos de água no consórcio milho-pastagem na microbacia hidrográfica do Rio Mundaú , Pernambuco. *Revista Brasileira de Recursos Hídricos*, *20*, 731–740.

Maia, N. G. (2012). *Caatinga : árvores e arbustos e suas utilidades.* (2nd ed.). Printcolor Grafica e Editora.

Mariano, D. A., Carlos, A. C., Wardlow, B. D., Anderson, M. C., Schiltmeyer, A. V, Tadesse, T., & Svoboda, M. D. (2018). Remote Sensing of Environment Use of remote sensing indicators to assess effects of drought and human- induced land degradation on ecosystem health in Northeastern Brazil. *Remote Sensing of Environment*, *213*(September 2017), 129–143. https://doi.org/10.1016/j.rse.2018.04.048

Miles, L., Newton, A. C., DeFries, R. S., Ravilious, C., May, I., Blyth, S., … Gordon, J. E. (2006). A global overview of the conservation status of tropical dry forests. *Journal of Biogeography*, *33*(3), 491–505. https://doi.org/10.1111/j.1365-2699.2005.01424.x

MMA / IBGE. (2007). [Brazil biomes]. Retrieved October 2017, from Global Forest Watch www.globalforestwatch.org

Mooney, H. A., Bullock, S. H., & Medina, E. (1995). Introduction. In S. H. Bullock, H. A. Mooney, & E. Medina (Eds.), *Seasonally Dry Tropical Forests* (pp. 1–8). Cambridge University Press. https://doi.org/10.1017/CBO9780511753398.001

Murphy, P. G., & Lugo, A. E. (1986). Ecology of Tropical Dry Forest. *Annual Review of Ecology and Systematics*, *17*(1), 67–88. https://doi.org/10.1146/annurev.es.17.110186.000435

Oliveira-Filho, A. T., Cardoso, D., Schrire, B. D., Lewis, G. P., Pennington, R. T., Brummer, T. J., … Lavin, M. (2013). Stability structures tropical woody plant diversity more than seasonality: Insights into the ecology of high legume-succulent-plant biodiversity. *South African Journal of Botany*, *89*, 42–57. https://doi.org/10.1016/j.sajb.2013.06.010

Oliveira, C. C. de, Zandavalli, R. B., Lima, A. L. A. de, & Rodal, M. J. N. (2015). Functional groups of woody species in semi-arid regions at low latitudes. *Austral Ecology*, *40*(1), 40–49. https://doi.org/10.1111/aec.12165.

Pennington, R. T., Prado, D. E., Pendry, C. A., & Botanic, R. (2000). Neotropical seasonally dry forests and Quaternary vegetation changes R., 261–273. https://doi.org/10.1046/j.1365-2699.2000.00397.x

Pereira, M. P. S., Justino, F., Malhado, A. C. M., Barbosa, H., & Marengo, J. (2014). The influence of oceanic basins on drought and ecosystem dynamics in Northeast Brazil. *Environmental Research Letters*, *9*(12), 124013. https://doi.org/10.1088/1748-9326/9/12/124013

Portillo-Quintero, C. A., & Sanchez-Azofeifa, G. A. (2010). Extent and conservation of tropical dry forests in the Americas. *Biological Conservation*, *143*(1), 144–155. https://doi.org/10.1016/j.biocon.2009.09.020

Prado, D. E., & Gibbs, P. E. (1993). Patterns of species distributions in the dry seasonal forests of South America. *Annals of the Missouri Botanical Garden*, 902–927.

Prado, D. E., & Gibbs, P. E. (1993). Patterns of species distributions in the dry seasonal forests of South America. *Annals of the Missouri Botanical Garden*, 902–927.

Prance, G. T. (2006). Tropical savannas and seasonally dry forests: An introduction. *Journal of Biogeography*, *33*(3), 385–386. https://doi.org/10.1111/j.1365-2699.2005.01471.x

QGIS Development Team (2019). Version 3.10.0-A Coruña. QGIS Geographic Information System. Open Source Geospatial Foundation Project. http://qgis.osgeo.org.

Redo, D., Aide, T. M., & Clark, M. L. (2013). Vegetation change in Brazil's dryland ecoregions and the relationship to crop production and environmental factors: Cerrado, Caatinga, and Mato Grosso, 2001–2009. *Journal of Land Use Science*, *8*(2), 123–153. https://doi.org/10.1080/1747423X.2012.667448

Ribeiro, E. M. S., Arroyo-Rodriguez, V., Santos, B. A., Tabarelli, M., & Leal, I. R. (2015). Chronic anthropogenic disturbance drives the biological impoverishment of the Brazilian Caatinga vegetation. *Journal of Applied Ecology*, *52*(3), 611–620. https://doi.org/http://dx.doi.org/10.5061/dryad.m7d8m

Ryan, C. M., Williams, M., Grace, J., Woollen, E., & Lehmann, C. E. R. (2017). Pre-rain green-up is ubiquitous across southern tropical Africa: Implications for temporal niche separation and model representation. *New Phytologist*, *213*(2), 625–633.

Salazar, A., Baldi, G., Hirota, M., Syktus, J., McAlpine, C., Salazar, A., … McAlpine, C. (2015). Land use and land cover change impacts on the regional climate of non-Amazonian South America: A review. *Global and Planetary Change*, *128*, 103–119. https://doi.org/10.1016/j.gloplacha.2015.02.009

Sampaio, E. V. S. B., & de Sa Barreto Sampaio, E. V. (1995). Overview of the Brazilian caatinga. In S. H. Bullock, H. A. Mooney, & E. Medina (Eds.), *Seasonally dry tropical forests* (pp. 35–63). Cambridge University Press. https://doi.org/10.1017/cbo9780511753398.003

Sanchez-Azofeifa, G. A., Quesada, M., Jon Paul Rodrıguez, Nassar, J. M., Stoner, K. E., Castillo, A., … Cuevas-Reyes, P. (2005). Research Priorities for Neotropical Dry Forests. *Biotropica*, *37*(4), 477–485.

Santos, J. C., Leal, I. R., Almeida-Cortez, J. S., Wilson Fernandes, G., & Tabarelli, M. (2011). Caatinga: the scientific negligence experienced by a dry tropical forest. *Tropical Conservation Science*, *4*(3), 276–286.

Särkinen, T., Iganci, J. R. V. V, Linares-Palomino, R., Simon, M. F., & Prado, D. E. (2011). Forgotten forests - issues and prospects in biome mapping using Seasonally Dry Tropical Forests as a case study. *BMC Ecology*, *11*(November). https://doi.org/10.1186/1472-6785-11-27

Schrire, B. D., Lavin, M., & Lewis, G. P. (2005). Plant Diversity and Complexity Patterns: Local, Regional and Global Dimensions. In I. Friis & H. Balslev (Eds.), *Biologiske skrifter* (Vol. 55, pp. 375–422). Copenhagen.

Siqueira-Filho JA de, Conceição AA, Rapini A, Coelho AOP, Zuntini AR, Joffily A, Vieira AOS, Prata APN, Machado AFP, Alves-Araújo AG, Melo AL, Amorim AMA, Fontana AP, Moreira ADR, Lima CT, Proença CEB, Luz CL, Kameyama C, Caires CS, Bove CP, Mynssen CM, S, S. V. (2012). *Flora of the caatingas of the São Francisco River: natural history and conservation*. (J. A. de S. Filho, Ed.). Rio de Janeiro: Andrea Jakobsson.

Staver, A. C., Archibald, S., & Levin, S. A. (2011). The global extent and determinants of savanna and forest as alternative biome states. *Science*, *334*(6053), 230–232. https://doi.org/10.1126/science.1210465

Tomasella, J., Silva, R. M., Vieira, P., Barbosa, A. A., Rodriguez, D. A., Oliveira, M. De, & Sestini, M. F. (2018). Desertification trends in the Northeast of Brazil over the period 2000 – 2016. *Int J Appl Earth Obs Geoinformation*, *73*(November 2017), 197–206. https://doi.org/10.1016/j.jag.2018.06.012

Vico, G., Thompson, S. E., Manzoni, S., Molini, A., Albertson, J. D., Almeida-Cortez, J. S., … Porporato, A. (2015). Climatic, ecophysiological, and phenological controls on plant ecohydrological strategies in seasonally dry ecosystems. *Ecohydrology*, *8*(4), 660–681. https://doi.org/10.1002/eco.1533

Webb, K. E. (1974). *The changing face of Northeast Brazil*. Columbia University Press.

Werneck, F. P. (2011). The diversification of eastern South American open vegetation biomes: Historical biogeography and perspectives. *Quaternary Science Reviews*, *30*(13–14), 1630–1648. https://doi.org/10.1016/j.quascirev.2011.03.009

Worbes, M., Blanchart, S., & Fichtler, E. (2013). Relations between water balance, wood traits and phenological behavior of tree species from a tropical dry forest in Costa Rica - A multifactorial study. *Tree Physiology*, *33*(5), 527–536. https://doi.org/10.1093/treephys/tpt028

II VEGETATION COVER CHANGES TEMPORAL SOIL MOISTURE DYNAMICS IN WATER-LIMITED ENVIRONMENTS: APPLICATION OF THE WAVELET TRANSFORM IN THE CAATINGA DRY FOREST

Introduction

Land use / land cover change is a mark of the Anthropocene era. Nowhere has this mark been more altering than in the dry tropical forests of South America (Janzen 1988). Defined by highly seasonal and often unpredictable rainfall patterns, these forests experience the highest rates of gross deforestation, as well as some of the highest rates of reforestation and regrowth (Aide et al. 2013; Hansen et al. 2013; Nanni et al. 2019). The Caatinga dry forest and shrubland of northeast Brazil is one of the most extensive and contiguous areas of tropical dry forest (Miles et al. 2006). Over the past several decades, this biome has lost between 45-52% of its original cover (Antongiovanni et al. 2016; Beuchle et al. 2015; Portillo-Quintero and Sanchez-Azofeifa 2010; Salazar et al. 2015) and gained forest cover on the order of 5-10% (Nanni et al. 2019). Such heterogenous landscape patterns are often driven by smaller holder agriculture (Sietz et al. 2006) such as 1) clearing of land for use as grazing and/or cultivation, 2) and which have access to water, 3) abandonment/fallow of land which leads, and 4) migration and/or land sub-division between generations, which leads to progressively small parcels. Abandonment of cropland often occurs during drought conditions (Dias et al. 2016). Moreover, land use practices commonly have a seasonal component. Throughout the year, cover alternates between bare ground during the dry season, and maize or grass during the wetter months, to help preserve the pasture and provide fodder for livestock (Sobrinho et al. 2016).

Currently, 25% of the total area of the Caatinga is agricultural, 30-50% is impacted by roads (Castelletti et al. 2000) and virtually all of the remaining natural vegetation is exposed to some type of disturbance (Antongiovanni et al. 2016). Increases in population density, clear-cutting, and grazing intensity continues to result in deforestation, altered vegetation structure, retarded regrowth, degradation, and often desertification (Marinho et al. 2016; Ribeiro et al 2015; Tomasella et al. 2018).

Importance of soil water

Soil water is at the nexus of understanding the ecohydrological impacts of deforestation because it is the integration of processes which potentially shift as land cover / land use shifts. These processes include climatological, physical and biological fluxes such as: solar radiation and temperature; soil hydraulic conductivity and infiltration; and plant-water uptake and hydraulic lift. Soil water is also tightly coupled to ecological response, such as soil respiration, primary production, microbial activity and nutrient cycling, especially in water-limited systems (Austin et al 2004; Collins et al. 2008; Choler et al. 2011; Heisler-White et al. 2008; Muldavin et al. 2008). For this reason, soil water has been at the core of foundational ecohydrological research. Extensive research has focused on deriving and predicting the relationship between rainfall and soil water using probabilistic models (Rodriguez-Iturbe 1999, Isham et al. 2005) and analytical soil water balance models (Penna et al. 2009; Teuling and Troch 2005; Teuling et al. 2007; Verrot and Destouni 2016). Still, it is difficult to incorporate complex multi-scalar forces interacting across time and space scales. To improve predictions regarding soil water patterns in space and time, we need to better characterizate the influence of soil and vegetation properties—datasets which are poorly represented across scales (Wilson et al. 2004). While a larger body of

research has focused on understanding how changes in land cover / land use in the tropics might affect fluxes such as runoff and stream flow, evapotranspiration, and infiltration (Alvarenga et al. 2016; Birkel et al. 2012; Levy et al. 2018; Salemi et al. 2013), few studies have looked specifically at how vegetation influences the temporal dynamic of soil water, and what such changes could mean at various scales. Practically none of these types of studies have been conducted in tropical dry forests, despite the apparently strong connection between drought-deciduous vegetation and available soil water.

Ecohydrological consequences of deforestation

Several studies in the dry tropics show that further changes in vegetation cover and land use can alter soil properties and related hydrologic fluxes. For example, the old forest site in the Caatinga had twice the infiltrability and more than more than five times the field saturated hydraulic conductivity than the abandoned grazed pasture site (Leite et al. 2018). Similar findings are reported for other sites in the dry tropics. For a woodland site in Burkina Faso, infiltrability was higher and surface runoff was lower under Shea trees compared to open areas, where even small rainfall events would result in surface runoff. Moreover, groundwater recharge reduced further away from trees than near trees, and was negligible when trees were absent (Ilstedt et al. 2016; Tobella et al. 2014;). In Nicaragua, preferential flow paths were more abundant in a forested vs. pasture site. Here, the density of standing woody vegetation significantly increased saturated hydraulic conductivity, and more so for fine-textured soils than in coarse-textured soils (Niemeyer et al. 2014). In India, forest disturbance, such as grazing, fuelwood / fodder extraction, and fire, resulted in a reduction of clay content and soil organic matter of surface soil and consequently, a reduction in soil water content decreased (Mehta et al. 2008). From an energy perspective,

the conversion of forested Caatinga to pasture results in reductions in relative humidity and latent heat flux, as well as increases in temperature, sensible heat flux, and albedo. Increases in albedo can lead to subsidence anomalies, which could reduce precipitation, even for neighboring regions such as northwestern Amazon (Salazar et al. 2015). Other semi-arid systems show that soil evaporation is higher in bare vs. forested sites due to lower direct solar radiation, temperature, and shading during the leaf out period (Breshears et al. 1998; Villegas et al. 2010). There are a few studies which compares evapotranspiration (ET) in forested vs. pasture sites in SDTF. These few studies include estimates from the Cerrado savanna in central Brazil show that forested areas report higher ET because trees generally have deeper roots and access to groundwater, compared to non-forested covers (Oliveira et al 2005); modelling studies predict similar findings (Silva et al. 2015). Additionally, several other studies show that woody vegetation in semi-arid systems affects the variation of soil water via interception (Owens et al. 2006) and hydraulic lift (Caldwell et al. 1998; Zou et al. 2005).

The role of vegetation in the temporal dynamics of soil water

If vegetation affects soil water, then we would expect this difference to be reflected in the temporal dynamics of soil water data collected across land cover types if soil type is held constant. At the pasture site, the soils have likely been compacted and infiltration reduced. Thus, at hourly to daily timescales, which are relevant to infiltration, we would expect a less apparent response in the soil water dynamics of the pasture compared to the forest site, particularly for more intense rainfall rates.

At the forested Caatinga site, there would be water loss via canopy storage and evaporation for small rain events. Thus, we expect that small rain events would not

produce a peak in soil water. For medium to large rain events, the canopy may capture water and promote stem flow. Thus, we would expect a potentially larger peak in soil water. After a rain pulse infiltrates and soil water reach field capacity, the draw-down will occur over 2 to 22 days due to root water uptake and transpiration in seasonally dry tropical forests (James et al. 2003). Thus, at the daily to weekly timescale we might expect the soil water signal in a forest to be "flashier" because of immediate utilization of soil water.

At the seasonal scale, soil water dynamics will be driven by the distinct wet-dry cycle of rainfall. Whether this variability will be strongest in the forested Caatinga vs. the abandoned pasture will depend on how hourly, daily and weekly soil water dynamics scale-up. If the forest site is highly responsive or sensitive to rainfall events, i.e. quickly utilizing available soil water, then the rainfall dynamics at the seasonal scale may be less apparent compared to the pasture site. Vegetation has a degree of buffering capacity and can grow during a dry period if the previous year was wet (Cunha et al. 2015). Thus, we would expect that the influence of interannual variability in rainfall will be less apparent in the soil water dynamics observed in the forest vs. pasture.

The role of soil texture

Soil textural differences between the two sites will affect soil water dynamics. Specifically, a higher percent of clay increases soil water holding capacity whereas a higher percent sand increases infiltration rates lowers soil water holding capacity. This means that clayey soils would be less dynamic. Sandy soils on the other hand, will probably not reach as high magnitudes of change but will be "flashier" as water is quickly flushed through the soil

profile. Similarly, rain pulses would propagate through to 40 cm depths more frequently in sandy soils.

Objectives

Since soil water is a key component in water balance studies and is a driver of ecological responses, then it is essential to understand how land use and land cover affect this measure. This is especially true for dry forests systems, which are so intimately linked to rainfall pulses and water availability. The objective of this study is to determine how and to what extent vegetation cover changes the temporal behavior of soil water. To provide insight into how soil water might be altered by agricultural conversion across timescales, we relied on a wavelet analysis approach to compared soil water dynamics by site, soil depth, and across hourly to seasonal timescales.

Methods

Study site

The study area is located at the Fazenda de Buenos Aires (07°56'50 "S and 38°23'29" W, 450m elevation), near the municipality of Serra Talhada, PE, Brazil (Figure II-1). The study area is typical of a dryland Caatinga mixed forest and shrub type called Sertão. The climate is tropical hot and dry. Mean annual precipitation is 733 mm and potential evapotranspiration is about 2,000 mm / year. The rainy season typically occurs from January to May, and accounts for ~75% of annual rainfall, although rainfall is highly erratic and unpredictable. Average monthly air temperatures range from 21 to 26 °C, with maximum temperatures of 31 °C and minimum temperatures of 17 °C (Griessen 2006; New LocClim 1.10). Entisol Orthent and Aridsol Argid (USDA 1999) are the predominant soils in the study areas.

We collected data from two sites: a forested Caatinga and an abandoned pasture, the same sites as those described in Leite et al. (2018). The forested site represents a more intact Caatinga. It is thought to have been relatively undisturbed since at least 1960, aside from light, free-roaming cattle and goat grazing. During the rainy season, herbaceous cover is present with areas of bare soil between woody plants. Most of the woody species are drought deciduous. The abandoned pasture represents a deforested site. In 1960, the area was cleared by slash and burn, then plowed and cultivated with cotton until 1980. After that, the area was sowed with buffelgrass (*Cenchrus ciliaris*) and turned into a pasture grazed by cattle and sheep until 2014. Currently, the pasture is abandoned. Patches of buffelgrass and forbs grow in the rainy season, during which there is light grazing of cattle.

Soil physical properties

Soil hydraulic properties were determined according to the Beerkan Estimation of Soil Transfer parameters, or the BEST method. This method relies on soil physical properties, namely particle size distribution, soil bulk density, and infiltration tests to define cumulative infiltration and the initial and final soil water contents. Infiltration tests were performed using modified single-rings (Bagarello et al. 2013; Lassabatere et al. 2006; Ursulino et al. 2019) for four soil profiles at each site, for depths of 10, 20, 30, and 40 cm and soil physical properties were also measured. The BEST method characterizes the soil water retention according to van Genuchten equation (van Genuchten 1980) and using the Burdine condition (Burdine 1953) and the hydraulic conductivity curve according to the Brooks and Corey equation (Brooks & Corey 1964). All parameters were obtained by the Beerkan-slope method for each depth in the soil profile using the “steady” version of the BEST algorithm (Bagarello et al. 2013; Leite et al. 2018;) within the Scilab platform,

except residual soil water content, which was inferred based on USDA textural classification and Rosetta look-up tables (Schaap et al. 2001; https://cals.arizona.edu/research/rosetta/).

Rainfall and soil water data

Rainfall (TE 525 WS-L, Texas Electronics, USA) soil temperature (108 Campbell Scientific Inc., USA), and soil volumetric water content (CS 616 Campbell Scientific Inc., USA) data was collected from an abandoned pasture and forested Caatinga study site. Soil temperature and volumetric water content were co-located at four depths per profile: 10 cm, 20 cm, 30 cm, and 40 cm (Figure II-2). All data were recorded at 30-minute intervals, gap-filled, and resampled to hourly data. Soil temperature data was then utilized to correct volumetric soil water.

Gap-filling

Data continuity is a severe limitation in wavelet analysis. Gap sizes should be reduced where possible and appropriate gap-fill techniques employed—ideally based on existing data as to avoid distorting temporal structure. We utilized a combination of linear interpolation for very small gaps, and bivariate linear analysis for larger gaps. When the general structure of the raw time series of soil water could be preserved, linear interpolation was utilized to preserve temporal autocorrelation. In the case of the pasture site, soil water data at 30 cm was completely absent, so it was interpolated as the average of volumetric water content at 20 cm and 40 cm to maintain data continuity across depth. Still interpretation of results at this depth for the Caatinga are approached with caution. For other missing data, there were two cases when a simple linear interpolation could not be used. The first case was for missing rainfall data at the pasture site. In this case we cross-

checked and filled the missing rainfall data with values from the Caatinga site because the presence of rainfall between the two sites aligned temporally, had relatively high correlation (~0.84, p-value <0.01), and the missing rainfall values in the pasture was less than 4%. The second case was air temperature and soil temperature at 40 cm also at the Caatinga site. Here, univariate linear models were used to predict missing values. Missing values in air temperature were filled based on pasture air temperature, because of high correlation (~0.88, p-value<0.01, r2=0.96). Similarly, missing values in soil temperature at 40 cm were filled based on soil temperature at 30 cm because of high correlation (~0.89, p-value<0.01, r2=0.92). Our continuous rainfall and soil water data was from December 1, 2016 to January 1, 2019, over two years.

Data correction

Raw soil water data was corrected in two ways. The first was to account for the influence of temperature on the dielectric permittivity of soil. The CS616 soil water probes use the water content reflectometer method for measuring soil water content. This is an indirect measurement that is sensitive to the dielectric permittivity of the material surrounding the probe rods. In soils, the dielectric permittivity can be influence by temperature in neutral, positive, or negative directions depending on the soil type and current water content. Thus, to adjust the raw data output we utilized a multiple regression following the equation:

$$\boldsymbol{VWC_{Tadj} = C_1 * VWC_{raw} + C_2 * T_{soil} + C_3} \qquad \text{Equation II-1}$$

Where VWC_{Tadj} is the temperature-adjusted volumetric water, VWC_{raw} is the raw volumetric water content, T_{soil} is the measured soil temperature and C_1, C_2, and C_3 are empirical coefficients. For the output of each probe, we selected three 24-hour periods over which to perform the multiple regression. These were periods in which there was no

rainfall, where soil water was similar at the start and end of the 24-hour period, and for which the period was considered either a low, medium, or high value within the range of the raw data.

Second, we also performed a min-max normalization on the soil water data using soil hydraulic properties. We assumed the that the range of raw soil water values corresponded to the saturated and residual soil water content, and all other values scaled proportionately. For each depth and site, the min-max normalization was applied using the formula:

$$\boldsymbol{VWC_{scaled} = \frac{VWC_i - VWC_{Min}}{VWC_{Max} - VWC_{Min}}} \qquad \text{Equation II-2}$$

Where VWC_{scaled} is the corrected soil volumetric water content, VWC_i is the temperature-adjusted volumetric water content or VWC_{Tadj} from the Equation II-1, VWC_{Max} is the saturated soil water content, and VWC_{Min} is the residual soil water content.

The continuous wavelet transform

We used a wavelet transform to reveal the frequency components of each time series soil water signal. For a non-stationary, aperiodic signal, x(t) the continuous wavelet transform is:

$$\boldsymbol{W(\tau, s) = \int_{-\infty}^{+\infty} x(t)\ \varphi^*\left(\frac{t - \tau}{s}\right) \delta t} \qquad \text{Equation II-3}$$

Where φ* denotes the complex conjugate wavelet, s is the scale, and t is the current time position in the time points, τ. The Morlet wavelet (Grossman and Morlet 1984) is often preferred because it optimizes time and frequency resolution (Heisenberg principle) and has wide application in earth sciences (Torrence and Compo 1998; Zhang and Moore 2011), hydrology (Gaucherel 2002) and ecology (Cazelles et al. 2008; Vargas et al. 2012).

Still, is important to note that many other wavelet functions can be used, which may be better in terms of time or frequency resolution (examples in Casagrande et al. 2015 for Morlet vs. DOG; Parent et al. 2006 for Morlet vs Mexican hat). The Morlet wavelet is defined as:

$$\varphi^{*}_{Morlet} = \pi^{-0.25} e^{-i2\pi ft} e^{-0.5t^2} \qquad \text{Equation II-4}$$

Where f is frequency. Because the central angular frequency of the Morlet wavelet is approximately 2π frequency is approximately equal the inverse of scale, and so scale and period are approximately equal (Cazelles et al. 2008).

Changing s and τ of the wavelet function—that is translating and dilating the wavelet—creates a series of "filters, allowing for a narrow window when the frequency is high and a broader window when the frequency is low. The result, the wavelet coefficients, W (τ, s), represent the contribution of the scales to the signal at different times. This means that the wavelet coefficients are the linear correlation between the chosen wavelet and the time series data, expressed at different scales and time locations. Hence, a large positive coefficient is a high positive correlation, and a large negative coefficient is a high negative correlation between the wavelet function and the time series. The wavelet coefficients can then be used to compute power, $\mathrm{W}(\tau,\ \mathrm{s})^2/s$ (rectified by Liu et al. 2007) to display the wavelet power spectrum. The power values correspond to variability in the time series signal and in this way reveals its temporal structure. Dramatic jumps or discontinuities are localized, and periodic components are displayed over a range of scales. Note that since wavelet power corresponds to variability, the units are in variance^2. In the case of volumetric soil water content, the units of power are $(m^3/m^3)^2$; i.e. unitless.

Results

Soil physical and hydraulic properties

We found that our temperature-corrected soil water values did not change much from raw soil water readings (Table II-1; C1>0.9 and C2 very small for all CS616 soil water probes). The min-max normalization of soil water data is physically consistent with physical properties described for each depth at the two sites and resulted in soil water values that were comparable between the sites and depths (Figure II-3) despite textural difference (Table II-2). At both sites, there is evidence of illuviation of clay from shallow to deeper soil layers because clay content increases with depth The Caatinga soils were classified as sandy loams throughout the top 40 cm. There was an increase in clay content with depth, doubling from the shallow 10 cm to deeper depths. Saturated soil water content was greater at the top 10 cm, indicating that soil porosity is also greater near the surface. The pasture soils were classified as sandy loam near the surface, then loam and sandy clay. Clay content also doubled from the shallow to deeper soils. Yet, the pasture soil also had twice the percentage of clay content compared to the corresponding Caatinga soils.

The soil water retention curve corresponds to soil textural classification (Figure II-4). For both sites at 10 and 20 cm where soil texture is a sandy loam, the soil water retention curves are very similar. For the pasture site at 40 cm soil depth, the curve is more gradual indicating that water is held more tightly. The soil hydraulic conductivity curve shows how hydraulic conductivity changes with increasing soil water content. There appears to be little difference in the behavior of unsaturated hydraulic conductivity (Figure II-5) until 40 cm depth. At this depth, the curves depart by site, being higher at the Caatinga. Although saturated soil hydraulic conductivity, Ks, differs greatly by site (Table

II-3); Ks is greater in the Caatinga than the Pasture site, the difference being more than four-fold at 10 cm soil depth.

Rainfall is a strong driver of the soil water time series regardless of site and soil depth (Figure II-3). The shallow soils are more responsive and more closely follow rainfall pulses. For example, for both the Caatinga and pasture site, a medium size rain event in July cause larger soil water peaks at 10 and 20 cm than at 30 and 40 cm. Although, the temporal dynamics seem to differ by site. The peaks in soil water content are more pronounced and the dry-down appears more immediate in the Caatinga site. Additionally, into the dry season (May to December) the Caatinga site quickly reaches a baseline level which approaches residual soil water content. In pasture site on the other hand, residual soil water content is approached only for the 10 cm depth and only near the end of the dry season. Note that the rainfall distribution is not identical by site by highly correlated (see gap-filling section above).

Wavelet power spectra

Wavelet power was plotted in the time-frequency domain to localize regions of high significant power (Figure II-6). The heat map is a plot of the power vs time and period (or time scale). Warm colors indicate regions of high power or high soil water variability, and cool colors indicate colors of low power or relative stability. The localized wavelet power was then averaged in the time and period domains to depict energy distribution (vertical and horizontal line plots, respectively). These plots depict power peaks in the time and period domains.

Generally, in the power spectra heat map, regions of high power (warm colors) align rainfall pulses across timescales, regardless of soil depth or site. This is consistent

with the vertical plots, which depict the alignment of soil moisture power peaks in the time-domain. Similarly, in the power spectra heat map, regions of high power become more apparent at 1 to 2 months in the deeper soils; i.e. the timescale at which changes in soil water occur increase with depth. This is consistent with the vertical time-domain plots. Larger or more intense rainfall create larger power peaks, but the detail of these peaks dissipates with depth for both sites. In the period domain, power peaks occurred at approximately 2-months regardless of site and depth.

Power decomposed by times scale

To better understand the short- and longer-timescale changes occurring at each site, we average power over specific timescales or periodic components. This is shown in Figures II-7 and II-8. Here, power is averaged for three timescales: 12 to 48 hours, 3 to 10 days, and 1 to 3 months—decomposing power into specific timescale bands. The timescales were chosen to better understand ecohydrological processes occurring at hourly to weekly timescales, like infiltration and evapotranspiration, as compared to those occurring over longer timescales, like the seasonality of vegetation activity as driven by the wet-dry cycles of rainfall.

To preserve time-localization—which is the main advantage of wavelet methods—Figure II-7 depicts average power over time for the three timescales. High-frequency variability, that is, average power for the shorter timescales, is clearly driven by rainfall pulses regardless of site and depth. Still the detail and/or magnitude of power peaks generally dissipates with depth at both sites. Low-frequency variability, that is average power over the longer 1 to 3 months timescale, was associated with rainfall seasonality;

power peaks occur in the wet season. Additionally, the size of the power peaks appeared smaller for the 2017 wet season than the 2018 wet season, particularly at the Caatinga site.

The average period-specific power by soil depth is shown in Figure II-8. Note that by averaging the power by soil depth, we have lost time-localization information. Soil water variability diverged by site, at the three timescales. Average power was greater in the Caatinga for all depths at the short timescales (12 to 48 hours and 3 to 10 days), meaning that high frequency changes are greater at the Caatinga site. This trend flipped at the 1 to 3 months timescale, meaning that soil water variability was greater in the pasture at lower frequencies. At this timescale, power was between 1.45 and 1.77 in the Caatinga, and between 1.74 and 2.15 in the pasture. Moreover, for both sites, power dissipates with depth at the short timescales but not necessarily for the longer timescale. At the 1 to 3 months timescale, power increases and then decreases with depth. At this timescale, the greatest soil water variability is at 30 cm in the Caatinga and at 20 cm in the pasture.

Discussion

We analyzed the soil water dynamics for two sites with different in land use / land cover. Although we used a technique which was computationally heavy, the lack of significance testing and replication means that we can only describe our results in a qualitative manner. To help support the limited replication in soil water data, physical and hydraulic parameters were also determined for soil four profiles per site.

Vegetation changes soil properties

We believe that the soil water dynamics for the two sites differ as a reflection of the interacting influence of vegetation on soil properties and water fluxes. As a result of vegetative and soil textural differences, it is likely that the upper soil layer, the A horizon,

has been eroded away at the Pasture site. At the pasture site, the clay content is already ~13% near the surface. While this difference may reflect soil heterogeneity given the small sample size, it is more likely that theses samples are indicative of the influence of land use / land cover on soil properties. As noted, the pasture area has a history of about 60 years of agricultural activity. During cotton cultivation, activities such as plowing, disturbed and exposed near surface soil layers. Consequent grazing meant that the soils were also likely compacted, reducing infiltration and soil hydraulic conductivity, and increasing runoff and erosion. Therefore, it is reasonable that after 60 years agricultural activities which impacted soils and reduced vegetation cover, the topsoil layer was lost to erosion.

Although previous field research did not find a difference in current erosion rates experience by the forested Caatinga vs. pasture sites (Leite et al. 2018), there is no known record of historical erosion rates. However, we found that saturated hydraulic conductivity was four times higher for the surface soils in the Caatinga vs. pasture site, as in previous research (Leite et al. 2018). At the Caatinga site, tree and shrubs roots can increase macro-porosity and promote soil structure through organic inputs, thus increasing infiltration and saturated hydraulic conductivity. As a result of these differences in soil texture and saturated hydraulic conductivity, we also found differences in temporal soil water dynamics. Specifically, we found that at short time scales, soil water in the Caatinga, which had sandier soils and greater hydraulic conductivity near the surface, was more dynamic than in the pasture.

Soil water dynamics have strong event-based and seasonal components

Through the univariate wavelet transform, we have shown that for both sites, wavelet power peaks aligned with rainfall events. This means that soil moisture variability is event

driven. This result is not surprising for seasonally water-limited areas such as Northeast Brazil. Moreover, our findings agree with other wavelet analysis performed at fine timescales. Parent et al. (2006) show that at the 1- to 48- hours scale, soil moisture is linked to precipitation occurrence, intensity and duration and at the 1 to 2 weeks scale, soil moisture is linked to periodicity of rainfall events. Lee and Kim (2019) used coherence analysis to show that soil moisture dynamics across a hillslope have a high coherence with rainfall at sub-daily and approximately biweekly scales. Soil water variability also had a strong seasonal component at both sites. This means the role of rainfall seasonality, i.e. wet vs. dry season, drives soil moisture variability at larger timescales. Again, the results are not surprising given high rainfall seasonality. Other studies show that soil moisture is more variable during a wet vs. dry stage (Costa et al. 2014; Lee and Kim 2019), reflecting both physical and biological processes, such as infiltration and plant water uptake.

Moreover, we show that soil acts as a low-pass filter on soil water variability, especially at the shorter timescales, because power decreases with depth. The dampening effect with increasing soil depth is related to the redness of the soil moisture spectra, where soil acts as a low-pass filter, removing high frequency fluctuations. These results agree with the literature. Wu et al. (2002) found that with depth, soil water variability shifted to lower frequencies—that is, variability occurring over longer durations. At shorter timescales, Parent et al. (2006) soil redistributes energy from precipitation, and that the influence of soil properties and seasonality become more pronounced with time since the rainfall event; i.e variability increases with timescale. Tang and Piechota (2009) used wavelet coherence to determine whether deep soil water can be an indicator of drought. Authors found that the soil water at 40 to 140 cm depth was significantly strongly

correlated with the Palmer Drought Severity Index at the 3- to 7- year frequency, corresponding to El Niño. Like Wu et al. (2002), these results show that climate can have a lasting effect on soil water reserves at depth.

Soil water seasonality is greater in the pasture than the forested Caatinga

Similar to soil, vegetation cam also buffers to seasonal variability in soil water. At the 1 to 3 months timescale, wavelet power in the Caatinga was lower than in the pasture. This means that the Caatinga vegetation also acts as low pass filter on soil water, which could be related to the seasonality in phenology and vegetation water. Like Potts et al. (2010), we found dampening of soil moisture variability in the forested Caatinga compared to the pasture. But unlike Potts et al. (2010), this dampening was strongest at the seasonal timescales, and was not apparent at the short timescales. Caatinga are shallowly rooted, with an effective rooting depth of 40cm. (Pinheiros et al. 2013); note that this does not mean that Caatinga species cannot be more deeply rooted. Shallow effective root depth probably why, within the top 40 cm and at the short-timescales (12 to 48 hours and 3 to 10 days), soil water variability was greater in the forested Caatinga than in the pasture—likely reflecting the immediate response of tree transpiration to rainfall pulses and greater soil infiltration and hydraulic conductivity. In regions where rainfall seasonality is weak and soils are deeper, soil water variability may be higher in a forested vs. pasture site. For example, in the Amazon river basin, Hodnett et al. (1995) found larger seasonal variation of water storage beneath the forest compared to pasture at 2 m depth. Moreover, between 0.2 and 0.4 m the changes in the forest and pasture were similar, but below 0.6 m, the changes in water content were consistently greater in the forest (Hodnett et al. 1995).

Several other studies show that vegetation considerably affects the variation of moisture in the soil profile (Caldwell et al. 1998; Seyfried et al. 2005; Zou et al. 2005; Zou et al. 2014).

Conclusion

Our findings show that land use history and vegetation cover can ultimately influence soil physical and hydraulic properties, resulting in change in ecohydrological fluxes such as soil water variability across hourly to seasonal timescales. We found that soil water variability is linked to rainfall pulses and seasonality. Thus, changes in rainfall regimes, such as increases in rainfall intensity and a shortening of the wet season, can great change the temporal dynamics and availability of soil water which supports forests and rain-fed agricultural activity. Moreover, we should expect changes in soil water to be greater for a forested site at short timescales, but less so at seasonal scales, particularly if changes in land cover also includes changes in soil physical and hydraulic properties. Thus, inter-annual changes in rainfall, such as wet vs. dry years, will have a greater impact on rain-fed agriculture, whereas forested areas may have some degree of buffer to seasonal and inter-annual changes in rainfall. The implications of these findings suggest that land use / land cover can lead to increased erosion and soil loss, changes in ecohydrological fluxes, promote land degradation and desertification, and make the system less resistant / resilient against climate change. Additional research should seek integrated measures of hydrology, such as runoff and stream discharge, as a function of land use / land cover to better understand potential changes in ecohydrological fluxes.

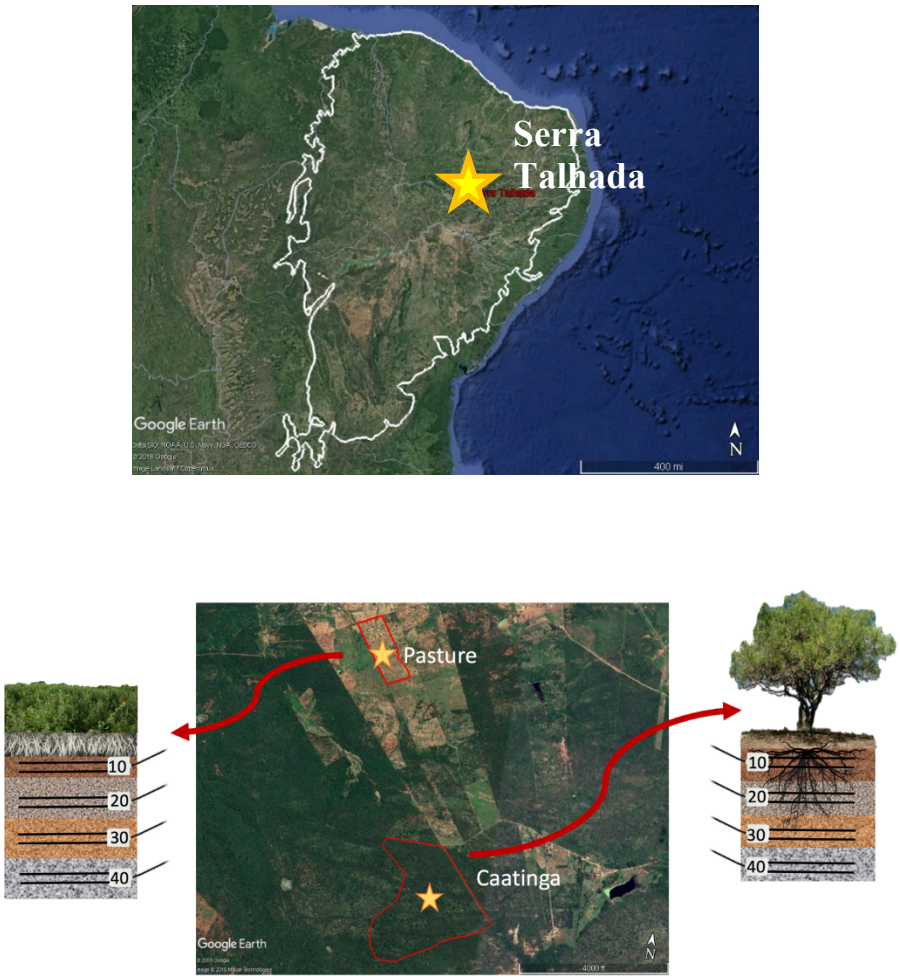

Figure II-1.The Caatinga biome (top) and the forested Caatinga and pasture sites (bottom) near Serra Talhada, PE, Brazil. Background images from Google (2018a, 2018b) and top biome outline from MMA / IBGE (2007).

Figure II-2. The forested Caatinga (top) and pasture (bottom) sites during the wet (left) and dry (right) season. Author's images.

Table II-1. Multiple regression coefficients to account for soil temperature.

Depth (cm)	C_1	C_2	C_3
Caatinga			
0 – 10	1.002	$1.300 * 10^{-5}$	$-5.175 * 10^{-4}$
10 – 20	0.997	$1.657 * 10^{-5}$	$6.930 * 10^{-5}$
20 – 30	0.997	$-5.218 * 10^{-5}$	$1.950 * 10^{-3}$
30 - 40	1.003	$-3.691 * 10^{-5}$	$1.088 * 10^{-3}$
Pasture			
0 – 10	0.977	$-3.2323 * 10^{-4}$	$1.497 * 10^{-2}$
10 – 20	0.970	$-6.006 * 10^{-4}$	$2.709 * 10^{-2}$
20 – 30	0.976	$-4.255 * 10^{-4}$	$1.918 * 10^{-2}$
30 – 40	0.981	$-1.863 * 10^{-4}$	$9.097 * 10^{-3}$

Table II-2. Soil physical properties.

Depth (cm)	% Sand (SD)		% Clay (SD)		USDA Texture Classification	Soil bulk density (g/cm^3) (SD)	
Caatinga							
0 – 10	68.53	(6.63)	6.38	(7.38)	sandy loam	1.20	(0.21)
10 – 20	64.45	(12.07)	11.29	(13.27)	sandy loam	1.39	(0.11)
20 – 30	61.83	(16.09)	13.42	(17.06)	sandy loam	1.43	(0.04)
30 – 40	62.71	(15.32)	13.30	(15.64)	sandy loam	1.49	(0.11)
Pasture							
0 – 10	59.85	(8.98)	12.72	(4.46)	sandy loam	1.38	(0.12)
10 – 20	52.51	(11.56)	18.49	(6.74)	sandy loam	1.47	(0.11)
20 – 30	49.22	(8.47)	19.18	(6.38)	loam	1.36	(0.09)
30 – 40	49.91	(13.25)	23.72	(9.82)	sandy clay loam	1.33	(0.14)

Table II-3. Soil hydraulic properties determined with the BEST method.

Depth (cm)	θ_s (m^3/m^3)	(SD)	θ_r (m^3/m^3)	Ks (mm/h)	(SD)
Caatinga					
0 – 10	0.548	(0.080)	0.039	274	(263)
10 – 20	0.477	(0.040)	0.039	46.7	(36.4)
20 – 30	0.470	(0.027)	0.039	30.3	(22.3)
30 – 40	0.438	(0.041)	0.039	21.0	(22.8)
Pasture					
0 – 10	0.479	(0.046)	0.039	62.0	(31.2)
10 – 20	0.445	(0.040)	0.061	17.4	(7.82)
20 – 30	0.486	(0.035)	0.061	28.1	(45.0)
30 – 40	0.497	(0.054)	0.063	14.9	(13.8)

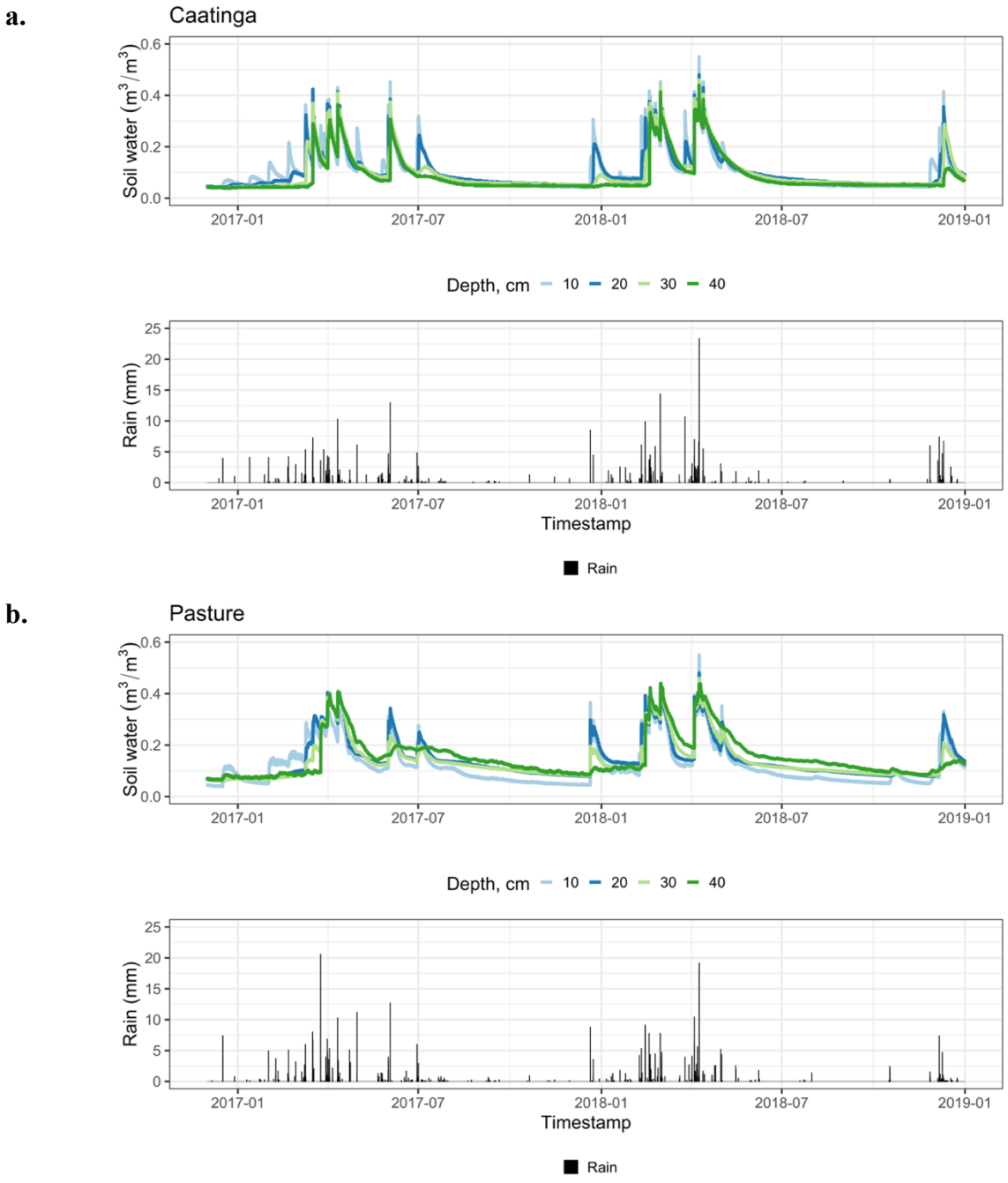

Figure II-3. Rainfall (bottom) and soil water (top) time series for the Caatinga (a) and Pasture (b) site.

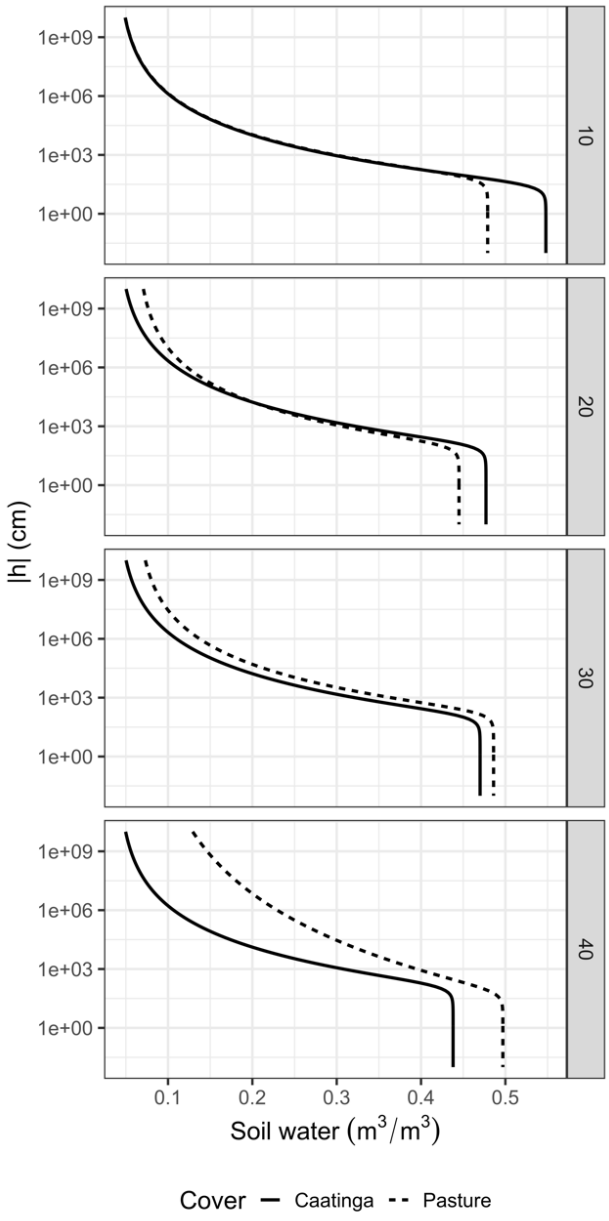

Figure II-4. Soil water retention curve by depth and site. The forested Caatinga site is the solid line and the pasture site is the dashed line.

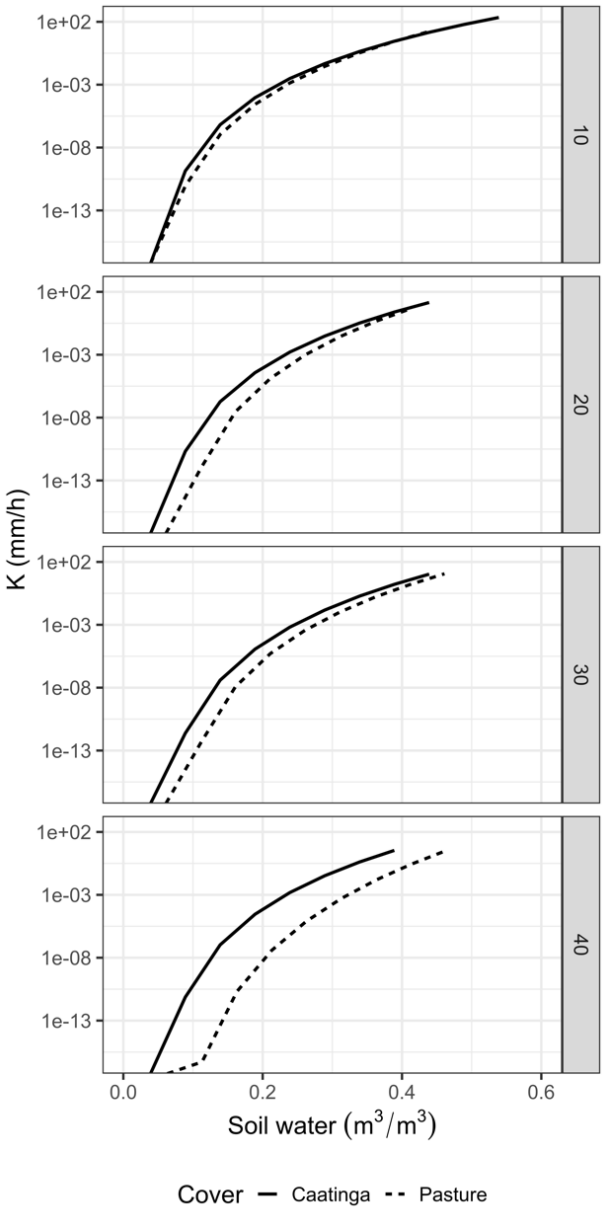

Figure II-5. Hydraulic conductivity curve by depth and site. The forested Caatinga site is the solid line and the pasture site is the dashed line.

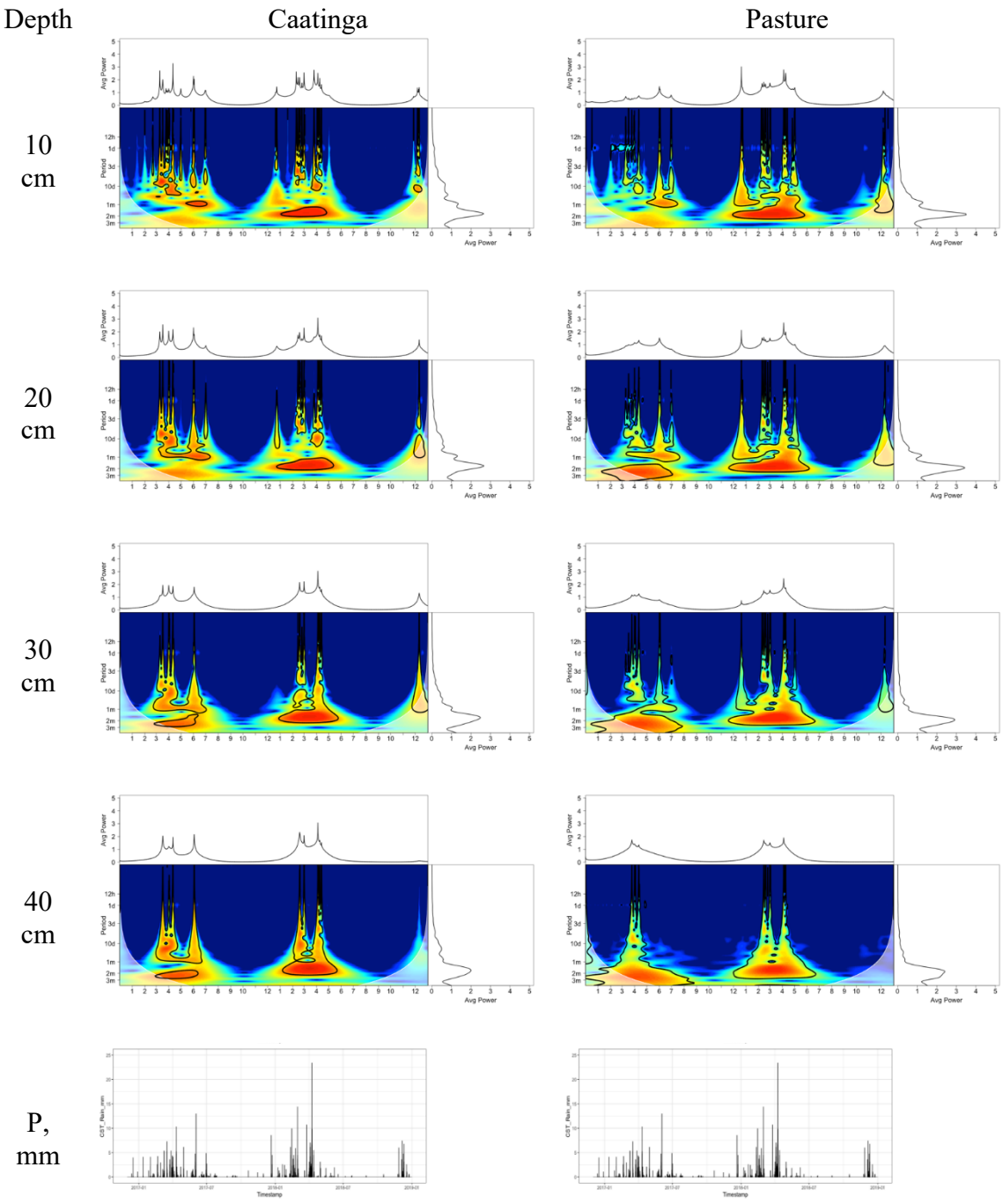

Figure II-6. Wavelet power spectra of soil moisture time series by cover type and soil depth. Warm colors indicate regions of high power, and cool colors indicate regions of low power. Significant high power regions (determined by AR (1) processes) are outlined in black, and the cone of influence is shaded in a transparent white. Power is plotted in the time and period domain. Top horizonal plot is the average power in the time domain, and right-side vertical plot is the average power in the period domain.

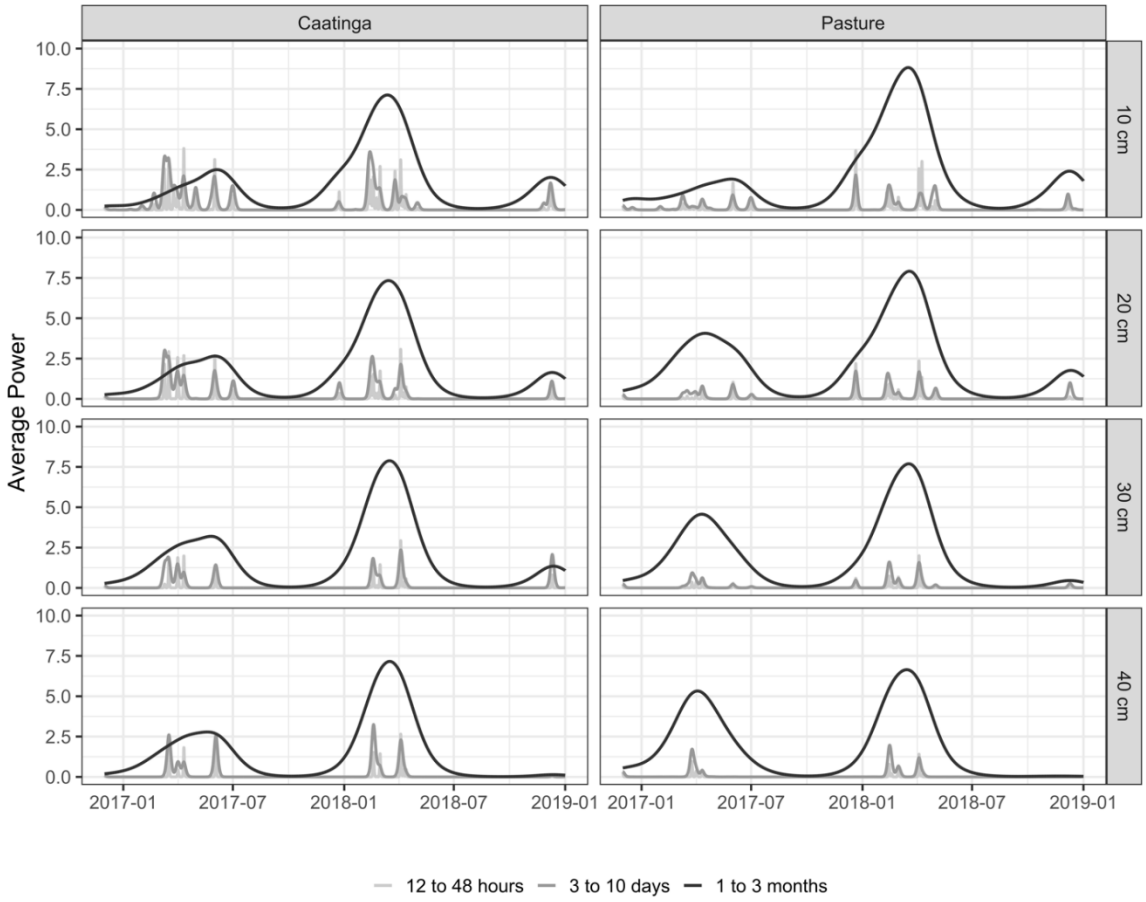

Figure II-7. Wavelet power averaged for three timescales: 12 to 48 hours (light grey), 3 to 10 days (dark grey), and 1 to 3 months (black) and across soil depth for the forested Caatinga site (left) and pasture site (right).

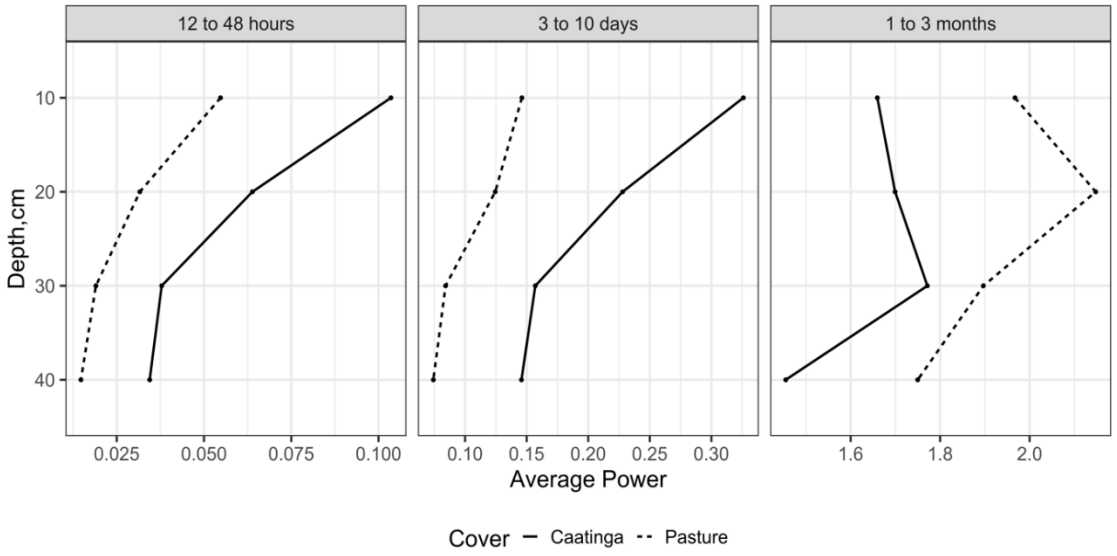

Figure II-8. Normalized power of the soil moisture spectra averaged for four depths in the soil profile and across three timescales: 12 to 48 hours, 3 to 7 days, and 1 to 3 months. The solid line is the forested Caatinga site and the dashed line is the pasture site. Note the different x-axes range.

References

Aide, T. M., Clark, M. L., Grau, H. R., López-Carr, D., Levy, M. A., Redo, D., … Muñiz, M. (2013). Deforestation and Reforestation of Latin America and the Caribbean (2001-2010). *Biotropica*, *45*(2), 262–271. https://doi.org/10.1111/j.1744-7429.2012.00908.x

Alvarenga, L. A., De Mello, C. R., Colombo, A., Cuartas, L. A., & Bowling, L. C. (2016). Assessment of land cover change on the hydrology of a Brazilian headwater watershed using the Distributed Hydrology-Soil-Vegetation Model. *Catena*, *143*, 7–17.

Antongiovanni, M., Venticinque, E. M., & Fonseca, C. R. (2018). Fragmentation patterns of the Caatinga drylands. *Landscape Ecology*, *33*(8), 1353–1367. https://doi.org/10.1007/s10980-018-0672-6

Austin, A. T., Yahdjian, L., Stark, J. M., Belnap, J., Porporato, A., Norton, U., … Schaeffer, S. M. (2004). Water pulses and biogeochemical cycles in arid and semiarid ecosystems. *Oecologia*, *141*(2), 221–235. https://doi.org/10.1007/s00442-004-1519-1

Bagarello, V., Castellini, M., Di Prima, S., Giordano, G., & Iovino, M. (2013). Testing a Simplified Approach to Determine Field Saturated Soil Hydraulic Conductivity. *Procedia Environmental Sciences*, *19*, 599–608. https://doi.org/10.1016/j.proenv.2013.06.068

Beuchle, R., Grecchi, R. C., Shimabukuro, Y. E., Seliger, R., Eva, H. D., Sano, E., & Achard, F. F. (2015). Land cover changes in the Brazilian Cerrado and Caatinga biomes from 1990 to 2010 based on a systematic remote sensing sampling approach. *Applied Geography*, *58*, 116–127. https://doi.org/10.1016/j.apgeog.2015.01.017

Birkel, C., Soulsby, C., & Tetzlaff, D. (2012). Modelling the impacts of land-cover change on streamflow dynamics of a tropical rainforest headwater catchment. *Hydrological Sciences Journal*, *57*(8), 1543–1561.

Breshears, D. D., Nyhan, J. W., Heil, C. E., & Wilcox, B. P. (2007). Effects of Woody Plants on Microclimate in a Semiarid Woodland: Soil Temperature and Evaporation in Canopy and Intercanopy Patches. *International Journal of Plant Sciences*, *159*(6), 1010–1017. https://doi.org/10.1086/314083

Burdine, N. T. (1953). Relative Permeability Calculations From Pore Size Distribution Data. *Journal of Petroleum Technology*, *5*(03), 71–78. https://doi.org/10.2118/225-G

Caldwell, M. M., Dawson, T. E., & Richards, J. H. (1998). Hydraulic lift: Consequences of water efflux from the roots of plants. *Oecologia*, *113*(2), 151–161. https://doi.org/10.1007/s004420050363

Casagrande, E., Mueller, B., Miralles, D. G., Entekhabi, D., & Molini, A. (2015). Wavelet correlations to reveal multiscale coupling in geophysical systems. *Journal of Geophysical Research*, *120*(15), 7555–7572. https://doi.org/10.1002/2015JD023265

Castelletti, C. H. M., da Silva, J. M. C., Tabarelli, M., & Santos, A. M. M. (2003). Quanto ainda resta da Caatinga? Uma estimativa preliminar. *Ecologia e Conservação Da Caatinga*, 777–796. https://doi.org/10.1590/S0103-40142005000200009

Cazelles, B., Chavez, M., Berteaux, D., Mendard, F., Vik, J. O., Jenouvrier, S., & Stenseth, N. C. (2008). Wavelet analysis of ecological time series. *Oecologia*, *156*(2), 287–304. https://doi.org/10.1007/s00442-008-0993-2

Choler, P., Sea, W., & Leuning, R. (2011). A Benchmark Test for Ecohydrological Models of Interannual Variability of NDVI in Semi-arid Tropical Grasslands. *Ecosystems*, *14*(2), 183–197. https://doi.org/10.1007/s10021-010-9403-9

Collins, S. L., Sinsabaugh, R. L., Crenshaw, C., Green, L., Porras-Alfaro, A., Stursova, M., & Zeglin, L. H. (2008). Pulse dynamics and microbial processes in aridland ecosystems. *Journal of Ecology*, *96*(3), 413–420. https://doi.org/10.1111/j.1365-2745.2008.01362.x

Cunha, A. P. M., Alvalá, R. C., Nobre, C. A., & Carvalho, M. A. (2015). Monitoring vegetative drought dynamics in the Brazilian semiarid region. *Agricultural and Forest Meteorology*, *214–215*, 494–505. https://doi.org/10.1016/j.agrformet.2015.09.010

Dias, L. C. P., Pimenta, F. M., Santos, A. B., Costa, M. H., & Ladle, R. J. (2016). Patterns of land use, extensification, and intensification of Brazilian agriculture. *Global Change Biology*, *22*(8), 2887–2903. https://doi.org/10.1111/gcb.13314

Dias, L. C. P., Macedo, M. N., Costa, M. H., Coe, M. T., & Neill, C. (2015). Effects of land cover change on evapotranspiration and streamflow of small catchments in the Upper Xingu River Basin, Central Brazil. *Journal of Hydrology: Regional Studies*, *4*, 108–122.

Gaucherel, C. (2002). Use of wavelet transform for temporal characterisation of remote watersheds. *Journal of Hydrology*, *269*(3–4), 101–121. https://doi.org/10.1016/S0022-1694(02)00212-3

Google. (2018a). [Northeast Brazil region]. Retrieved October 2018, from Google Earth Pro 7.3. SIO, NOAA, U.S. Navy, NGA, GEBCO. IBCAO. Landsat / Copernicus.

Google. (2018b). [Area near Serra Talhada, PE]. Retrieved July 2019, from Google Earth Pro 7.3. Maxar Technologies 2019.

Grossmann, A., & Morlet, J. (1984). Decomposition of Hardy Functions Into. *SIAM Journal on Mathematical Analysis*, *15*(4).

Hansen, M. C., Potapov, P. V, Moore, R., Hancher, M., Turubanova, S. A. A., Tyukavina, A., … others. (2013). High-resolution global maps of 21st-century forest cover change. *Science*, *342*(6160), 850–853.

Heisler-White, J. L., Knapp, A. K., & Kelly, E. F. (2008). Increasing precipitation event size increases aboveground net primary productivity in a semi-arid grassland. *Oecologia*, *158*(1), 129–140. https://doi.org/10.1007/s00442-008-1116-9

Hodnett, M. G., da Silva, L. P., da Rocha, H. R., & Cruz Senna, R. (1995). Seasonal soil water storage changes beneath central Amazonian rainforest and pasture. *Journal of Hydrology*, *170*(1–4), 233–254. https://doi.org/10.1016/0022-1694(94)02672-X

Ilstedt, U., Bargués Tobella, A., Bazié, H. R., Bayala, J., Verbeeten, E., Nyberg, G., … Malmer, A. (2016). Intermediate tree cover can maximize groundwater recharge in the seasonally dry tropics. *Scientific Reports*, *6*(February), 1–12. https://doi.org/10.1038/srep21930

Isham, V., Cox, D. R., Rodríguez-Iturbe, I., Porporato, A., & Manfreda, S. (2005). Representation of space-time variability of soil moisture. *Proceedings of the Royal Society A: Mathematical, Physical and Engineering Sciences*, *461*(2064), 4035–4055. https://doi.org/10.1098/rspa.2005.1568

James, S. A., Meinzer, F. C., Goldstein, G., Woodruff, D., Jones, T., Restom, T., … Campanello, P. (2003). Axial and radial water transport and internal water storage in tropical forest canopy trees. *Oecologia*, *134*(1), 37–45.

Janzen, D. H. (1988). Management of Habitat Fragments in a Tropical Dry Forest : Growth. *Annals of the Missouri Botanical Garden*, *75*(1), 105–116. https://doi.org/10.2307/2399468

Lassabatère, L., Angulo-Jaramillo, R., Soria Ugalde, J. M., Cuenca, R., Braud, I., & Haverkamp, R. (2006). Beerkan Estimation of Soil Transfer Parameters through Infiltration Experiments—BEST. *Soil Science Society of America Journal*, *70*(2), 521. https://doi.org/10.2136/sssaj2005.0026

Leite, P. A. M., Souza, E. S. de S., Santos, E. S. do, Gomes, R. J., Cantalice, J. R., & Wilcox, B. P. (2018). The influence of forest regrowth on soil hydraulic properties and erosion in a semiarid region of Brazil. *Ecohydrology*, *11*(3), 1–12. https://doi.org/10.1002/eco.1910

Levy, M. C., Lopes, A. V, Cohn, A., Larsen, L. G., & Thompson, S. E. (2018). Land use change increases streamflow across the arc of deforestation in Brazil. *Geophysical Research Letters*, *45*(8), 3520–3530.

Liu, Y., Liang, X. S., & Weisberg, R. H. (2007). Rectification of the bias in the wavelet power spectrum. *Journal of Atmospheric and Oceanic Technology*, *24*(12), 2093–2102. https://doi.org/10.1175/2007JTECHO511.1

MMA / IBGE. (2007). [Brazil biomes]. Retrieved October 2017, from Global Forest Watch www.globalforestwatch.org

Marinho, F. P., Mazzochini, G. G., Manhães, A. P., Weisser, W. W., & Ganade, G. (2016). Effects of past and present land use on vegetation cover and regeneration in a tropical dryland forest. *Journal of Arid Environments*, *132*, 26–33. https://doi.org/10.1016/j.jaridenv.2016.04.006

Mehta, V. K., Sullivan, P. J., Walter, M. T., Krishnaswamy, J., & DeGloria, S. D. (2008). Impacts of disturbance on soil properties in a dry tropical forest in Southern India. *Ecohydrology*, *1*(2), 161–175. https://doi.org/10.1002/eco.15

Muldavin, E. H., Moore, D. I., Collins, S. L., Wetherill, K. R., & Lightfoot, D. C. (2008). Aboveground net primary production dynamics in a northern Chihuahuan Desert ecosystem. *Oecologia*, *155*(1), 123–132. https://doi.org/10.1007/s00442-007-0880-2

Nanni, A. S., Sloan, S., Aide, T. M., Graesser, J., Edwards, D., & Grau, H. R. (2019). The neotropical reforestation hotspots: A biophysical and socioeconomic typology of contemporary forest expansion. *Global Environmental Change*, *54*, 148–159. https://doi.org/10.1016/j.gloenvcha.2018.12.001

Niemeyer, R. J., Fremier, A. K., Heinse, R., Chavez, W., & DeClerck, F. A. J. (2014). Woody Vegetation Increases Saturated Hydraulic Conductivity in Dry Tropical Nicaragua. *Vadose Zone Journal*, *13*(1). https://doi.org/10.2136/vzj2013.01.0025

Oliveira, A. R. S., Bezerra, L., Davidson, E. A., Pinto, F., Klink, C. A., Nepstad, D. C., & Moreira, A. (2005). Deep Root Function in Soil Water Dynamics in Cerrado Savannas of Central Brazil. *Functional Ecology*, *19*(4), 574–581.

Owens, M. K., Lyons, R. K., & Alejandro, C. L. (2006). Rainfall partitioning within semiarid juniper communities: effects of event size and canopy cover. *Hydrological Processes: An International Journal*, *20*(15), 3179–3189.

Parent, A.-C., Anctil, F., & Parent, L.-E. (2006). Characterization of temporal variability in near-surface soil moisture at scales from 1 h to 2 weeks. *Journal of Hydrology*, *325*(1–4), 56–66. https://doi.org/10.1016/j.jhydrol.2005.09.027

Penna, D., Borga, M., Norbiato, D., & Dalla Fontana, G. (2009). Hillslope scale soil moisture variability in a steep alpine terrain. *Journal of Hydrology*, *364*(3–4), 311–327. https://doi.org/10.1016/j.jhydrol.2008.11.009

Pinheiro, E. A. R., Costa, C. A. G., & de Araujo, J. C. (2013). Effective root depth of the Caatinga biome. *Journal of Arid Environments*, *89*, 1–4. https://doi.org/10.1016/j.jaridenv.2012.10.003

Portillo-Quintero, C. A., & Sanchez-Azofeifa, G. A. (2010). Extent and conservation of tropical dry forests in the Americas. *Biological Conservation*, *143*(1), 144–155. https://doi.org/10.1016/j.biocon.2009.09.020

Potts, D. L., Scott, R. L., Bayram, S., & Carbonara, J. (2010). Woody plants modulate the temporal dynamics of soil moisture in a semi-arid mesquite savanna. *Ecohydrology*, *3*(1), 20–27. https://doi.org/10.1002/eco.91

Ribeiro, E. M. S., Arroyo-Rodriguez, V., Santos, B. A., Tabarelli, M., & Leal, I. R. (2015). Chronic anthropogenic disturbance drives the biological impoverishment of the Brazilian Caatinga vegetation. *Journal of Applied Ecology*, *52*(3), 611–620. https://doi.org/http://dx.doi.org/10.5061/dryad.m7d8m

Rodriguez-Iturbe, I., D'Odorico, P., Porporato, a., & Ridolfi, L. (1999). On the spatial and temporal links between vegetation, climate, and soil moisture. *Water Resources Research*, *35*(12), 3709–3722. https://doi.org/10.1029/1999WR900255

Salazar, A., Baldi, G., Hirota, M., Syktus, J., McAlpine, C., Salazar, A., … McAlpine, C. (2015). Land use and land cover change impacts on the regional climate of non-Amazonian South America: A review. *Global and Planetary Change*, *128*, 103–119. https://doi.org/10.1016/j.gloplacha.2015.02.009

Salemi, L. F., Groppo, J. D., Trevisan, R., de Moraes, J. M., de Barros Ferraz, S. F., Villani, J. P., … Martinelli, L. A. (2013). Land-use change in the Atlantic rainforest region: Consequences for the hydrology of small catchments. *Journal of Hydrology*, *499*, 100–109.

Schaap, M. G., Leij, F. J., & Van Genuchten, M. T. (2001). Rosetta: A computer program for estimating soil hydraulic parameters with hierarchical pedotransfer functions. *Journal of Hydrology*, *251*(3–4), 163–176. https://doi.org/10.1016/S0022-1694(01)00466-8

Seyfried, M. S., Schwinning, S., Walvoord, M. A., Pockman, W. T., Newman, B. D., Jackson, R. B., & Phillips, F. M. (2005). Ecohydrological Control of Deep Drainage in Arid and Semiarid Regions. *Ecology*, *86*(2), 277–287. https://doi.org/10.1890/03-0568

Sietz, D., Untied, B., Walkenhorst, O., Lüdeke, M. K. B., Mertins, G., Petschel-Held, G., & Schellnhuber, H. J. (2006). Smallholder agriculture in Northeast Brazil: assessing heterogeneous human-environmental dynamics. *Regional Environmental Change*, *6*(3), 132–146.

Silva, B. B. da, Wilcox, B. P., Silva, V. de P. R. da, Montenegro, S. M. G. L., & Oliveira, L. M. M. de. (2015). Changes to the energy budget and evapotranspiration following conversion of tropical savannas to agricultural lands in São Paulo State, Brazil. *Ecohydrology*, *8*(7), 1272–1283.

Sobrinho, M. S., Tabarelli, M., Machado, I. C., Sfair, J. C., Bruna, E. M., & Lopes, A. V. (2016). Land use, fallow period and the recovery of a Caatinga forest. *Biotropica*, *48*(5), 586–597. https://doi.org/10.1111/btp.12334

Tang, C., & Piechota, T. C. (2009). Spatial and temporal soil moisture and drought variability in the Upper Colorado River Basin. *Journal of Hydrology*, *379*(1–2), 122–135. https://doi.org/10.1016/j.jhydrol.2009.09.052

Teuling, A. J., Uijlenhoet, R., Hurkmans, R., Merlin, O., Panciera, R., Walker, J. P., & Troch, P. A. (2007). Dry-end surface soil moisture variability during NAFE'06. *Geophysical Research Letters*, *34*(17). https://doi.org/10.1029/2007GL031001

Teuling, A. J., & Troch, P. A. (2005). Improved understanding of soil moisture variability dynamics. *Geophysical Research Letters*, *32*(5), 1–4. https://doi.org/10.1029/2004GL021935

Tobella, A., Reese, H., Almaw, A., Bayala, J., Malmer, A., Laudon, H., & Ilstedt, U. (2014). The effect of trees on preferential flow and soil infiltrability in an agroforestry parkland in semiarid Burkina Faso A. *Water Resources Research*, *50*, 3342–3354. https://doi.org/10.1111/j.1752-1688.1969.tb04897.x

Tomasella, J., Silva, R. M., Vieira, P., Barbosa, A. A., Rodriguez, D. A., Oliveira, M. De, & Sestini, M. F. (2018). Desertification trends in the Northeast of Brazil over the period 2000 – 2016. *Int J Appl Earth Obs Geoinformation*, *73*(November 2017), 197–206. https://doi.org/10.1016/j.jag.2018.06.012

Torrence, C., & Compo, G. P. (1995). A Practical Guide to Wavelet Analysis. *Bulletin of the American Meteorological Society*.

United States Department of Agriculture. (1999). Soil taxonomy: A basic system of soil classification for making and interpreting soil surveys. USDA Washington, USA.

Ursulino, B. S., Montenegro, S. M. G. L., Coutinho, A. P., Coelho, V. H. R., Araújo, D. C. dos S., Gusmão, A. C. V., … Angulo-Jaramillo, R. (2019). Modelling soil water dynamics from soil hydraulic parameters estimated by an alternative method in a

tropical experimental basin. *Water (Switzerland)*, *11*(5), 4–6. https://doi.org/10.3390/w11051007

van Genuchten, M. Th. (1980). A closed-form equation for predicting the hydraulic conductivity of unsaturated soils. *Soil Science Society of America Journal*, *44*, 892–898. Retrieved from https://hwbdocuments.env.nm.gov/Los Alamos National Labs/TA 54/11569.pdf

Vargas, R., Collins, S. L., Thomey, M. L., Johnson, J. E., Brown, R. F., Natvig, D. O., & Friggens, M. T. (2012). Precipitation variability and fire influence the temporal dynamics of soil CO 2 efflux in an arid grassland. *Global Change Biology*, *18*(4), 1401–1411. https://doi.org/10.1111/j.1365-2486.2011.02628.x

Verrot, L., & Destouni, G. (2016). Data-model comparison of temporal variability in long-term time series of large-scale soil moisture. *Journal of Geophysical Research*, *121*(17), 10056–10073. https://doi.org/10.1002/2016JD025209

Villegas, J. C., Breshears, D. D., Zou, C. B., & Royer, P. D. (2010). Seasonally Pulsed Heterogeneity in Microclimate: Phenology and Cover Effects along Deciduous Grassland–Forest Continuum. *Vadose Zone Journal*, *9*(3), 537. https://doi.org/10.2136/vzj2009.0032

Wilson, D. J., Western, A. W., & Grayson, R. B. (2004). Identifying and quantifying sources of variability in temporal and spatial soil moisture observations. *Water Resources Research*, *40*(2), W025071–W02507110. https://doi.org/10.1029/2003WR002306

Wu, W., Geller, M. A., & Dickinson, R. E. (2002). The Response of Soil Moisture to Long-Term Variability of Precipitation. *Journal of Hydrometeorology*, *3*(5), 604–613. https://doi.org/10.1175/1525-7541(2002)003<0604:trosmt>2.0.co;2

Zhang, Z., & Moore, J. C. (2011). Improved significance testing of wavelet power spectrum near data boundaries as applied to polar research. *Advances in Polar Science*, *22*(3), 192–198. https://doi.org/10.3724/SP.J.1085.2011.00192

Zou, C. B., Barnes, P. W., Archer, S., & McMurtry, C. R. (2005). Soil moisture redistribution as a mechanism of facilitation in savanna tree–shrub clusters. *Oecologia*, *145*(1), 32–40.

Zou, C., Turton, D., & Will, R. (2014). Alteration of hydrological processes and streamflow with juniper (Juniperus virginiana) encroachment in a mesic grassland catchment. *Hydrological Processes*, *6182*(December 2013), 6173–6182. https://doi.org/10.1002/hyp

III PLANT WATER USE STRATEGIES DIVERGE ALONG PLANT FUNCTIONAL TYPES IN THE CAATINGA DRY FOREST

Introduction

Seasonally dry tropical dry forests (SDTFs) are understudied (Azofeifa et al. 2005) despite being model biomes for advancing eco-hydrological understanding (Mendez-Alonzo et al. 2012; Wright et al. 2017). Mean annual rainfall is relatively low for the tropics, ranging from 1,600 to 2,000 mm / year with four to seven months of severe water shortages and drought-deciduous forests (Bullock et al., 1995; Dirzo et al., 2011; Janzen, 1988). This high rainfall seasonality (Feng et al. 2013) means that vegetation must balance trade-offs between acquisitive and conservative strategies or between carbon gain and water conservation (Pineda-Garcia et al. 2013; Scwhinning and Ehleringer 2001) under alternating periods of abundance and stress. Moreover, SDTF have a relatively high biodiversity, meaning that tree species employ a range of water use and conservation strategies which allows for successful establishment and coexistence, particularly in the late successional stages (Esquivel-Muelbert et al. 2017; Lebrija-Trejos et al. 2010; Lohbeck et al. 2013; Pineda-Garcia et al. 2015). Although SDTFs are amongst the biomes most prone to hydraulic failure and drought-induced mortality (Allen et al. 2010), few studies have documented ecophysiological responses over a wide range of species. Hence, our understanding of how these species either tolerate or avoid drought in these biomes remains limited.

Central to understanding tree adaptations and responses to water-stress and drought is the characterization of plant form and function. Yet, tropical biomes are complex and

hyper-diverse. Compared to other semiarid systems, this is true even for the dry tropics (Pennington et al. 2009). Functional type classification schemes are intended to simplify this complexity by grouping species based on similar responses to specific environmental conditions or disturbances. Thus, the utility of identifying functional types, if indeed they exist, is their extrapolative and predictive power.

Classifying plant function types usually means observing functional traits, or plant features which reflect ecological strategies and responses. Generally, leaf and wood traits are thought to be coordinated into so-called economic spectra, reflecting the trade-offs associated with the allocation of a limited resources for one purpose vs. another and defining the boundaries within which trees function (Chave et al. 2009; Diaz et al. 2016; Reich 2014; Wright et al. 2004). In SDTFs, studies show a clear coordination between wood density and phenology and thus, these traits have been used to define functional types (Borchert 1994; Lima and Rodal 2010; Lima et al. 2012, Oliveira et al. 2013) and predict resource acquisition and conservation strategies (Mendez-Alonzo et al. 2012).

Wood density is a central trait because it encompasses many aspects of a tree's physiological and ecological function. Wood density is related to structural integrity and is associated with hydraulic function, carbon allocation, and growth and mortality. Wood anatomy and hydraulic function are inter-related, where xylem fibers provide much of the structural support (Martinez-Cabrera et al. 2009) and vessels represent the water transport conduits. In the dry tropics, wood density has been negatively correlated with stem hydraulic conductance (Markesteijn et al. 2011) stomatal conductance, and daily transpiration (Bucci et al. 2004; Worbes et al. 2013). Thus, high wood density generally

means greater mechanical support, but also smaller vessel diameter and sometimes higher vessel density (Gelder et al. 2006; Hacke et al. 2001; Preston et al. 2006;).

For SDTF in particular, of the low wood density trees occur as stem succulents (Avila-Lovera and Ezcurra 2016). These tree forms have significantly larger vessel areas and greater stem water storage capacity than co-existing non-succulent trees (Borchet 1994; Lima et al. 2012; Pratt and Jacobsen 2017; Worbes et al. 2013). Larger vessel areas indicate a greater water transport capacity, i.e. stem hydraulic conductivity (Chave et al. 2009; Zanne et al. 2010). Stem succulents have also been shown to have a low tolerance of very negative leaf water potentials, pronounced midday drops in stomatal conductance, and an early onset of leaf fall (Butz et al. 2016; Lima et al. 2012; Pineda-Garcia et al. 2015; Worbes et al 2013). A low tolerance of very negative leaf water potentials equates to a low resistance to cavitation, which is more a function of xylem mechanical strength than it is vessel area or wood density itself (Jacobsen et al. 2005; Lachenbruch and McCulloh 2014; Venturas et al. 2017). Generally, less negative midday leaf water potential indicates a low tolerance of drought (Hacke et al. 2001; Markesteijn et al. 2011; Pratt and Jacobsen 2017;). However, high stem water storage could be important for buffering changes in xylem pressure (Meinzer et al. 2009) and therefore leaf water potentials, meaning that stem succulents have developed a highly specialized by little-regarded water use strategy (Worbes et al. 2013).

On the contrary, it follows that in SDTF high wood density trees would be expected to have smaller vessel areas with reduced stem hydraulic conductivity, increased resistance to cavitation and embolism, thereby withstanding more negative leaf water potentials, are would be associated with greater drought tolerance, and late shedding of leaves. This

suggests that in SDTF, wood density could be a useful predictor of hydraulic function. As predicted by "safety vs. efficiency" tradeoffs, a large water transport capacity and a low tolerance to drought means that low wood density trees, including stem succulents, will also have a higher rate of carbon gain and growth rate at least during active periods (Pineda-Garcia et al. 2015; King et al. 2006). For these reasons low wood density trees have often been associate with rapid resource acquisition strategies and high wood density trees have been associated with conservative resource acquisition strategies (Pineda-Garcia et al. 2015).

In relation to leaf traits, high wood density trees generally have lower specific leaf area and greater leaf density (Bucci et al. 2004; Wilson et al. 1999). High wood density trees are also more tolerant to competition and exert a strong competitive effect; low wood density trees are less competitive (Kunstler et al. 2016). Still, high wood density trees generally have, and are associated with greater construction costs and slower growth rates than low wood density species (Kunstler et al. 2016; Poorter et al. 2008; Reich 2014). Wood density is also a highly conservative trait and to some degree reflects evolutionary history; although there is strong variation within the Fabaceae family (Swenson and Enquist 2007).

Besides being an apparent and defining feature of SDTFs, phenological patterns reflect ecophysiological functioning and water use and access (Markesteijn et al. 2010; Mendez-Alonzo et al. 2012; Schotz et al. 2014; Valdez-Hernández et al. 2010). In particular, leaf fall is a common drought-avoidance strategy. Some modeling studies suggest that it is phenology rather than physiological traits which is the dominant control on plant-water-carbon interactions (Vico et al. 2017). Still, we know very little regarding

the mechanisms which allow these species to display difference in the timing of leaf flush and fall despites under the same abiotic stresses. That is, there is still substantial variation in leaf flush, fall, bud break, and fruiting amongst species in SDTF (Machado et al. 1997). These offsets suggest that trees have different strategies for conserving water that allows for temporal partitioning of water use and phenological activity (Lasky et al. 2016). Additionally, the presence of evergreen species ecosystems indicates that these species are either accessing stable deeper water sources or that these species are highly specialized and efficient drought-avoiders compared to less drought-tolerant deciduous species (Hasselquist et al. 2010; Jackson et al. 1995). Studies based on more detailed leaf traits data, though, has little predictive power in SDTFs (Powers and Tiffin 2010).

Objective

Previous research has revealed classification schemes of plant types based on coordinated wood and leaf functional traits. Whether these traits actually manifest in unique defining functions has not be directly tested. More specifically, we do not know if PFTs defined by wood density and phenology can be used to predict water use strategies. If wood density can be used as a proxy for hydraulic transport and storage, and if deciduousness can be used as an indicator of drought-stress avoidance, then it would follow that PFTs defined by these traits would also results in unique and diverge hydraulic function. That is, the variations in wood density and phenological pattern for these co-existing species indicates that they experience and cope with the same water stress conditions in very different way. On this basis, we aim to assess whether or not we can use PFTs to predict water use strategies.

Methods

Site Description

The study area is part of the Caatinga, a seasonally dry tropical forest and shrubland biome in northeast Brazil. The forest is tropical drought-deciduous, and the climate is tropical hot and dry (BShw Koppen classification) with a strong precipitation seasonality (D'Odorico and Bhattachan 2012). Mean annual precipitation is 733 mm and potential evapotranspiration is about 2,000 mm / year. The rainy season typically occurs from December to May, and accounts for about 75 % of annual rainfall; although, interannual trends are erratic and unpredictable. Average monthly air temperatures range from 21 to 26 °C, with maximum temperatures of 31 °C and minimum temperatures of 17 °C (Griessen 2006; New LocClim 1.10).

This study was conducted within a relatively old (50+years) Caatinga forest stand located near the municipality of Serra Talhada, PE, on the Fazenda de Buenos Aires (07°56'50" S and 38°23'29" W, 450 m elevation; see Figure III-1.) in northeast Brazil. The area is rather unique in that few intact and contiguous stands of this size remain (Antongiovanni et al. 2018). The understory is composed of a thick herbaceous that quickly dies off during the dry season. The forested area forms part of a large multiple-use area with portions of pasture and other forest stands of varying age.

Entisol Orthent and Aridsol Argid (USDA 1999) are the predominant soils in the study areas. During the dry season, the clayey soils at 40 to 50 cm depth become compacted and hard. The forest stand is subject to light grazing by free-roaming cattle. The study plot is an area of about 90 m x 90 m. The rich diversity of tree species and

morphologies in the Caatinga dry forest make it ideal biome to document a range of plant traits under water-limited conditions.

Ancillary Data

Hydrometeorology is continuously monitored at this site by the National Observatory of Water and Carbon Dynamics in the Caatinga project (ONDACBC; https://ondacbc.eco.br/). This includes rainfall (mm; TE 525 WS-L, Texas Electronics, USA), air temperature (°C) (model HMP45C, Vaisala, Campbell Scientific Inc., Logan, UT, USA). Soil moisture was also monitored within the study plot at five depths of 5 cm, 10 cm, 20 cm, 35 cm, 50 cm (5TM, Decagon Devices, Inc., Pullman, WA). Raw soil moisture readings were corrected for temperature and scaled by minimum residual and maximum saturation values described by measure soil textural properties (Table III-1).

Species selection

We selected sixteen dominant Caatinga forest species classified into three plant functional types based on wood density and phenology (Lima et al. 2012). The **deciduous low wood density, DLWD,** species include *Amburana cearensis, Commiphora leptophloeos, Jatropha mollissima, Manihot epruinosa, Pseudobombax marginatum,* and *Spondias tuberos.* The **evergreen high wood density, EV,** species including *Cynophalla flexuosa* and *Ziziphus joazeiro*. The **deciduous high wood density, DHWD,** species including *Anadenanthera colubrine, Aspidosperma pyrifolium, Bauhinia cheilantha, Cenostigma pyramidale, Croton blanchetianus, Enterolobium species, Myracrodruon urundeuva,* and *Piptadenia stipulacea.* These species are also representative of SDTF in general (Pereira et al. 2003; Sarkinen et al. 2011). A brief description of each species, based on Lorenzi 2008,

2016a, 2016b and Maia 2012, and field observations, is given below and is summarized in Tables III-2 and III-3

Description of the DLWD species

All of the DLWD species we measured are also considered stem-succulent tree species.

Spondias tuberosa This species, commonly known as umbuzeiro, is endemic to the Caatinga and is also one of the most symbolic species of northeast Brail. Most distinctly, this species has large, spongy root tuber that can reach 20 cm in diameter and up to 4 kg in weight as it accumulates water and nutrients. The tubers as well as the fruit, are edible and sweet; the roots can be dried and used as a flour; and young leaves can be eaten directly. Even for cleared forests, this species was often spared because of its utility. It is a short tree, about 4-7 m tall, with a thick trunk that can reach 10 m in diameter, with convoluted branches. This species has a thicker grey bark. The canopy is concave, forming a natural shelter for people and cattle. Leaf flush occurs immediately after the first rains, flowering and fruiting during the rainy season, and leaf fall is characterized by leaf color change to yellow, orange and pink. This species is recommended for reforestation because it is considered to survive long droughts and can create a more favorable micro-climate through shading and moisture capture.

Amburana cearensis, umburana de cheiro, is native to Argentina, Bolivia, Paraguay, Peru and Brazil, and is known for its sweet vanilla-like smell arising from high coumarin content and its bark has medical properties; another common name is cumaru. Other uses include wood, coal, forage, bee nectar during the dry season, and ornamental purposes. This species develops a thick root tuber for water and nutrient storage which

helps the tree survive the dry season. As observed in the field, it quickly loses all leaf cover during the early dry season, and flowering and fruiting shortly follow. The leaves are smooth and may change to a yellow or yellowish red color before falling. The yellowish-red stem trunk has smooth bark which peels into fine transparent paper-like layers.

Commiphora leptophloeos, or umburana de cambão, is similar in that the bark also peels into fine layers and often has a green, likely photosynthetic trunk. This species tends flowers before the rainy season begins, and leaf flush begins in the early part of the rainy season. The leaves are pubescent. The tree height ranges from 6 to 9 m. This species has a deep history of cultural significance in northeast Brazil. Its uses included wood, coal, medicinal properties, edible fruits and is used as an ornamental tree. Often, hollows form in the trunk, which are utilized by bees. This species is recommended for reforestation and restoration and can be used as a natural barrier or live fence. It is called *umbu-rana* because it is considered the "false" umbu. This species is characteristic of the Caatinga but can also be found in the Patanal or Chaco.

Jatropha mollissima, or pinhão-bravo, is endemic to the Caatinga. Like some of the other species, it is characterized by bark with peels into fine paper-like layers, revealing a green, likely photosynthetic bark. Also characteristic to this species is the large, pubescent leaves which quickly wilt and fall at the start of the dry season. Other similar *Jatropha* species can be found in semiarid forests and shrublands. Because this species flowers during the late dry season, it is an important source of pollen for bees. It is a small, stem succulent shrub/tree. Further, it has a history of medicinal uses, including the treatment of wounds, hemorrhage and inflammation.

Manihot epruinosa, or maniçoba, is a wild cassava species native to the Caatinga. It has a succulent dark-colored trunk, large glabrous leaves, and starchy root tubers which store water and nutrients (Matos et al. 2005).

Pseudobombax marginatum, or embiratanha, has a distinct green, likely photosynthetic trunk that is either smooth or wrinkly. The leaves, which are large and leathery leaves, fall during the late rainy season to early dry season. As its common name indicates, the wood fibers can be used to create strong cords. The large swollen taproot is edible and may store water and nutrients especially when young. Flowering is usually in the early dry season, with large white flowers that open at dusk and close at dawn, possibly attracting moths and birds at night. It is characteristic of the Caatinga but occurs throughout Brazil, Bolivia, Paraguay, and Peru.

Description of the EV high wood density species

Cynophalla flexuosa, or feijão bravo, is a woody species that occurs in shrub or liana form. This species reaches up to 6 m height and the diameter is relatively small, 12 to 15 cm when in liana form. The leaves are small, thick, and leathery, 4 to 10 cm length and 1 to 5 cm width. This species is found as far north as Mexico and Florida, throughout Central America and Brazil. It is recommended for reforestation and tolerates salinized soils

Ziziphus joazeiro or joaziero, is another endemic and emblematic species of the Caatinga drylands. Historically, this species was often preserved during clear-cutting, and is easily distinguished during the dry season as its green canopy dots the landscape. It is one of the few species with edible fruits and provides shade for people and cattle year-round. It has broad far-reach roots and is thought to be deeply rooted, relying on deeper, more stable water sources. When in tree form, it is multi-stemmed with a broad canopy. In

the study plot, this species appeared in shrub from, which may indicate that deeper water sources are absent. It is an important source of pollen and nectar during the dry season.

Description of the DHWD species

Anadenanthera colubrina, or angico, is found through the Caatinga, as well as the Patanal and Atlantic rainforest. The bark is distinct in that it has thick horn-like protuberances or spines. It is a taller tree, reaching up to 15 m in the Caatinga. The canopy is sparse, the leaves are bipinnately compound and often close during very dry conditions. This species has several woody root tubers which are usually lost and replaced by more developed lateral roots as it matures. It is an adaptable and fast-growing species. Leaf fall begins at the start of the dry season and leaf flush begins before or after the first rains.

Aspidosperma pyrifolium, or periero, is endemic to the Caatinga. This species generally flushes at the start of the rainy season and loses leaves during the dry season. Flowering occurs after leaf fall and before leaf flush, i.e. before the start of the rains. This species is known to grow in harsh dry conditions but can also tolerate some level of flooding and water-saturated soils. It is a good lumber source, has medicinal properties, provides pollen and nectar for bees during the dry season, and is recommended for reforestation, particularly for areas suffering from desertification. Even so, this species is considered threatened.

Bauhinia cheilantha is locally known as mororó or pata-de-vaca because of the shape of its leaves resembles a cow's hoof; it is also a good forage resource. This species can occur in shrub or liana form, with a small diameter of 8-10 cm. Flushing occurs after the full rains and full canopy cover is reach in 5 to 6 weeks. Leaf fall occurs in the dry

season. The radial roots help protect soil against erosion and the species is recommend for reforestation. The wood is often used for fencing, firewood or coal, and the bark has medicinal properties.

Cenostigma pyramidale (botanical synonymy *Caesalpinia* or *Poincianella pyramidalis* Tul*)* or catinguiera, is endemic to and widely distributed across the Caatinga. It is usually 4 to 6 m height but can reach up to 12 m in favorable conditions. The canopy is generally sparse and/or irregular. It is characterized by a distinct unpleasant smell and is adapted to various conditions. It is thought to have deep roots. The trunk can be straight or twisted. It is often used as a source of wood for construction or coal, as forage, and has medical properties. This species is also recommended for reforestation and agroforestry.

Croton blanchetianus, or marmeleiro, can occur in shrub or liana form. The leaves are simple, pubescent, and can be burned to use the smoke as a mosquito repellant. Flushing occurs vigorously with the first rains, immediately followed by flowering and fruiting. Leaf fall occurs at the start of the dry season. The roots are laterally spread. The species is common in semiarid biomes, including most of the Caatinga. The wood can be used to build fences or small materials, the bark is medicinal, the leaves serve as forage, and this species is also recommended for reforestation.

There is limited information regarding the occurrence of *Enterolobium species.* or tamboril, in the Caatinga. While the individuals were not identified to the species level, they are believed to be *E. maximum* Ducke or *E. contortisiliquum* (Vell.) Morong because of the shape of the leaves, trunk, and possible occurrence of seed pod known as orelha de macaco or monkey's ear. This species is similar in appearance to *C. pyramidale*, but at this

site was higher in the canopy with a more erect trunk and white flowers. Leaf flush was observed during the rainy season and leaf fall into the dry season.

Myracrodruon urundeuva, or aroeira, is found across the Caatinga and Cerrado, as well as more humid biomes such as the Atlantic rainforest and Patanal. The common name of this species indicates that it is "a bird's home" possibly because it reaches up to 20 m in the Caatinga. As described in Maia (2012), when young, the main root takes on a tuber-like form which is thought to serve as a reserve for food and nutrients.

Piptadenia stipulacea, or jurema-branca, is endemic to the Caatinga. This species is characterized by binpinnately compound leaves, thorn-covered stems, and a light grey colored trunk (to differentiate from close cousin *Mimosa tenuiflora* (Willd.) Poir. or jurema-preta which has a dark brownish-black colored trunk). Leaf flush and flowering occurring during the wet season. This species is a nitrogen-fixing legume and is recommended for reforestation. Additional uses are wood for construction or coal, forage for livestock, and its yellow flowers pollen for bees.

Other species found near the study site, but which were not measured, include *Schinopsis brasiliensis* Engl. or baraúna; *Ceiba glaziovii* (Kuntze) K. Schum or barriguda, *Cnidoscolus quercifolius* Pohl or faveleira, *Mimosa tenuiflora* (Willd.) Pior or jurema-branca, and *Combretum leprosum* Mart or mofumbo. At the stand-level, the canopy closed at the peak of the wet season, then gradually opened up as the dry season progressed; the canopy was almost completely open by mid-dry season.

Data Collection

We examined water use strategy with regards to deciduousness and tolerance to water stress, water access and rooting depths, and water use efficiency. Tolerance to water stress

was measured via pre-dawn and mid-day leaf water potential, Ψ_{PD} and Ψ_{MD}, water access was measured via water isotope tracers, δ^2H and $\delta^{18}O$, and water use efficiency was measured via $\delta^{13}C$. Data was collected during the wettest month of the rainy season until middle of the dry season (Figure III-2) and followed Pérez-Harguindeguy et al. (2013).

Leaf measurements

Our measure of tolerance to water stress is based on pre-dawn and mid-day leaf water potential, Ψ_{PD} and Ψ_{MD}. Leaf water potential is an indicator of leaf hydration and is related, in part, to stomatal closure. The more negative the value, the more dehydrated the leaf—conditions we would expect when VPD is high. Comparing pre-dawn and mid-day leaf water potentials indicates the degree of stomatal closure that species may experience as a response to water stress, since temperatures and VPD usually max out in the afternoon.

We measured leaf water potentials from April 11 to August 22, 2018 on a bi-weekly basis, or as long as the individual had leaf cover. Measurements were made with a Scholander pressure chamber (Model 1505D PMS Instrument Company, Albany, OR) which uses tanks of nitrogen gas within a closed system to apply pressure. Pre-dawn leaves (4:30 to 6:00 AM) and mid-day (11:30-1:00 PM) leaves were clipped, bagged, and kept in a cooler with ice, and immediately measured in-situ. The pressure in the nitrogen tanks was sufficient to make most measurements (665 total leaves), with the exception of one measurement, at which point the pressure in the nitrogen tanks (5.8 MPa) was not high enough. Because the pressure in the nitrogen tanks slowly declines as measurements progress, we prioritized the species which we expected to have more negative pressure

potentials. The maximum pressure we measured was for *C. pyramidale* at 7.5 MPa on July 21, 2018.

Our measure of plant water use efficiency is based on stable isotopes of carbon, foliar $\delta^{13}C$. Water use efficiency is the ratio between the gain of CO2 or biomass in photosynthesis to the loss of water through transpiration. Different species can exhibit a wide range of carbon gain to a unit of water. Some species are expected to be more water-efficient, that is having greater C gain or biomass growth for the same amount of water than less water-efficient species. How water efficient a tree is can be reflected in foliar $\delta^{13}C$ because photosynthetic enzymes more readily use the lighter ^{12}C isotope relative to the heavier ^{13}C isotope. The extent of this discrimination over longer time scales (i.e. not instantaneous) will depend on the mole fraction of CO2 in the substomatal cavity, and thus on stomatal regulation. We measured foliar $\delta^{13}C$ for leaves collected is from April 28 to August 22, 2018 on a bi-weekly basis, or as long as the individual had leaf cover.

After leaf water potential field measurements, the leaves were re-bagged and subsequently oven-dried at 75 to 80 °C for at least 48 hours. The leaves were transported to the Stable Isotopes for Biosphere Science (SIBS) Laboratory at Texas A&M University, College Station for grinding, weighing and packing. Once packed, the samples were analyzed for foliar carbon content and $\delta^{13}C$ using an Elemental Analyzer (Costech Analytical Technologies, Valencia, CA, USA) coupled to a Thermo Scientific Delta V Isotope Ratio Mass Spectrometer (EA-IRMS; Thermo Fisher Scientific, Waltham, MA, USA). Stable isotope ratios are expressed in delta notation ($\boldsymbol{\delta}$) as the ratio of the sample (R_{sample}) relative to the standard ($R_{standard}$) as follows:

$$\boldsymbol{\delta}\,(‰) = (R_{sample}/R_{standard} - 1) * 1000 \qquad \text{Equation III-1}$$

Calibration for $\delta^{13}C$ was performed using certified standards, USGS (United States Geological Survey) Glutamic Acid 40 ($\delta^{13}C$ = –26.39 ‰) and Glutamic Acid 41 ($\delta\ ^{13}C$ = 37.63 ‰). Quality control is performed using in-house plant standards ($\delta^{13}C$ = –12.78 ‰ and $\delta^{13}C$= –39.88 ‰).

Stem measurements

Our measure of plant water source is based on naturally occurring stable isotopes of water, δ^2H and $\delta^{18}O$, in stems, soils, and precipitation. δ^2H and $\delta^{18}O$ can serve as tracers if δ^2H and $\delta^{18}O$ can be characterized for the possible water sources. In this case, we relied on a gradient of δ^2H and $\delta^{18}O$ ratios across soil layers, which occurs when the near surface soils become evaporatively enriched in the heavier isotopes, ^2H and ^{18}O. The δ^2H and $\delta^{18}O$ ratios are then compared to the δ^2H and $\delta^{18}O$ of stems for a relative understanding of "shallow" for "deeper" soil water sources. Soil and stem samples for δ^2H and $\delta^{18}O$ were collected on April 10, 2018 to represent wet conditions, June 12, 2018 to represent dry conditions, and an additional collection of the EV group only on September 19, 2018 since the EV species *Cynophalla flexuosa and Ziziphus joazeiro* maintained leaf cover during the dry season.

Soil and stem samples were collected for analysis of stable isotopes of water. Soils were collected from seven pits within the study plot, at three integrated depths: 5-15 cm, 20-30 cm, and 40-50 cm. During dry conditions, it became increasing difficult to collect soil samples from the 40-50 cm depth. As the clay content was usually higher at these depths, dry soils shrank and became compact and hard. Soil for each depth interval was

placed into a plastic bag, homogenized, and subsampled into 12ml glass vials with PolyCone-lined phenolic caps sealed with parafilm. The vials were immediately stored in a cooler with ice. Two to three stems were cut for each individual tree. The bark was left on (to avoid the influence of evaporation that would occur if the bark was stripped in-situ in arid conditions) and the stems were subsampled into two vials per tree. Again, vials were immediately stored in a cooler with ice.

Rainwater and through fall samples were collected approximately bi-weekly from January 2018 until the last rain event of the season, on June 2018. The next rain event was not until December 2018, the start of the next rainy season, meaning that we the isotopic signatures of rainfall were captured for one full wet season. Rainwater was collected at one point above the canopy, and throughfall was collected at three to four points beneath the canopy. Water collectors were wrapped with aluminum foil and a layer of paraffin oil used poured inside to reduce evaporation (IAEA 2014). Other water samples were opportunistically collected on August 11. These include groundwater and surface water samples from the surrounding area. These water samples were not included in the meteoritic water line but were not significantly different from it. Precipitation samples with debris were filtered (0.2 μm) to remove particles.

All soil and stem samples were kept frozen, and rainwater was kept cold, until they were transported in a cooler with ice packs to the SIBS Laboratory at Texas A&M University, College Station. In the lab, water was extracted from stems and soils via cryogenic vacuum distillation (West et al. 2006). One side of the vacuum line containing the sample was kept in a water bath of boiling water (100 °C). Extractions generally lasted 2.5 - 3 hours for stems and 3 or more hours for soils. The extraction was considered

complete when no more water condensed, and no more water vapor could be seen on the liquid nitrogen side of the line.

All water samples were analyzed using a High Temperature Conversion/ Elemental Analyzer coupled to a Delta V Advantage Isotope Ratio Mass Spectrometer (TC/EA-IRMS). Stable hydrogen isotopic composition is expressed in delta notation ($\boldsymbol{\delta}$; see above). Calibration was performed using in-house water standards: SIBS-wA ($\delta^2H = -390.8 \pm 1.6$ ‰, $\delta^{18}O = -50.09 \pm 0.33$ ‰) and SIBS-wP ($\delta^2H = -34.1 \pm 1.9$ ‰, $\delta^{18}O = -4.60 \pm 0.24$ ‰). Quality control was performed using an in-house water standard, SIBS-wU ($\delta^2H = -120.2 \pm 1.5$ ‰, $\delta^{18}O = -15.95 \pm 0.27$ ‰). These in-house standards were calibrated using IAEA standards (VSMOW2, SLAP, and GISP). All water isotope values are reported in VSMOW-SLAP scale.

To describe the tree species according to their functional groups, we measured stem-specific wood density. Specific stem wood density was measured for three individuals per species outside of the study plot, except for *Cynophalla flexuosa* and *Enterolobium species*. We found only two individuals of *C. flexuosa* outside of the study plot. For the *Enterolobium species*, we could not find an individual outside the plot and thus sampled only one individual found within the plot. Branches were cut in the field and processed in the lab. In the lab, the branches were cut into approximately cylindrical 2-3 cm pieces, stripped of bark and submerged in water for at least 2 days, until saturated. The saturated stem left to sit so that excess water would drain off and then weighted for saturated mass. Then, the sample was submerged in graduated cylinder filled with distilled water on a mass balance. The cylinder with water was tared before the sample was submerged. A needle was used to submerge the sample without touching the walls or

bottom of the cylinder. Thus, the mass reading on the balance equals the volume of the sample (because water density is ~1g/cm3). The wood sample were then oven-dried at 105 °C for at least 72 hours and re-weighted for dried mass to calculated wood density (Table III-2).

Statistical Analysis

Our question is, do PFTs predict plant water use strategies? To test for this across time, we conducted repeated measures ANOVA using linear mixed-effects modeling in the R package nlme (Pinheiro et al. 2019). The response traits we modeled were$\Psi_{MD\text{-}PD}$, Ψ_{MD}, Ψ_{PD}, stem δ^2H, stem $\delta^{18}O$, and foliar $\delta^{13}C$. To test for significance, we applied Tukey's post-hoc for linear mixed models using the R package multcomp (Hothorn et al. 2008). First, we modeled PFTs as the fixed effects factor and date and species as the random effects factor (i.e. repeated measures). Species was included as a random effect to account for the random selection of species that pertains to each PFT (we could have selected other representative species). Second, we split the data into three groups to test species association to each PFT. Within each PFT, we modeled species as a fixed effects factor and date as the random effects factor. For all models, we confirmed homogeneity in the variance of the residuals.

Results

General hydroclimate

The start of the rainy season was observed with the first large event pulses on December 24, 2017 (24 mm registered in Serra Talhada city and 10 mm registered nearest the field

site at the Cachoeira weir, http://www.apac.pe.gov.br). Based on rainfall data for 2018, we defined the end of the rainy season as the end of April. April was the wettest month of 2018, with a total rainfall of 230 mm. By May, total monthly rainfall dropped to 15 mm. Average monthly temperature increased from 24.6 °C in April to 25.7 °C in August; the minimum average daily temperature recorded was 22.8 °C and the maximum average daily temperature was 27.8 °C. Soil volumetric water content responded to rainfall, peaking in April and decreasing to lows during the dry season (Figure III-3). Our measurements were conducted from April 10 to August 22, 2018. The "wet" period collection of stems and soils for stable isotope analysis occurred the day after a large rain, registered as a 77 mm event; the "dry" period collection occurred after 40 days without any rain events larger than 5 mm; the second "dry" was a collection for the EV species, which were the only trees with noticeable canopy cover.

Plant functional type trends

Plant functional type Ψ_{PD} and Ψ_{MD}

Leaf water potential varied significantly by PFT. First, there were significant differences in Ψ_{MD} between the three PFTs (Table III-4). Similarly, there were also significant differences in the change in leaf water potential, $\Psi_{MD\text{-}PD,}$ between the three groups. The smallest change occurred for the DLWD (CI_{lower} = -0.88 and CI_{upper} = 0.35), followed by the DLWD (CI_{lower} = -1.14 and CI_{upper} = -0.66) and then the EV groups (CI_{lower} = -2.46 and CI_{upper} = -0.92). In terms of Ψ_{PD}, only the DLWD group differed significantly; there was no difference between the high wood density groups DHWD and EV. The Ψ_{PD} was generally less negative for the DLWD group. Over time, the DLWD group exhibited more stable

Ψ_{PD} and Ψ_{MD} values that were less than -1 MPa, whereas as the DHWD and EV groups because increasingly negative. For example, Ψ_{MD} values for DHWD began just above an average of -1 MPa in April and reached and average of almost -5 MPa in July. For EV, Ψ_{MD} values began at less than an average of -1 MPa in April and reached just below -4 MPa in July. The Ψ_{MD} values for the DLWD group remained below -1 MPa (Figure III-4).

Plant functional type $\delta^{18}O$ and $\delta^{2}H$ stem water ratios

Stem water isotope ratios ($\delta^{2}H$ - $\delta^{18}O$) are shown in Figure III-5 for April 10 and June 12, to represent wet and dry conditions respectively; regression lines are listed in Table III-5. Precipitation collected above and below the canopy were not significantly different ($\delta^{18}O$ Wilcoxon test p-value = 0.49; $\delta^{2}H$ unpaired t-test p-value = 0.92; Table III-6) and were used to plot the local meteoritic water line, LMWL (Dansgaard 1964; Kendall and McDonnell 1998). The soil water samples collected on April 10 plot on or slightly below the LMWL. The soils were very wet when collected and therefore reflect values similar to rainwater. Regardless of PFT, stem waters plot below both the rainwater and soil water lines, indicating that plant water sources are likely a mixture of waters not derived solely the recent rain event. The DLWD group plots above the DHWD and EV, that is, the $\delta^{2}H$ and $\delta^{18}O$ ratios are more positive. Although, this difference is only significant between DLWD and DHWD groups according to $\delta^{2}H$ values (Tukey's p-value=0.0074 for DLWD vs DWHD; Table III-6).

The soil samples collected on Jun. 12 during the dry season plot further away from the LMWL with more positive $\delta^{2}H$ and $\delta^{18}O$ ratios. These forms the evaporation line which is due to enrichment of heavy isotopes caused by fractionation during evaporation (Sprenger et al. 2016). The stem water for the DLWD group plots between the LMWL and

the soil water samples, which defines the boundary conditions for this group. The DHWD and EV regression lines overlap with each other but fall below the DLWD group. This means that relative to DLWD, the two high wood density groups are depleted in in heavy $\delta^{18}O$ and $\delta^{2}H$, i.e. lighter $\delta^{18}O$ and $\delta^{2}H$. This difference between low and high wood density groups in significant according to $\delta^{2}H$ ratios (Tukey's p-value<$1e^{-4}$ for DLWD vs. EV and for DLWD vs. DHWD; Table III-6)

Plant functional type foliar $\delta^{13}C$

Average foliar $\delta^{13}C$ varied significantly by PFT (Figure III-6; Table III-7). For the DLWD type, foliar $\delta^{13}C$ decreases over time, from an average of -28.4 ‰ to -29.3 ‰ $\delta^{13}C$ and was significantly different from the two high wood density PFTs (Tukey's p-value = 0.0476 vs. DHWD and was <0.001 vs. EV; Table III-7). The EV group on the other hand remained relatively stable over time, with the average foliar $\delta^{13}C$ just below -27.0 ‰. The DHWD group generally increased from initial values near -28.5 ‰ similar to the DLWD to values more similar to the EV, -27.7 ‰, but was still significantly different from both of those groups (Tukey's p-value = 0.0476 vs. DLWD and 0.0434 vs. EV; Table III-7).

Species-level trends

Species-level Ψ_{PD} and Ψ_{MD}

To better understand whether PFTs are a good predictor of plant water use strategies, we examined variations within PFTs by looking at species-level trends. Species-level Ψ_{PD} and Ψ_{MD} over time are shown in Figure III-7. To avoid water loss, many of the DLWD species quickly lost all leaf cover as the dry season progressed. The exceptions to this trend are the DLWD species *Commiphora leptophloeos* and *Spondias tuberosa.* These two DLWD species also maintained less negative pre-dawn to mid-day Ψ_{leaf}.

The species for both the EV and DHWD groups had similar trends; and the DHWD species generally maintained leaves for longer. Most species in these two groups experienced gradually more negative Ψ_{PD} and Ψ_{MD} as the dry season progressed. *Aspidosperma pyrifolium* and *Croton blanchetianus,* on the other hand, had relatively stable Ψ_{PD} and Ψ_{MD} from April to June, but then changed more abruptly and lost all leaf cover soon after. For *A. pyrifolium,* Ψ_{PD} and Ψ_{MD} remained at ~1.5 to -2 MPa before dropping to -3 MPa in July and ~5 MPa in August. For *C. blanchetianus*, Ψ_{PD} and Ψ_{MD} remained close to -1 MPa but for June 9 and July 7, Ψ_{MD} was much more negative, at approximately -2 MPa and -5 MPa respectively. Patterns for *Myracrodruon. urundeuva* were more similar to that of DLWD group, remaining less negative and stable through the dry season.

Species-level stem water $\delta^{18}O$ and $\delta^{2}H$ ratios

For most species regardless of PFT, there was general shift towards heavy-enriched $\delta^{18}O$ into the dry season (Figure III-8). Still, this shift was more apparent within the DLWD species, and strongest for the species with large leaf areas, like *Jatropha mollissima, Manihot epruinosa,* and *Pseudobombax marginatum*. Smaller shifts occurred for *Commiphora leptophloeos* and *Spondias tuberosa* which maintained some leaf cover for a relatively longer period, and also maintained less negative $\Psi_{leaf.}$

The shift towards heavier $\delta^{18}O$ was less apparent for the species in the DHWD group. Within this group, the species that experienced greater shifts towards heavier $\delta^{18}O$ were ENSP and *Commiphora leptophloeos* and the *Enterolobium species*. Different from

all the species sampled, *Ziziphus joazeiro*, and evergreen species, was the only one that seemed to shift to lighter $\delta^{18}O$ values.

Species-level foliar $\delta^{13}C$

We found high variation in species-level foliar $\delta^{13}C$ (Figure III-9). Species which tended to have less negative foliar $\delta^{13}C$ were *Amburana cearensis*, *Cynophalla flexuosa*, *Aspidosperma pyrifolium*, *Cenostigma pyramidale*, and *Enterolobium species* (arbitrarily above -28‰). With the exception of *C. flexuosa*, these species all belong to the Fabaceae family. Decreasing trends in foliar $\delta^{13}C$ occurred for most of the DLWD species. The same was not true for *P. marginatum* nor *Manihot epruinosa.* Regarding the DHWD species, more negative ratios of ~30 ‰ were found for *Bauhinia cheilanth* and *Croton blanchetianus.*

Discussion

PFT predicts tolerance to water stress, with some exceptions

In the Caatinga SDTF, the PFT framework is a strong predictor of plant water status and tolerance to water stress. Our findings agree with several studies which define PFTs for the dry tropics based on wood density and phenology, including Borchert (1994) in Costa Rica, and Lima et al. (2012) and Oliveira et al. (2015) conducted in the Caatinga dry forest. In these studies, less negative leaf or stem water potentials was associated with early-deciduous low wood density species, often stem succulents, with high stem water storage capacity. Like these studies, we also found plant water status was associated with phenology and stem water storage capacity. It was these associations that lead the authors to propose the PFT we have used as a framework. But unlike these studies we also measured $\Psi_{MD.}$ We found significant differences in Ψ_{MD} between the three PFTs (Table II-

6). This indicates that even on a daily PFTs have different water use since water demand is generally highest during mid-day hours and when net radiation, temperature, and vapor pressure deficit peak.

We used $\Psi_{MD\text{-}PD}$ can be an indicator of stomatal control because it is related to the degree of stomatal closure in a tree will experience. Our results suggest that DLWD group had greater stomatal control compared to the high DHWD and EV group, meaning that the DLWD species are more isohydric because they maintain a relatively constant Ψ_{MD} even as soil dries and soil Ψ drops. One reason the DLWD species can maintain stable, less negative leaf water potentials is likely because these species have high water storage capacity. Water stored in plant tissues are helps stem succulent species avoid drought stress. Conversely, the high wood density species found in the DHWD and EV group are more anisohydric because they allow Ψ_{MD} to decline nearly in parallel with Ψ_{soil} (Meinzer et al. 2016). Thus, our findings also support the idea that anisohydric species like those in EV and DHWD functional types are more tolerant of water stress and could potentially be less prone to drought-induced mortality (McDowell et al. 2008).

Exceptions to general PFT trends occurred in the DHWD types, namely *Aspidosperma pyrifolium, Croton blanchetianus,* and *Myracrodruon urundeuva.* For *A. pyrifolium* and *C. blanchetianus,* Ψ_{leaf} was less negative during the early part of the dry season, but then became more negative after July. *C. blanchetianus* soon after lost all leaf cover, while *A. pyrifolium* maintain a diminished level of leaf cover throughout the duration of sampling. Some have reported that under more favorable conditions, *A. pyrifolium* can maintain leaf cover year-round (Maia 2012). This species is characterized

by thick waxy coriaceous leaves that may be important to minimizing water loss and help maintain less negative $\Psi_{leaf.}$ It is unclear how *M. urundeuva*, was able to maintain stable $\Psi_{MD\text{-}PD}$ since this species does not seem to have access to relatively deeper, more stable water sources.

PFT generally have access to the same water, except for some evergreen species

The differences in plant water status and tolerance to drought though, is likely not because species have access to different water sources or employ different rooting strategies. Regardless of PFT, stem waters plot below both the rainwater and soil water lines, indicating that plant water sources are likely a mixture of waters not derived solely the recent rain event. The lack of a significant difference in stem $\delta^{18}O$ indicates that all PFTS have access to the same water and seem to be very shallowly rooted. within the top 50cm. This does not mean that species cannot develop deeper roots, but rather that the shallow soils at this site prevent trees from relying heavily on deeper water sources. Although into the dry season, based on $\delta^{2}H$ values there might be a slight vertical partitioning of water sources within the top 50cm between the DLWD and DHWD groups. The stem water for the DLWD group plots between the LMWL and the soil water samples. This indicates that water sources for DLWD is likely bound between this year's rainwater and soil water up to a depth of 50cm. The shift towards heavier $\delta^{18}O$ particularly for the DLWD species also suggests that deeper water sources are not being used by most of the species measured; this shift is likely reflective of the seasonal change in $\delta^{18}O$ of rainwater. Note that *Ziziphus joazeiro* as the only species that shifted to lighter $\delta^{18}O$, which means that this evergreen that might be tapping slightly deeper water sources.

Our findings are unique in that previous studies tend to focus plant-water sourcing a function of deciduousness (Hasselquist et al. 2010; Jackson et al. 1995), not wood density. Furthermore, Drake and Franks (2003) have suggested that for a seasonally dry tropical forest located along a riparian zone, species which exhibited large decreases in Ψ_{PD} were likely dependent on shallow water sources. Our findings are contradictory to this in that the species with the smallest decrease in Ψ_{PD}, which were in the DLWD type, are likely relying on shallow soil water sources and likely storing some of this water for use during the dry season. A similar pattern was found by Pivovaroff et al. (2017) in a Mediterranean forest, where species that had more negative midday leaf water potential during the growing season also showed access to deeper water sources based on δ^2H ratios. This means that temporal partitioning of water resources could explain how stem succulent and high wood density and evergreen tree species are able to co-exist under the same high-water stress conditions, and this temporal partitioning is evident because some species, i.e. DLWD, have a higher water storage capacity and some species, i.e. DHWD and EV, have evolved a greater tolerance more negative leaf water potentials and are likely more resistant to cavitation. Moreover, the significant difference in Ψ_{PD} for the DLWD vs the DHWD and EV group again indicates that store stem water could provide a more readily accessible water source that soil water which is held under more negative pressure potentials.

PFT predicts water use efficiency but masks species-level variation

In this study, PFT generally predicted intrinsic water use efficiency (WUE_i) based on foliar $\delta^{13}C$ was significantly different at the PFT level but masked highly variable species-level trends. Finding that PFT can be used to predict WUE_i by PFT contradicts previous work

conducted in the Caatinga. Previous research failed to find a significant difference between DHWD and EV groups in the Caatinga (Souza et al. 2015). One reason for contrasting results could be because Souza et al. (2015) measured more EV species over a shorter time frame. While Souza et al. (2015) maybe have better characterized the EV as group (5 vs. 2 evergreen species) it was only during the wet season, when water use efficiency differences might be less important since resources are abundant. Moreover, compared to this study, our foliar δ13C were about 4 ‰ more negative.

Additionally, we found high variation at the species-level. This means that the PFT framework masks species-level variations in WUE_i. In particular, some species from the Fabaceae family tended to have less negative foliar $\delta^{13}C$, which could indicate some level of phylogentic conservationism. These species were *Amburana cearensis*, *Aspidosperma pyrifolium*, *Cenostigma pyramidale*, and *Enterolobium species*

Decreasing trend in foliar $\delta^{13}C$ are often related to an increasing dependence of recycled respired carbon dioxide (Cernusak et al. 2011; Pfanz et al. 2002; Worbes et al. 2013). As mentioned, the DLWD species in this study are also considered stem succulent trees, and many of these tree forms have photosynthetic stems. Fleshy often green to yellow trunks were observed for *Amburana cearensis*, *Commiphora leptophloeos*, *Jatropha mollissima*, and *Pseudobombax marginatum*, could indicating that these trunks are likely photosynthetic. Although the same decreasing trend was not observed for *P. marginatum,* which had mostly stable foliar $\delta^{13}C$ over time. One reason for this could be that *P. marginatum* was also early deciduous, and so sampling was limited to shorter time period. Similarly, *Manihot epruinosa* also maintained relatively stable foliar $\delta^{13}C$ values

and had a small sampling time-window, but this species had a dark almost black colored trunk that is not likely to be photosynthetic.

Regarding the DHWD species we found lower water use efficiency for *Bauhinia cheilantha,* and *Croton blanchetianus,* both which occur in liana form. Some studies that show that lianas can be deeply rooted and may shift to deeper soil water sources during the dry season (Andrade et al. 2005) but may also be more aggressive in water use (Guzman et al. 2017) Our stem water $\delta^{18}O$ and $\delta^{2}H$ findings do not agree. Instead the reason that these laiana species may have a low water use efficiency is because, in addition to having a high wood density and thin xylem vessels, these species also have relatively small diameters. Consequently, water transport is likely low and less efficient. Still, it is unclear how *C. blanchetianus* managed to maintain low Ψ_{PD} and Ψ_{MD} levels.

Conclusion

Our findings demonstrate the utility of PFT as a framework for predicting water use strategies in the Caatinga SDTF. Still, in some cases, PFT classification masks species-level patterns and variation. Additionally, we also found that stem water storage is a highly specialized and perhaps little-appreciated water use and conservation strategy that many low wood density stem succulent species employ to help them avoid drought-stress conditions, essentially decoupling trees from drying soils. We confirmed the association between wood density and phenology and provided further insight into specific water use strategies employed by PFTs and species of the Caatinga SDTF. To our knowledge this is the first time that stem water $\delta^{18}O$ and $\delta^{2}H$ findings has been reported for this biome and these species, and it is also the first time that water making this a pioneer study for the Caatinga SDTF. Additionally, we report finding on many species' endemic to the

Caatinga, information that is scarce in scientific literature. Beyond the Caatinga, our findings provide insight into gaining a better understanding on the strategies that species employ to survive highly seasonal water-limited environments.

The importance of using leaf and wood traits to predict water use strategies is important for several reasons. First, these forests are amongst the most impacted by land use change (Hansen et al. 2013). Thus, understanding species strategies for coping with drought can inform reforestation and conservation recommendations (Lohbeck et al. 2013; Nathan et al. 2016; Werden et al. 2018). Moreover, understanding the boundary conditions within which PFTs operate may also be important to understanding and predict community-level composition and dynamics. Lastly organizing species variation into PFTs can help us understand and model forest response to climate change predictions.

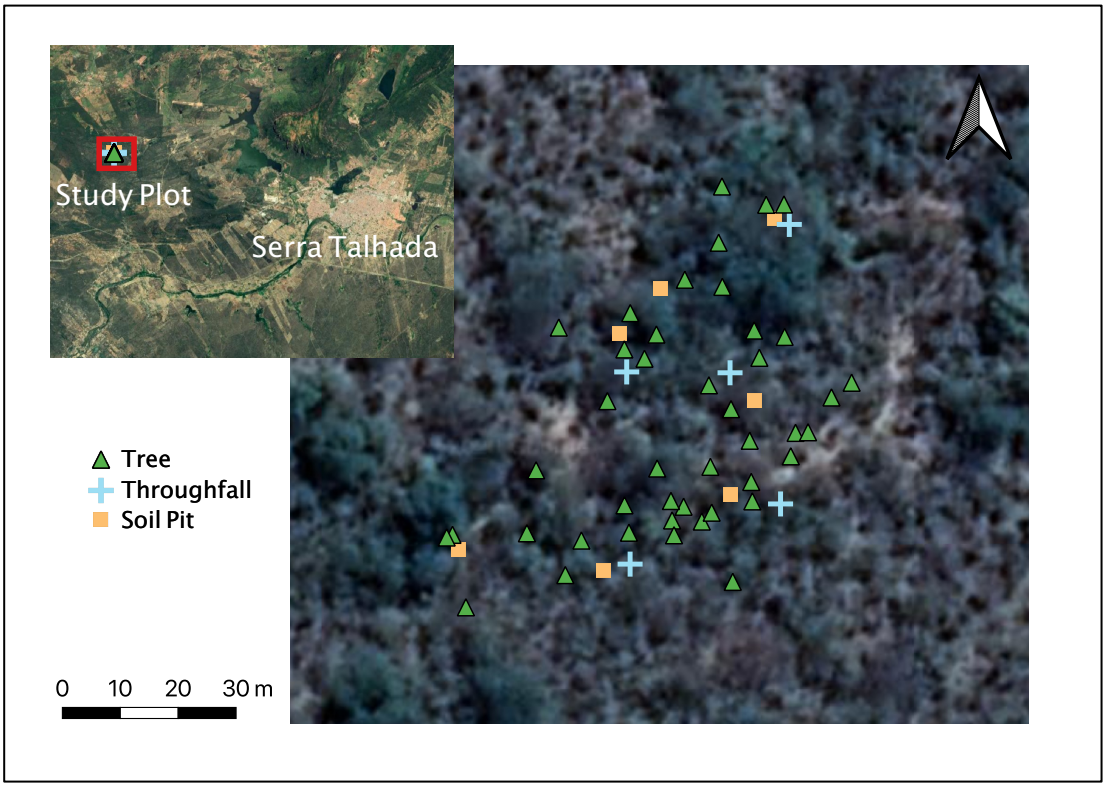

Figure III-1. Map of the study area near Serra Talhada, PE, Brazil, and the study plot where sampling occurred. Background images from Google (2019) using QGIS (2019).

Table III-1. Soil physical properties of the study site.

Depth (cm)	Sand (%)	Clay (%)	Textural Class	Min. θ (m^3/m^3)	Max θ (m^3/m^3)
0 to 10	68.5	6.4	sandy loam	0.039	0.548
10 to20	64.5	11.3	sandy loam	0.039	0.477
20 to 30	61.8	13.4	sandy loam	0.039	0.470
30 to 40	62.7	13.3	sandy loam	0.039	0.438
40 to 50	62.6	15.0	sandy loam	0.039	0.437

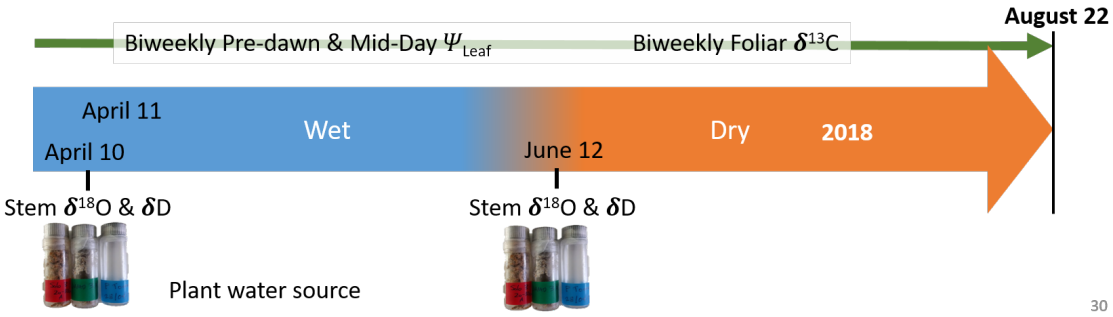

Figure III-2. Timeline of field measurements and collections.

Table III-2. Wood and rooting characteristics of the 16 selected species. +Color codes plant functional type: deciduous low wood density, DLWD; evergreen high wood density, EV; deciduous high wood density, DHWD. * Stem specific wood density from field samples. ** description from Maia (2012).

+ID	Family	Species	Plant form	Wood Density (g/cm^3)*	Rooting** characteristics
AMCE	Fabaceae	*Amburana cearensis* (Allemao) A.C.Sm.	Stem succulent	0.44 (0.03)	Root tubers and long fibrous fine roots
COLE	Burseraceae	*Commiphora leptophloeos* (Mart.) Gillett	Stem succulent	0.25 (0.06)	--
JAMO	Euphorbiaceae	*Jatropha mollissima* (Pohl) Baill.	Stem succulent	0.26 (0.03)	--
MAEP	Euphorbiaceae	*Manihot epruinosa* Pax & K. Hoffm.	Stem succulent	0.34 (0.04)	Starchy tubers (wild cassava)
PSSP	Bombacaceae	*Pseudobombax marginatum* (A.St.-Hil, Juss & Cambess.) K.Schum	Stem succulent	0.28 (0.05)	Swollen root
SPTU	Anacardiaceae	*Spondias tuberosa* Arruda	Stem succulent	0.42 (0.03)	Lateral roots and large tubers
CYFL	Capparaceae	*Cynophalla flexuosa* (L.) J. Presl	Liana	0.49 (0.05)	--
ZIJO	Rhamnaceae	*Ziziphus joazeiro* Mart.	Tree	0.56 (0.02)	Deep radial roots
ANCO	Fabaceae	*Anadenanthera colubrina* (Vell.) Brenam	Tree	0.63 (0.01)	Shallow lateral roots
ASPY	Apocynaceae	*Aspidosperma pyrifolium* Mart.	Tree	0.54 (0.02)	--

Table III-2. Continued.

+ID	Family	Species	Plant form	Wood Density (g/cm^3)*	Rooting** characteristics
BACH	Fabaceae	*Bauhinia cheilantha* (Bong.) Steud.	Liana	0.61 (0.04)	Lateral roots
CEPY	Fabaceae	*Cenostigma pyramidale* (Tul.) E. Gagnon & G. P. Lewis	Tree / shrub	0.64 (0.02)	Deep main root
CRBL	Euphorbiaceae	*Croton blanchetianus* Baill.	Liana / shrub	0.72 (0.01)	Lateral roots
ENSP	Fabaceae	*Enterolobium sp.*	Tree	0.61 (--)	--
MYUR	Anacardiaceae	*Myracrodruon urundeuva* Allemão	Tree	0.53 (0.02)	Deeply rooted
PIST	Fabaceae	*Piptadenia stipulacea* (Benth.) Ducke	Tree	0.56 (0.05)	--

Table III-3. Leaf characteristics of the sixteen Caatinga tree species. + Color codes plant functional type: deciduous low wood density, DLWD; evergreen high wood density, EV; deciduous high wood density, DHWD. * Observed in the field; see Methods. ** description from Maia (2012).

+ID	*Family*	*Species*	*Leaf Morphology**	*Leaf Texture*)*	*Leaf Flush***	*Leaf Fall***
AMCE	Fabaceae	*Amburana cearensis* (Allemao) A.C.Sm.	Pinnately compound	Glabrous	Wet season	Dry season
COLE	Burseraceae	*Commiphora leptophloeos* (Mart.) Gillett	Pinnately compound	Pubescent	Wet season	Dry season
JAMO	Euphorbiaceae	*Jatropha mollissima* (Pohl) Baill.	Palmately compound	Pubescent	Wet season	Dry season
MAEP	Euphorbiaceae	*Manihot epruinosa* Pax & K. Hoffm.	Palmately compound	Glabrous	Wet season	*Dry season
PSSP	Bombacaceae	*Pseudobombax marginatum* (A. St.-Hil., Juss., & Cambess.) A. Robyns	Palmately compound	Coriaceous / rugose	Wet season	Dry season
SPTU	Anacardiaceae	*Spondias tuberosa* Arruda	Pinnately compound	Glabrous	First rains	Year long
CYFL	Capparaceae	*Cynophalla flexuosa* (L.) J. Presl	Simple	Coriaceous	Evergreen	Evergreen
ZIJO	Rhamnaceae	*Ziziphus joazeiro* Mart.	Simple	Glabrous / coriaceous	Height of dry season	Evergreen

Table III-3. Continued.

+ID	*Family*	*Species*	*Leaf Morphology**	*Leaf Texture*)*	*Leaf Flush***	*Leaf Fall***
ANCO	Fabaceae	*Anadenanthera colubrina* (Vell.) Brenam	Bipinnately compound	Glabrous	End of dry season/beginning of wet season	Early of dry season
ASPY	Apocynaceae	*Aspidosperma pyrifolium* Mart.	Simple	Coriaceous	End of dry season/beginning of wet season	Dry season
BACH	Fabaceae	*Bauhinia cheilantha* (Bong.) Steud.	Palmately compound	Pubescent	First rains	Dry season
CEPY	Fabaceae	*Cenostigma pyramidale* (Tul.) E. Gagnon & G. P. Lewis	Bipinnately compound	Coriaceous / scabrose	First rains	Dry season
CRBL	Euphorbiaceae	*Croton blanchetianus* Baill.	Simple	Pubescent	First rains	Early dry season
ENSP	Fabaceae	*Enterolobium sp.*	Bipinnately compound	Coriaceous / scabrose	Wet season	*Late dry season
MYUR	Anacardiaceae	*Myracrodruon urundeuva* Allemão	Pinnately compound	Pubescent	Wet season	Dry season
PIST	Fabaceae	*Piptadenia stipulacea* (Benth.) Ducke	Bipinnately compound	Glabrous	Wet season	Dry season

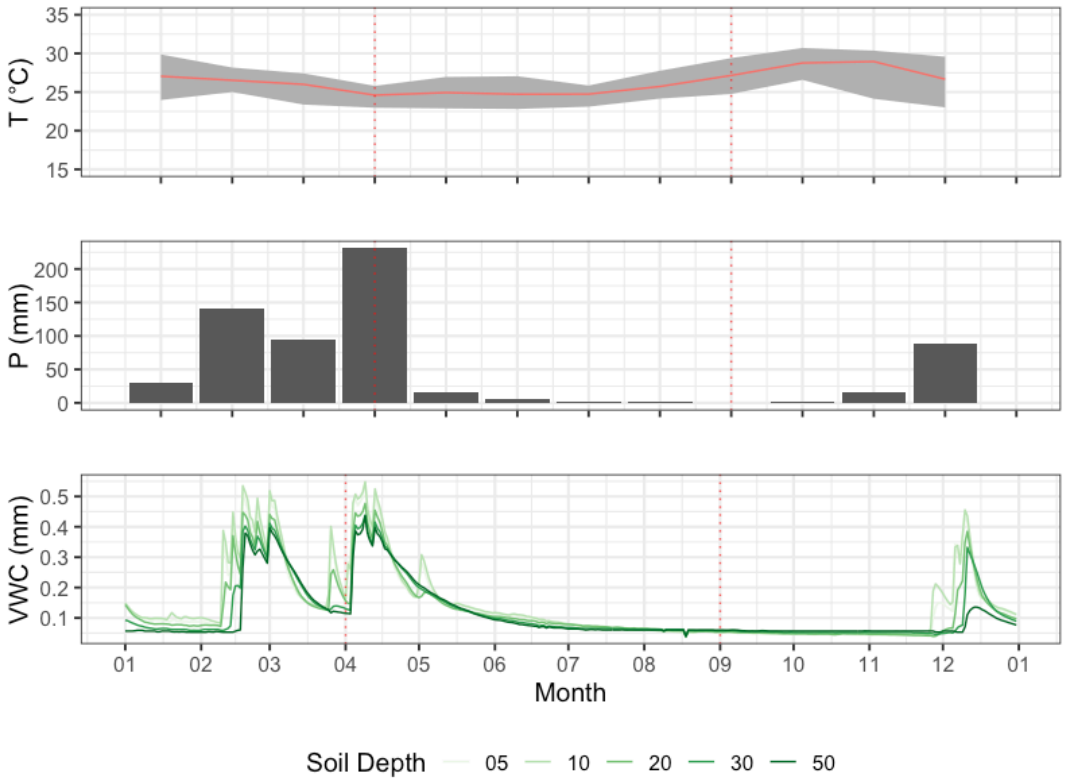

Figure III-3. Average monthly air temperature, with minimum and maximum bounds in grey (top); total monthly rainfall observed near the study plot (middle); and continuous volumetric water content observed in the study plot(bottom). Red dashed line marks the measurement period from April 11 to August 22, 2018.

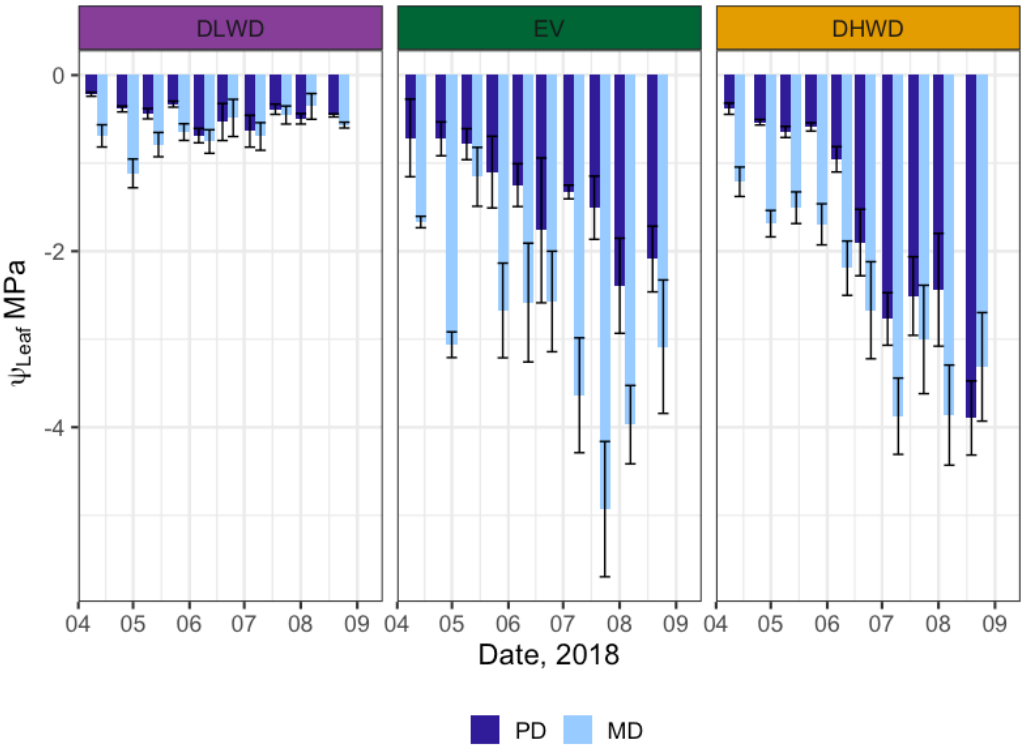

Figure III-4. Plant functional type pre-dawn (dark blue, PD) and mid-day, (light blue, MD) leaf water potentialΨLeaf from April 11 to August 22, 2018. Error bars are standard deviations and panels are color-coded to plant functional types: : deciduous low wood density, DLWD; evergreen high wood density, EV; deciduous high wood density, DHWD.

Table III-4.Linear mixed models of pre-dawn and mid-day leaf water potential. The model used PFT as a fixed effect, and Date and Species as random effects. Significance levels are: * at 0.05 confidence level, ** at 0.01 confidence level; * at 0.001 confidence level. Plant functional types are: deciduous low wood density, DLWD; evergreen high wood density, EV; deciduous high wood density, DHWD.**

PFT	*CI lower*	*CI upper*	*Tukey's p-value*	
			EV	**DHWD**
Leaf Ψ_{MD-PD}				
DLWD	-0.88	0.35	***< 0.001	**0.0023
DHWD	-1.14	-0.66	**0. 0081	
EV	-2.46	-0.92		
Leaf Ψ_{MD}				
DLWD	-1.93	0.04	***<1e^{-4}	***<1e^{-4}
DHWD	-3.04	-2.07	0.5030	
EV	-4.08	-1.77		
Leaf Ψ_{PD}				
DLWD	-1.60	-0.09	0.0861	***<0.001
DHWD	-2.07	-1.01	0.2597	
EV	-2.15	-0.37		

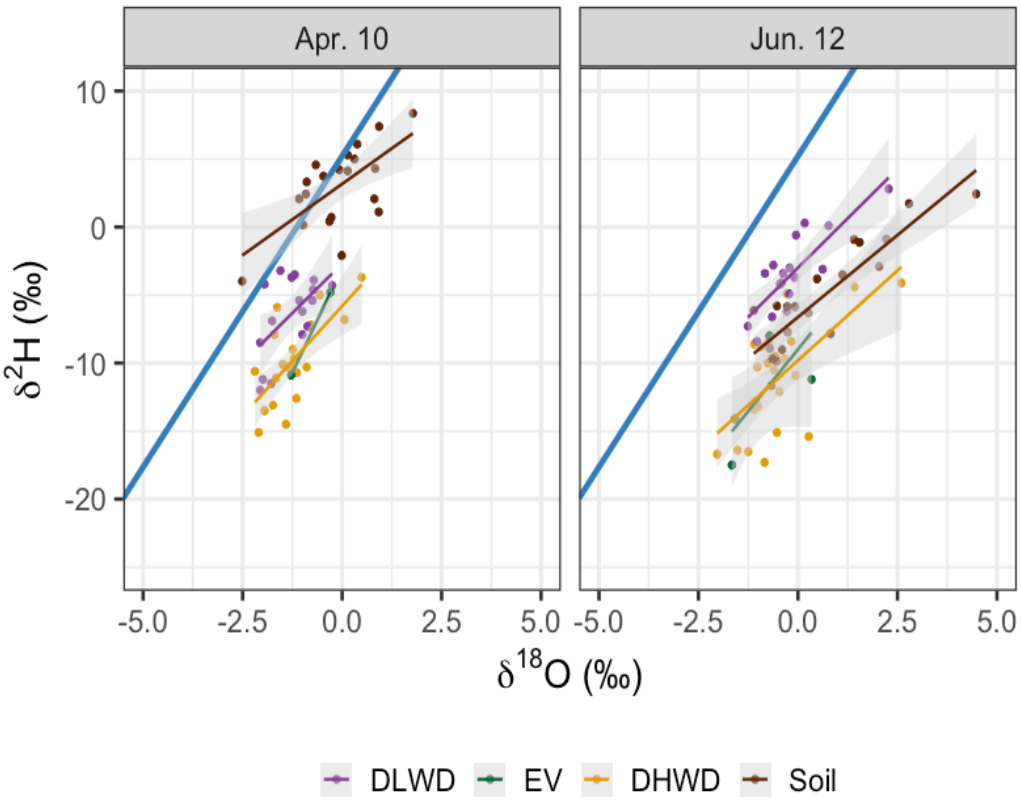

Figure III-5. Plant functional type δ18O and δ2H for stem and soil water ratios. The local meteoritic line for precipitation is plotted in blue. Grab samples of the wet season, April 10, 2018 and dry season, June 12, 2018. Stem water is plotted by plant functional type: deciduous low wood density, DLWD; evergreen high wood density, EV; deciduous high wood density, DHWD. Soil water is plotted in brown and represents three depths, 5 to 15cm, 20 to 30cm, and 40 to 50cm. Grey shading is standard deviation for the linear fit for stem and soil water.

Table III-5. Linear regression equations for δ18O and δ2H by plant functional type and season. Plant functional types are: deciduous low wood density, DLWD; evergreen high wood density, EV; deciduous high wood density, DHWD.

Sample Type	Equation	R^2	n
Local meteoric water line	y = 4.76x + 6.40	0.88	55
Wet Season, April 10, 2018			
DLWD	y = 2.91x – 2.69	0.32	17
EV	y = 6.16x – 3.01	1	3
DHWD	y = 3.22x – 5.81	0.48	22
Soils	y = 2.09x + 3.17	0.43	20
Dry Season, June 12, 2018			
DLWD	y = 2.90x – 2.99	0.67	17
EV	y = 3.63x – 8.99	0.48	7
DHWD	y = 2.64x – 9.81	0.42	23
Soils	y = 2.41x – 6.62	0.78	20
Dry Season, September 19, 2018			
EV	y = 2.90x – 2.99	0.67	5
Soils	y = 1.77x – 6.41	0.89	17

Table III-6. Linear mixed models of stem δ18O and δ2H by collection date. Values of n found in Table -5. The modeled included PFT as a fixed effect, and Date and Species as random effects. Significance levels are: * at 0.05 confidence level, ** at 0.01 confidence level; * at 0.001 confidence level. Plant functional types are: deciduous low wood density, DLWD; evergreen high wood density, EV; deciduous high wood density, DHWD.**

	CI lower	*CI upper*	*Tukey's p-value*	
			EV	**DHWD**
Stem $\delta^{18}O$ April 10, 2018				
DLWD	-2.31	-0.28	0.1870	0.9500
DHWD	-1.81	-0.65	0.2370	
EV	-2.02	0.77		
Stem $\delta^{2}H$ April 10, 2018				
DLWD	-11.64	-1.24	0.9466	****0.0074**
DHWD	-12.57	-7.05	0.3403	
EV	-14.12	-0.02		
Stem $\delta^{18}O$ June 12, 2018				
DLWD	-1.59	1.27	0.0989	0.4242
DHWD	-1.31	0.27	0.4266	
EV	-2.72	0.65		
Stem $\delta^{2}H$ June 12, 2018				
DLWD	-9.36	2.45	*****<1e^{-4}**	*****<1e^{-4}**
DHWD	-14.40	-7.96	0.6190	
EV	-19.87	-5.77		

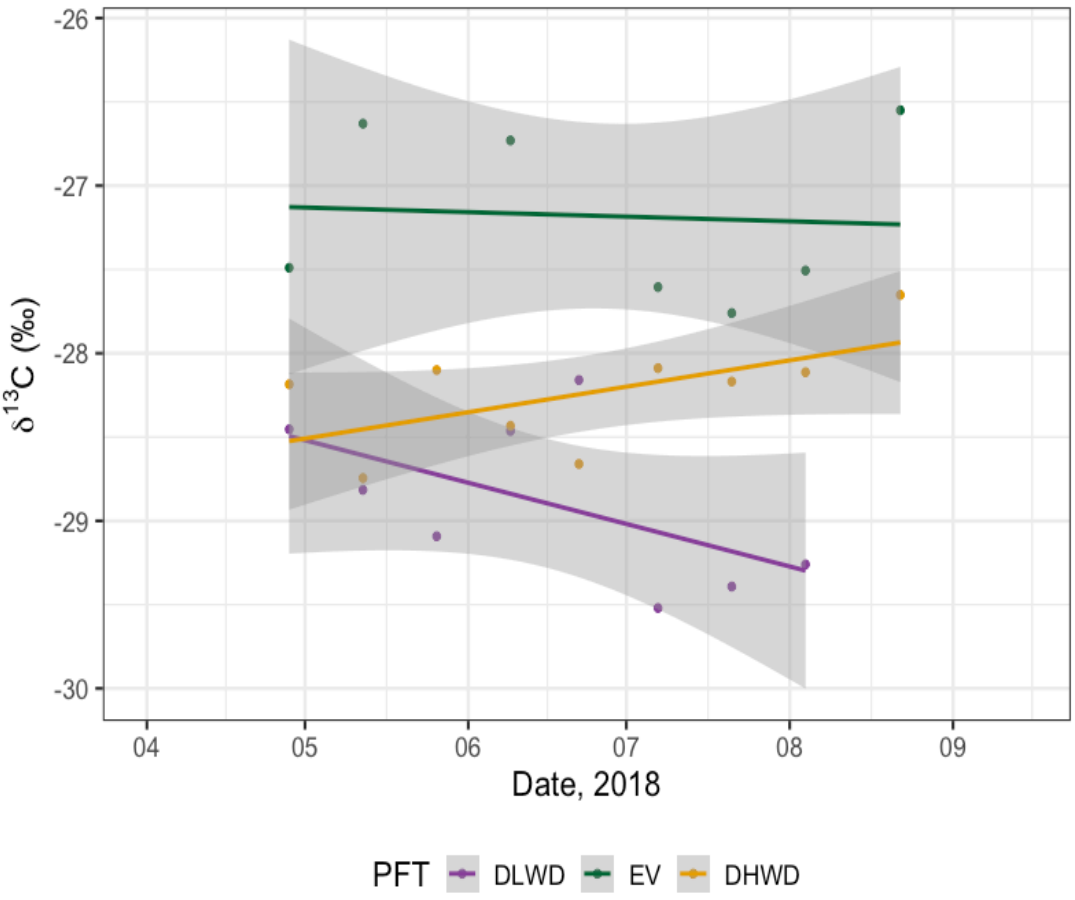

Figure III-6. Plant functional type, PFT, average foliar $\delta^{13}C$ from April 28 to August 22, 2018. Each point represents a mean ratio for all species and samples of the plant functional types, PFTs, are: deciduous low wood density, DLWD; evergreen high wood density, EV; deciduous high wood density, DHWD. Grey shading depicts the standard deviation associated with the linear regression fit

Table III-7. Linear mixed models of foliar $\delta^{13}C$. The model used PFT as a fixed effect, and Date and Species as random effects. Significance levels are: * at 0.05 confidence level, ** at 0.01 confidence level; * at 0.001 confidence level. Plant functional types are: deciduous low wood density, DLWD; evergreen high wood density, EV; deciduous high wood density, DHWD.**

PFT	*CI lower*	*CI upper*	*Tukey's p-value* EV	DHWD
Foliar $\delta^{13}C$				
DLWD	-29.61	-28.15	***<0.001	*0.0476
DHWD	-28.60	-28.07	*0.0434	
EV	-28.48	-26.67		

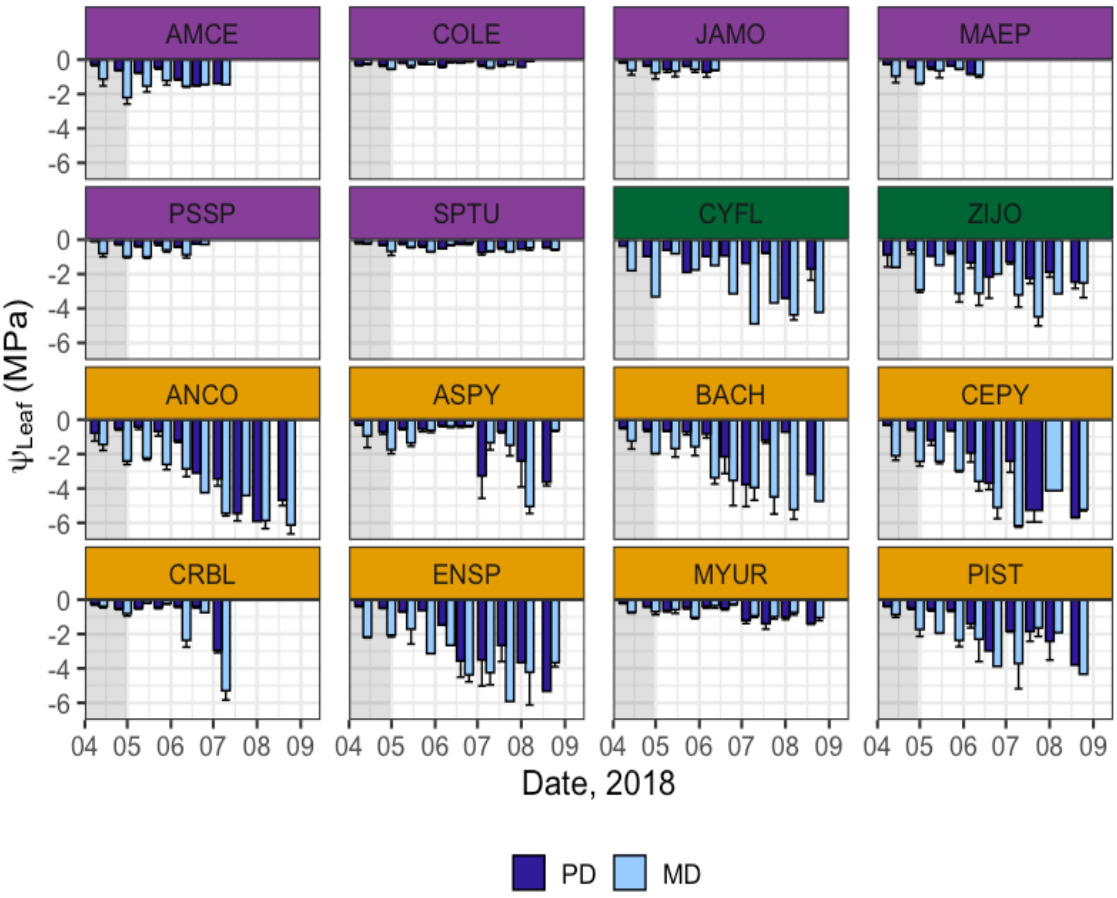

Figure III-7. Species-level biweekly pre-dawn (dark blue, PD) and mid-day, (light blue, MD) leaf water potential, Ψ_{Leaf}, from April 11 to August 22, 2018. Error bars are standard deviation. Shaded region marks the end of the wet season. Species are labeled and color-coded to plant functional types: deciduous low wood density, DLWD; evergreen high wood density, EV; deciduous high wood density, DHWD.

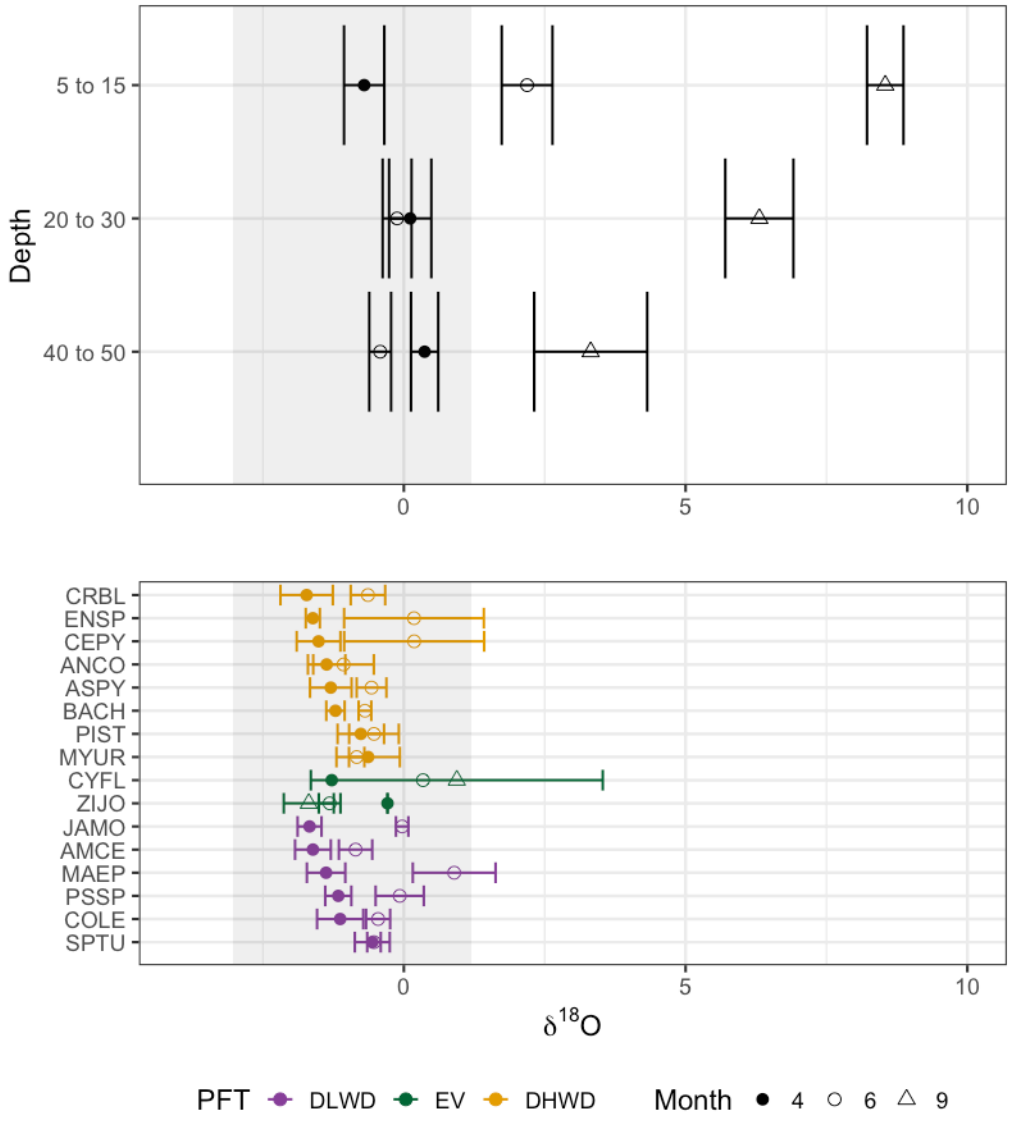

Figure III-8. Species-level soil and stem water $\delta^{18}O$ ratios (top and, bottom respectively). Soil water for three depth intervals, 5 to 15cm, 20 to 30cm, and 40 to 50cm. Grey shading depicts the average and standard deviation of rainwater $\delta^{18}O$. Grab samples of the wet season, April 10, 2018 (filled circle), and dry season, June 12, 2018 (circle outline) and September 19, 2018 (triangle outline). Species are color-coded to plant functional types: deciduous low wood density, DLWD; evergreen high wood density, EV; deciduous high wood density, DHWD.

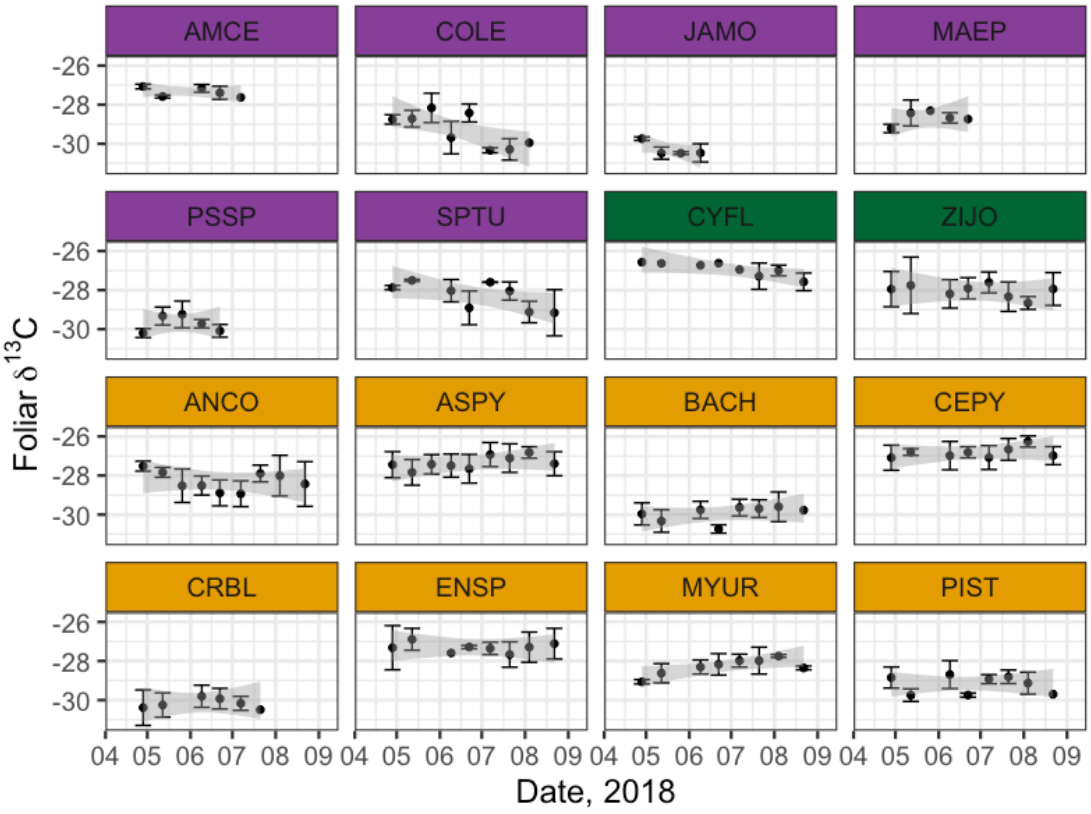

Figure III-9. Species-level foliar $\delta^{13}C$ over time. Species are color-coded to plant functional types: deciduous low wood density, DLWD; evergreen high wood density, EV; deciduous high wood density, DHWD. Grey shading depicts the standard deviation associated with the linear regression fit.

References

Allen, C. D., Macalady, A. K., Chenchouni, H., Bachelet, D., McDowell, N., Vennetier, M., … Hogg, E. H. T. (2010). A global overview of drought and heat-induced tree mortality reveals emerging climate change risks for forests. *Forest Ecology and Management*, *259*(4), 660–684.

Allen, K., Dupuy, J. M., Gei, M. G., Hulshof, C., Medvigy, D., Pizano, C., … Waring, B. G. (2017). Will seasonally dry tropical forests be sensitive or resistant to future changes in rainfall regimes? *Environmental Research Letters*, *12*(2).

Andrade, J. L., Meinzer, F. C., Goldstein, G., & Schnitzer, S. A. (2005). Water uptake and transport in lianas and co-occurring trees of a seasonally dry tropical forest. *Trees - Structure and Function*, *19*(3), 282–289. https://doi.org/10.1007/s00468-004-0388-x

Antongiovanni, M., Venticinque, E. M., & Fonseca, C. R. (2018). Fragmentation patterns of the Caatinga drylands. *Landscape Ecology*, *33*(8), 1353–1367. https://doi.org/10.1007/s10980-018-0672-6

Ávila-Lovera, E., & Ezcurra, E. (2016). Stem-succulent trees from the Old and New World tropics. In *Tropical Tree Physiology* (pp. 45–65). Springer.

Borchert, R. (1994). Soil and Stem Water Storage Determine Phenology and Distribution of Tropical Dry Forest Trees. *Ecology*, *75*(5), 1437–1449.

Bucci, S. J., Goldstein, G., Meinzer, F. C., Scholz, F. G., Franco, A., & Bustamante, M. (2004). Functional convergence in hydraulic architecture and water relations of tropical savanna trees: From leaf to whole plant. *Tree Physiology*, *24*(8), 891–899. https://doi.org/10.1093/treephys/24.8.891

Bullock, S. H., Mooney, H. A., & Medina, E. (1995). *Seasonally dry tropical forests*. (S H Bullock, H. A. Mooney, & E. Medina, Eds.), *Seasonally dry tropical forests*.

Butz, P., Raffelsbauer, V., Graefe, S., Peters, T., Cueva, E., Hölscher, D., & Bräuning, A. (2017). Tree responses to moisture fluctuations in a neotropical dry forest as potential climate change indicators. *Ecological Indicators*, *83*, 559–571. https://doi.org/10.1016/j.ecolind.2016.11.021

Cernusak, L. A., & Hutley, L. B. (2011). Stable isotopes reveal the contribution of corticular photosynthesis to growth in branches of Eucalyptus miniata. *Plant Physiology*, *155*(1), 515–523.

Chapotin, S. M., Razanameharizaka, J. H., & Holbrook, N. M. (2006). A biomechanical perspective on the role of large stem volume and high water content in baobab trees

(Adansonia spp.; Bombacaceae). *American Journal of Botany*, *93*(9), 1251–1264. https://doi.org/10.3732/ajb.93.9.1251

Chapotin, S. M., Razanameharizaka, J. H., & Holbrook, N. M. (2006). Baobab trees (Adansonia) in Madagascar use stored water to flush new leaves but not to support stomatal opening before the rainy season. *New Phytologist*, *169*, 549–559.

Chapotin, S. M., Razanameharizaka, J. H., & Holbrook, N. M. (2006). Water relations of baobab trees (Adansonia spp. L.) during the rainy season: Does stem water buffer daily water deficits? *Plant, Cell and Environment*, *29*(6), 1021–1032. https://doi.org/10.1111/j.1365-3040.2005.01456.x

Chave, J., Muller-Landau, H. C., Baker, T. R., Easdale, T. A., Hans Steege, T. E. R., & Webb, C. O. (2006). Regional and phylogenetic variation of wood density across 2456 neotropical tree species. *Ecological Applications*, *16*(6), 2356–2367. https://doi.org/10.1890/1051-0761(2006)016[2356:RAPVOW]2.0.CO;2

D'Odorico, P., & Bhattachan, A. (2012). Hydrologic variability in dryland regions: Impacts on ecosystem dynamics and food security. *Philosophical Transactions of the Royal Society B: Biological Sciences*, *367*(1606), 3145–3157. https://doi.org/10.1098/rstb.2012.0016

Dansgaard, W. (1964). Stable isotopes in precipitation. *Tellus*, *16*(4), 436–468.

Guzman, M. E., Santiago, L. S., Schnitzer, S. A., & Álvarez-Cansino, L. (2017). Trade-offs between water transport capacity and drought resistance in neotropical canopy liana and tree species. *Tree Physiology*, *37*(10), 1404–1414. https://doi.org/10.1093/treephys/tpw086

Dirzo, R., Young, H. S., Mooney, H. A., & Ceballos, G. (2011). *Seasonally dry tropical forests: ecology and conservation*. Island Press.

Drake, P. L., & Franks, P. J. (2003). Water resource partitioning, stem xylem hydraulic properties, and plant water use strategies in a seasonally dry riparian tropical rainforest. *Oecologia*, *137*(3), 321–329. https://doi.org/10.1007/s00442-003-1352-y

Esquivel-Muelbert, A., Galbraith, D., Dexter, K. G., Baker, T. R., Lewis, S. L., Meir, P., … Phillips, O. L. (2017). Biogeographic distributions of neotropical trees reflect their directly measured drought tolerances. *Scientific Reports*, *7*(1), 1–11. https://doi.org/10.1038/s41598-017-08105-8

Feng, X., Vico, G., & Porporato, A. (2012). On the effects of seasonality on soil water balance and plant growth. *Water Resources Research*, *48*(5), 1–12. https://doi.org/10.1029/2011WR011263

Gelder, H. A. van, Poorter, L., Sterck, F., van Gelder, H. A., Poorter, L., & Sterck, F. (2006). Wood mechanics, allometry, and life-history variation in a tropical rain forest tree community. *New Phytologist*, *171*(2), 367–378. https://doi.org/10.1111/j.1469-8137.2006.01757.x

Griesser, J. (2006). New LocClim 1.10. Rome, Italy: Agrometeorology Group, FAO/SDRN.

Google. (2019). [Area near Serra Talhada, PE and zoomed in image of forested study area]. Retrieved from Google Satellite in QGIS Version 3.10.0-A Coruña. CNES / Airbus 2019, Maxar Technologies 2019,

Hacke, U. G., Sperry, J. S., Pockman, W. T., Davis, S. D., & McCulloh, K. A. (2001). Trends in wood density and structure are linked to prevention of xylem implosion by negative pressure. *Oecologia*, *126*(4), 457–461. https://doi.org/10.1007/s004420100628

Hansen, M. C., Potapov, P. V, Moore, R., Hancher, M., Turubanova, S. A. A., Tyukavina, A., … others. (2013). High-resolution global maps of 21st-century forest cover change. *Science*, *342*(6160), 850–853.

Hasselquist, N. J., Allen, M. F., & Santiago, L. S. (2010). Water relations of evergreen and drought-deciduous trees along a seasonally dry tropical forest chronosequence. *Oecologia*, *164*(4), 881–890. https://doi.org/10.1007/s00442-010-1725-y

Hothorn, T., Bretz, F., & Westfall, P. (2008). Simultaneous inference in general parametric models. *Biometrical Journal*, *50*(3), 346–363. https://doi.org/10.1002/bimj.200810425

IAEA. (2014). IAEA/GNIP precipitation sampling guide, International Atomic Energy Agency.

Jackson, P. C., Cavelier, J., Goldstein, G., Meinzer, F. C., Holbrook, N. M., & Url, S. (1995). Partitioning of Water Resources among Plants of a Lowland Tropical Forest. *Oecologia*, *101*(2), 197–203. https://doi.org/10.1007/BF00317284

Jacobsen, A. L., Ewers, F. W., Pratt, R. B., Paddock, W. A., & Davis, S. D. (2005). Do Xylem Fibers Affect Vessel Cavitation Resistance? *Plant Physiology*, *139*(1), 546–556. https://doi.org/10.1104/pp.104.058404

Janzen, D. H. (1988). Management of Habitat Fragments in a Tropical Dry Forest : Growth. *Annals of the Missouri Botanical Garden*, *75*(1), 105–116. https://doi.org/10.2307/2399468

Kendall, C., & McDonnell, J. J. (2012). *Isotope tracers in catchment hydrology*. (C. Kendall & J. J. McDonnell, Eds.). Elsevier.

King, D. A., Davies, S. J., Tan, S., & Noor, N. S. M. (2006). The role of wood density and stem support costs in the growth and mortality of tropical trees. *Journal of Ecology*, *94*(3), 670–680. https://doi.org/10.1111/j.1365-2745.2006.01112.x

Kunstler, G., Falster, D., Coomes, D. A., Hui, F., Kooyman, R. M., Laughlin, D. C., … Westoby, M. (2016). Plant functional traits have globally consistent effects on competition. *Nature*, *529*(7585), 204–207. https://doi.org/10.1038/nature16476

Lachenbruch, B., & Mcculloh, K. A. (2014). Traits, properties, and performance: How woody plants combine hydraulic and mechanical functions in a cell, tissue, or whole plant. *New Phytologist*, *204*(4), 747–764. https://doi.org/10.1111/nph.13035

Lasky, J. R., Uriarte, M., & Muscarella, R. (2016). Synchrony, compensatory dynamics, and the functional trait basis of phenological diversity in a tropical dry forest tree community: Effects of rainfall seasonality. *Environmental Research Letters*, *11*(11). https://doi.org/10.1088/1748-9326/11/11/115003

Lebrija-Trejos, E., Meave, J. A., Poorter, L., Pérez-García, E. A., & Bongers, F. (2010). Pathways, mechanisms and predictability of vegetation change during tropical dry forest succession. *Perspectives in Plant Ecology, Evolution and Systematics*, *12*(4), 267–275. https://doi.org/10.1016/j.ppees.2010.09.002

Lima, A. L. A. de, & Rodal, M. J. N. (2010). Phenology and wood density of plants growing in the semi-arid region of northeastern Brazil. *Journal of Arid Environments*, *74*(11), 1363–1373. https://doi.org/10.1016/j.jaridenv.2010.05.009

Lima, A. L. A., Sampaio, E. V. S. B., Castro, C. C. de, Rodal, M. J. N., Antonino, A. C. D., Melo, A. L. de, … de Melo, A. L. (2012). Do the phenology and functional stem attributes of woody species allow for the identification of functional groups in the semiarid region of Brazil? *Trees*, *26*(5), 1605–1616. https://doi.org/10.1007/s00468-012-0735-2

Lohbeck, M., Poorter, L., Lebrija-Trejos, E., Martinez-Ramos, M., Meave, J. A., Paz, H., … Bongers, F. (2013). Successional changes in functional composition contrast for dry and wet tropical forests, *94*(March), 1211–1216.

Lorenzi, H. (2008). *Árvores brasileiras: Manual de identificação e cultivo de plantas arbóreas nativas do Brasil Vol.01* (5th ed.). Nova Odessa: Instituto Plantarum de Estudos da Flora.

Lorenzi, H. (2016). *Árvores brasileiras: Manual de identificação e cultivo de plantas arbóreas nativas do Brasil Vol.02* (5th ed.). Nova Odessa: Instituto Plantarum de Estudos da Flora.

Lorenzi, H. (2016). *Árvores brasileiras: Manual de identificação e cultivo de plantas arbóreas nativas do Brasil Vol.03* (2nd ed.). Nova Odessa: Instituto Plantarum de Estudos da Flora.

Machado, I. C., Marivando Barros, L., & Sampaio, E. V. de S. B. (1997). Phenology of Caatinga Species at Serra Talhada , PE , Northeastern Brazil Author. *Biotropica*, *29*(1), 57–68.

Maia, N. G. (2012). *Caatinga : árvores e arbustos e suas utilidades.* (2nd ed.). Printcolor Grafica e Editora.

Markesteijn, L., Iraipi, J., Bongers, F., & Poorter, L. (2010). Seasonal variation in soil and plant water potentials in a Bolivian tropical moist and dry forest. *Journal of Tropical Ecology*, *26*(5), 497–508. https://doi.org/10.1017/S0266467410000271

Markesteijn, L., Poorter, L., Paz, H., Sack, L., & Bongers, F. (2011). Ecological differentiation in xylem cavitation resistance is associated with stem and leaf structural traits. *Plant, Cell and Environment*, *34*(1), 137–148. https://doi.org/10.1111/j.1365-3040.2010.02231.x

Martínez-Cabrera, H. I., Jones, C. S., Espino, S., & Jochen Schenk, H. (2009). Wood anatomy and wood density in shrubs: Responses to varying aridity along transcontinental transects. *American Journal of Botany*, *96*(8), 1388–1398. https://doi.org/10.3732/ajb.0800237

Matos, D. S. de, Guim, A., Batista, Â. M. V., Pereira, O. G., & Martins, e V. (2005). Composição Química E Valor Nutritivo Da Silagem De Maniçoba (Manihot Epruinosa). *Archivos de Zootecnia*, *54*(208), 619–629. Retrieved from http://www.redalyc.org/articulo.oa?id=49520804

McDowell, N., Pockman, W. T., Allen, C. D., Breshears, D. D., Cobb, N., Kolb, T., … Yepez, E. A. (2008). Mechanisms of plant survival and mortality during drought: Why do some plants survive while others succumb to drought? *New Phytologist*, *178*(4), 719–739. https://doi.org/10.1111/j.1469-8137.2008.02436.x

Meinzer, F. C., Johnson, D. M., Lachenbruch, B., McCulloh, K. A., & Woodruff, D. R. (2009). Xylem hydraulic safety margins in woody plants: Coordination of stomatal control of xylem tension with hydraulic capacitance. *Functional Ecology*, *23*(5), 922–930. https://doi.org/10.1111/j.1365-2435.2009.01577.x

Meinzer, F. C., Woodruff, D. R., Marias, D. E., Smith, D. D., McCulloh, K. A., Howard, A. R., & Magedman, A. L. (2016). Mapping 'hydroscapes' along the iso- to anisohydric continuum of stomatal regulation of plant water status. *Ecology Letters*, *19*(11), 1343–1352. https://doi.org/10.1111/ele.12670

Méndez-Alonzo, R., Paz, H., Cruz Zuluaga, R., Rosell, J. A., & Olson, M. E. (2012). Coordinated evolution of leaf and stem economics in tropical dry forest trees. *Ecology*, *93*(11), 2397–2406.

Méndez-Alonzo, R., Pineda-García, F., Paz, H., Rosell, J. A., & Olson, M. E. (2013). Leaf phenology is associated with soil water availability and xylem traits in a tropical dry forest. *Trees - Structure and Function*, *27*(3), 745–754. https://doi.org/10.1007/s00468-012-0829-x

Oliveira, C. C. de, Zandavalli, R. B., Lima, A. L. A. de, & Rodal, M. J. N. (2015). Functional groups of woody species in semi-arid regions at low latitudes. *Austral Ecology*, *40*(1), 40–49. https://doi.org/10.1111/aec.12165

Pennington, R. T., Lavin, M., & Oliveira-Filho, A. (2009). Woody Plant Diversity, Evolution, and Ecology in the Tropics: Perspectives from Seasonally Dry Tropical Forests. *Annual Review of Ecology, Evolution, and Systematics*, *40*(1), 437–457. https://doi.org/10.1146/annurev.ecolsys.110308.120327

Pereira, I. M., Andrade, L. A., Sampaio, E., & Barbosa, M. R. V. (2003). Use-history effects on structure and flora of caatinga. *Biotropica*, *35*(2), 154–165. https://doi.org/10.1111/j.1744-7429.2003.tb00275.x

Pérez-Harguindeguy, N., Díaz, S., Garnier, E., Lavorel, S., Poorter, H., Jaureguiberry, P., … Cornelissen, J. H. C. (2013). New handbook for standardised measurement of plant functional traits worldwide. *Australian Journal of Botany*, *61*(3), 167–234. https://doi.org/10.1071/BT12225

Pfanz, H., Aschan, G., Langenfeld-Heyser, R., Wittmann, C., & Loose, M. (2002). Ecology and ecophysiology of tree stems: corticular and wood photosynthesis. *Naturwissenschaften*, *89*(4), 147–162.

Pineda-García, F., Paz, H., & Meinzer, F. C. (2013). Drought resistance in early and late secondary successional species from a tropical dry forest: The interplay between xylem resistance to embolism, sapwood water storage and leaf shedding. *Plant, Cell and Environment*, *36*(2), 405–418. https://doi.org/10.1111/j.1365-3040.2012.02582.x

Pineda-García, F., Paz, H., Meinzer, F. C., & Angeles, G. (2015). Exploiting water versus tolerating drought: Water-use strategies of trees in a secondary successional tropical dry forest. *Tree Physiology*, *36*(2), 208–217. https://doi.org/10.1093/treephys/tpv124

Pivovaroff, A. L., Pasquini, S. C., De Guzman, M. E., Alstad, K. P., Stemke, J. S., & Santiago, L. S. (2016). Multiple strategies for drought survival among woody plant species. *Functional Ecology*, *30*(4), 517–526. https://doi.org/10.1111/1365-2435.12518

Poorter, L., Wright, S. J., Paz, H., Ackerly, D. D., Condit, R., Ibarra-Manríquez, G., … Wright, I. J. (2008). Are functional traits good predictors of demographic rates? Evidence from five neotropical forests. *Ecology*, *89*(7), 1908–1920. Retrieved from http://www.ncbi.nlm.nih.gov/pubmed/18705377

Powers, J. S., & Tiffin, P. (2010). Plant functional type classifications in tropical dry forests in Costa Rica: Leaf habit versus taxonomic approaches. *Functional Ecology*, *24*(4), 927–936. https://doi.org/10.1111/j.1365-2435.2010.01701.x

Pratt, R. B., & Jacobsen, A. L. (2017). Conflicting demands on angiosperm xylem: Tradeoffs among storage, transport and biomechanics. *Plant Cell and Environment*, *40*(6), 897–913. https://doi.org/10.1111/pce.12862

Preston, K. A., Cornwell, W. K., & DeNoyer, J. L. (2006). Wood density and vessel traits as distinct correlates of ecological strategy in 51 California coast range angiosperms. *New Phytologist*, *170*(4), 807–818. https://doi.org/10.1111/j.1469-8137.2006.01712.x

QGIS Development Team (2019). Version 3.10.0-A Coruña. QGIS Geographic Information System. Open Source Geospatial Foundation Project. http://qgis.osgeo.org.

Reich, P. B. (2014). The world-wide "fast-slow" plant economics spectrum: A traits manifesto. *Journal of Ecology*, *102*(2), 275–301. https://doi.org/10.1111/1365-2745.12211

Sanchez-Azofeifa, G. A., Quesada, M., Jon Paul Rodrıguez, Nassar, J. M., Stoner, K. E., Castillo, A., … Cuevas-Reyes, P. (2005). Research Priorities for Neotropical Dry Forests 1 2 , 9 , 10 ,. *Biotropica*, *37*(4), 477–485.

Särkinen, T., Iganci, J. R. V. V, Linares-Palomino, R., Simon, M. F., & Prado, D. E. (2011). Forgotten forests - issues and prospects in biome mapping using Seasonally Dry Tropical Forests as a case study. *BMC Ecology*, *11*(November). https://doi.org/10.1186/1472-6785-11-27

Scholz, F. G., Bucci, S. J., Goldstein, G., Meinzer, F. C., Franco, A. C., & Miralles-Wilhelm, F. (2007). Biophysical properties and functional significance of stem water storage tissues in Neotropical savanna trees. *Plant, Cell and Environment*, *30*(2), 236–248. https://doi.org/10.1111/j.1365-3040.2006.01623.x

Scholz, F. G., Bucci, S. J., Goldstein, G., Meinzer, F. C., Franco, A. C., & Miralles-Wilhelm, F. (2008). Temporal dynamics of stem expansion and contraction in savanna trees: Withdrawal and recharge of stored water. *Tree Physiology*, *28*(3), 469–480. https://doi.org/10.1093/treephys/28.3.469

Scholz, F. G., Bucci, S. J., Goldstein, G., Meinzer, F. C., Franco, A. C., & Salazar, A. (2008). Plant- and stand-level variation in biophysical and physiological traits along tree density gradients in the Cerrado. *Brazilian Journal of Plant Physiology*, *20*(3), 217–232.

Schwinning, S., & Ehleringer, J. R. (2010). Water use trade-offs and optimal adaptations arid ecosystems. *Journal of Ecology*, *89*, 464–480.

Souza, B. C. de, Oliveira, R. S., Araujo, F. S. de, Lima, A. L. A., & Rodal, M. J. N. (2015). Divergências funcionais e estratégias de resistência à seca entre espécies decíduas e sempre verdes tropicais. *Rodriguésia*, *66*(1), 21–32.

Swenson, N. G., & Enquist, B. J. (2007). Ecological and evolutionary determinants of a key plant functional trait: Wood density and its community-wide variation across latitude and elevation. *American Journal of Botany*, *94*(3), 451–459. https://doi.org/10.3732/ajb.94.3.451

United States Department of Agriculture. (1999). Soil taxonomy: A basic system of soil classification for making and interpreting soil surveys. USDA Washington, USA.

Valdez-Hernández, M., Andrade, J. L., Jackson, P. C., & Rebolledo-Vieyra, M. (2010). Phenology of five tree species of a tropical dry forest in Yucatan, Mexico: Effects of environmental and physiological factors. *Plant and Soil*, *329*(1), 155–171. https://doi.org/10.1007/s11104-009-0142-7

Venturas, M. D., Sperry, J. S., & Hacke, U. G. (2017). Plant xylem hydraulics: What we understand, current research, and future challenges. *Journal of Integrative Plant Biology*, *59*(6), 356–389. https://doi.org/10.1111/jipb.12534

Vico, G., Dralle, D., Feng, X., Thompson, S., & Manzoni, S. (2017). How competitive is drought deciduousness in tropical forests? A combined eco-hydrological and eco-evolutionary approach. *Environmental Research Letters*, *12*(6). https://doi.org/10.1088/1748-9326/aa6f1b

Werden, L. K., Alvarado J., P., Zarges, S., Calderón M., E., Schilling, E. M., Gutiérrez L., M., & Powers, J. S. (2018). Using soil amendments and plant functional traits to select native tropical dry forest species for the restoration of degraded Vertisols. *Journal of Applied Ecology*, *55*(2), 1019–1028. https://doi.org/10.1111/1365-2664.12998

West, A. G., Patrickson, S. J., & Ehleringer, J. R. (2006). Water extraction times for plant and soil materials used in stable isotope analysis. *Rapid Communications in Mass Spectrometry*, *20*(8), 1317–1321. https://doi.org/10.1002/rcm.2456

Wilson, P. J., Thompson, K., & Hodgson, J. G. (1999). Specific leaf area and leaf dry matter content as alternative predictors of plant strategies. *New Phytologist*, *143*(1), 155–162. https://doi.org/10.1046/j.1469-8137.1999.00427.x

Worbes, M., Blanchart, S., & Fichtler, E. (2013). Relations between water balance, wood traits and phenological behavior of tree species from a tropical dry forest in Costa Rica - A multifactorial study. *Tree Physiology*, *33*(5), 527–536. https://doi.org/10.1093/treephys/tpt028

Wright, C., Kagawa-Viviani, A., Gerlein-Safdi, C., Mosquera, G. M., Poca, M., Tseng, H., & Chun, K. P. (2018). Advancing ecohydrology in the changing tropics: Perspectives from early career scientists. *Ecohydrology*, *11*(3), 1–18. https://doi.org/10.1002/eco.1918

Wright, I. J., Reich, P. B., Westoby, M., Ackerly, D. D., Baruch, Z., Bongers, F., … Villar, R. (2004). The worldwide leaf economics spectrum. *The Quarterly Review of Biology*, *428*(3), 821-. https://doi.org/10.1007/sll466-009-0028-z

Zanne, A. E., Westoby, M., Falster, D. S., Ackerly, D. D., Loarie, S. R., Arnold, S. E. J. J., & Coomes, D. A. (2010). Angiosperm wood structure: Global patterns in vessel anatomy and their relation to wood density and potential conductivity. *American Journal of Botany*, *97*(2), 207–215. https://doi.org/10.3732/ajb.0900178

IV STEM WATER STORAGE CAPACITY AND SAP FLUX PATTERNS FOR TWO SPECIES OF CONTRASTING WOOD DENSITIES

Introduction

Stem water storage is important for understanding tree water relations. This stored water determines phenology and degree of desiccation (Borchert 2004; Borchert and Pockman 1996; Bucci et al. 2004; Lima et al. 2012; Nilsen et al. 1990), contributes to daily (Carrasco et al. 2015; Mathney et al. 2015; Scholz et al. 2007; Scholz et al. 2008a; Scholz et al. 2008b; Yu et al. 2019) and seasonal water demands (Chapotin et al. 2006a), and thus is relevant to whole-tree water use (Christoffersen et al. 2016; Huang et al. 2017). Stem water storage may have a particularly strong role in seasonally dry tropical forests (SDTF), where severe water stress occurs four to seven months of the year (Bullock et al. 1995; Dirzo et al. 2011; Janzen, 1988). While all trees to some extent store water in their roots, trunks, and leaves, a sizeable volume of stored stem water is a potentially critical reservoir during the prolonged periods of droughts experienced in SDTF.

Sarcocauls are unique tree forms prevalent in SDTF. They are characterized by large, often swollen, fleshy trunks, translucent exfoliating bark with photosynthetic cells, and non-succulent, drought-deciduous leaves (Avila-Lovera and Ezcurra 2016). Stem water storage capacity in these is high because they have low wood density and large amounts of undifferentiated parenchyma. Moreover, photosynthetic bark allows for re-fixation and recycling of respiratory CO2 so that carbohydrates supplies can be maintained during leafless months (Avila-Lovera et al. 2017; Holbrook 1995). To avoid water loss, leaf fall often occurs early in the dry season (Chapotin et al. 2006c; Sande et al. 2016;).

On the other hand, non-succulent, high wood density trees also occur in SDTF. These trees often dominate community composition during early successional stages (Poorter et al. 2019) and are generally associated with drought-tolerance strategies (Mendez-Alonzo et al. 2013). Generally, high wood density is associated with higher cavitation and embolism thresholds, greater tolerance of more negative leaf water potentials, and tardy deciduousness compared to low wood density trees (Bucci et al. 2004; Esquivel-Muelber et al. 2017; Lima et al. 2012; Markesteijn et al. 2011; Mendez-Alonzo et al. 2012; Preston et al. 2006; Jacobsen et al. 2005; Valdez-Hernández et al. 2010; Worbes et al. 2013). Trees with dense wood often have smaller trunk diameters, i.e. smaller active sapwood area, and slower growth, and greater water use efficiency compared to trees with low wood density (Esquivel-Muelber et al. 2017; Kunstler et al. 2016; Poorter et al. 2008; Reich 2014; Worbes et al. 2013; Zanne et al. 2010). Higher wood density also translates to a lower capacity for stem water storage (Borchert 2004; Lima et al. 2012).

Trees with higher wood density generally have low water transport efficiency and narrow conducting area (Hacke et al. 2001). Although, to conduct a unit volume of water through smaller vessel diameters of high wood density trees would require a faster sap flux density. In low wood density sarcocauls, sap flux must be slow enough to allow reserves to build up but not so easily utilized that reserves are depleted prior to the onset of severe water stress. Thus, it is apparently paradoxical that sarcocauls, which would have greater hydraulic conductivity may also be conducting water at a slower rate compared to high wood density trees. Sap flux density as a function of wood density varies and the direction of this relationship seems to reflect trade-offs between efficiency and safety (Bucci et al. 2004) and biophysical constraints (Gao et al. 2015).

Since SDTF have long periods of drought and since tree exhibit a wide range of wood densities, these trees must also be utilizing water at very different rates in order to deal with water stress. Specifically, we ask 1) How does sap flux differ between a species that has a large stem water storage capacity vs. one that has a small stem water storage capacity? 2) What is the role of stem water storage in buffering tree sap flux response to VPD and in tree sensitivity to available soil water? 3) Does the sensitivity of sap flux to VPD change in wet vs. dry conditions. By comparing sap flux density between two species of contrasting wood density, we expect to better understand which species is more tolerant of water stress and less sensitive to drought conditions vs. which species is more aggress in its water use but less resistant to drought conditions. This insight is important to understanding how SDTF might adapt to climate change scenarios which predict increased drought and changes in rainfall regime. Additionally, a more detailed understanding of plant water fluxes is vital to quantifying components the hydrologic cycle in seasonal systems, and hence better management of ecosystems for water-providing services.

Methods

Study site

This study was conducted within a relatively old (50+years) Caatinga forest stand located near the municipality of Serra Talhada, PE, on the Fazenda de Buenos Aires (07°56'50 "S and 38°23'29" W, 450m elevation; Figure IV-1). The Caatinga is a seasonally dry tropical forest and shrubland biome in northeast Brazil. The forest is drought-deciduous, and the climate is tropical hot and dry (BShw Koppen classification BShw) with a strong precipitation seasonality (D'Odorico and Bhattachan 2012). Mean annual precipitation is 733 mm and potential evapotranspiration is about 2,000 mm / year. The rainy season

typically occurs from December to May (Figure IV-2), and accounts for 75% of annual rainfall; although, interannual trends are erratic and unpredictable. Average monthly air temperatures range from 21 to 26 °C, with maximum temperatures of 31 °C and minimum temperatures of 17 °C (Griessen 2006; New LocClim 1.10). The predominant soils in the study site are Entisol Orthent and Aridsol Argid (USDA 1999).

Species selection and phenology

Two species were selected based on their wood density: the sarcocaul (low wood density) species, *Commiphora leptophloeos* (Mart.) Gillett; and the high wood density species *Cenostigma pyramidale* (Tul.) E. Gagnon & G. P. Lewis (botanical synonymy *Caesalpinia (Poincianella) pyramidalis* Tul; Maia 2012; Gasson et al. 2009), (Table IV-1; Figure IV-3). *C. leptophloeos* is native and can be found in other SDTFs. *C. pyramidalis* is endemic to the Caatinga (Maia 2012). Based on field observations and core sampling, the depth to sapwood depth for both species was shallow, but the total sapwood area for *C. pyramidale* is likely much smaller than that of *C. leptophloeos*. Five individuals per species were selected with a small area (~30 m x 30 m) of the forest stand.

Because there is strong relationship between wood density and phenology for Caatinga, trees, and because water use is linked to phenological activity, monthly ocular estimations of the percent of the canopy with buds, leaf flush, leaf fall, flowers and fruits from December 21, 2018 to July 26, 2019. Ocular estimations were made on a semi-quantitative scale of 0 to 4, where 0 = 0 or no visible leaves, 1 = 1–25%, 2 = 26–50%, 3 = 51–75% and 4 = 76–100% of the canopy were in any phenophase, according to the method proposed by Fournier (1974) and as described in Morellato et al. (2010). This estimate is

then converted to the percent of the phenophase intensity of each individual and then summarized by species using the following equation:

$$\%\ FI = [\sum_{i=1}^{n} x_i/(n * 4)]*100 \qquad \text{Equation IV-1}$$

Where % FI is the Intensity of the Fournier Index, n is the number of individuals sampled (in this case 5) and x_i is the value according to estimation scale for individual *i*.

Sap flux probe construction and data pre-processing

To measure sap flux density, thermal dissipation sensors were constructed following Granier (1985). Each sensor consisted of two probes: a heater probe and a reference probe constructed from stainless steel with a type-T thermocouple (copper-constantan). The probes were 10 mm long (half the size of Granier's original design), with the thermocouples located at 5 mm. The heater probe, additionally, is wrapped with constantan wire and inserted into an aluminum sleeve to ensure that heat is evenly distributed. The probes are inserted into the tree trunk, 10 cm apart, with the heater probe above the reference probe. The probes are then routed through a voltage regulator and data logger (1000X Campbell Scientific, Inc., Logan, UT).

Raw voltage was converted to temperature differentials, dT, based on metal properties of the thermocouple wires. Then, the timeseries was filtered for noise using a maximal overlap discrete wavelet transform (MODWT) and partial summation of the decomposition components. By summing only select low-pass octave bands, we removed the high frequency noise associate with sensor data. This filtering methods ensures that we can quickly and objectively remove high frequency noise, without having to make subjective and tedious manual cleans. We visually examined all partial summations to make sure that only high frequency noise was removed. The MODWT methods were

implemented using the R package wmtsa (Percival and Walden 2000; https://CRAN.R-project.org/package=wmtsa). Then dT is convert to sap flux density, Js, via the equation:

$$Js = \alpha K^{\beta} \quad \text{Equation IV-2}$$

Where, α and β are Granier's original constants and K is a unitless flow index calculated as:

$$K = (dT_{max} - dT) - 1. \quad \text{Equation IV-3}$$

Where dT_{max} is the maximum temperature differential at which zero-flow conditions are assumed.

We processed dT data using the Baseliner software (Oishi et al. 2008). Baseliner is an open-source software for processing data from Granier-style TD sensors using a combination of automated steps, visualization, and manual editing. Through Baseliner, zero-flow reference value or baselines are defined as 1) nighttime hours, 2) relatively stable dT, and 3) when VPD values approaching zero. It is important to note that the original Granier design can underestimate flows by more than 25% (Flo et al. 2019) and up to 60% in other cases (Pasqualotto et al. 2019; Steppe et al. 2010). This underestimation is due to several factors including ambient thermal gradients, steep radial gradients across active sapwood and even across the sensor length, sensors partially placed in non-conducting sapwood, inability to identify baselines, bidirectional flows, wounding artifacts, and general noise in the signal due to low flows, improper heat regulation, and signal transmission (Moore et al., in review). To reduce ambient thermal gradients, we use reflective foil insulation to protect TD sensors. To avoid placing sensors in non-conducting sapwood, we shortened the original Granier probe length to 2 cm for all sensors. This was especially important for *C. pyramidale*, which has a shallow depth to the active sapwood.

To account for shifting baselines present in our dataset, we manually selected dTmax values within a seven- to ten-day window. These manually selected dTmax values occurred at nighttime hours and for relatively stable dT but at which VPD did not necessarily approach zero. While this approach removed the effect of shifting baselines, it does not account for sap flux underestimation when night-time VPD is high and nighttime transpiration likely. Some studies considered that nighttime sap flux in the sarcocaul is mainly a reflection of seasonal stem water replenishment (Chapotin et al. 2006a), which could be confirmed with night-time measurements of stomatal conductance for example. Lastly, network wires routed from sensor to data logger were buried to reduce transmission noise and destruction from cattle and wildlife.

Despite these efforts, noise is still present in the data and if large enough, can preclude our ability to capture species-level differences. Hence, to quantify the comparability of our dataset, a power analysis for sample size determination was performed post-hoc. After discarding faulty sensors, sap flux data was reduced to a total of seven sensors for *C. leptophloeos* and a total of eight sensors for *C. pyramidale*, representing five individuals of each species. These data were used to perform the power analysis on the daily total sap flux density for a sub-sample period from February 1- May 31, 2019 (n=119). The results confirmed that we were able to capture species-level differences even with this limited number of sensors (Moore et al. in review).

Meteorological data

Concurrent meteorological data is continuously logged and monitored at this site by the ONDA CBC group (https://ondacbc.eco.br). This data and includes rainfall (mm; TE 525 WS-L, Texas Electronics, USA), vapor pressure deficit (kPa), and relative humidity (%)

and air temperature (°C) (model HMP45C, Vaisala, Campbell Scientific Inc., Logan, UT, USA). We used nearby station data to fill in any missing data, including net radiation for the entire measurement period. Station data was downloaded from the Brazilian National Institute of Meteorology (http://www.inmet.gov.br). Additionally, volumetric soil water content was also monitored for one profile approximately central to the thermal dissipation sensor network. Measurements were logged every half hour at five depths: 5 cm, 10 cm, 20 cm, 35 cm, 50 cm (5TM probes, METER Group, Inc., Pullman, WA). To calibrate soil water content, we scaled raw data based on minimum residual and maximum saturation values based on soil textural properties (see Chapter 3 of this dissertation). All data was re-sampled to an hourly frequency.

Data analysis

To quantify the role of stored stem water and the time lag between Js and VPD for wet and dry conditions, we used a hysteresis index, H_{index}, calculated using the shoelace formula (Braden 1986) and a paired t-test, as in Gimenez et al. (2019). The H_{index} measure allows us to quantitatively compare the area of the hysteresis loops between contrasting species. The H_{index} is calculated as an area of a polygon, A, in the following equation:

$$\boldsymbol{A = \frac{1}{2} + \left| \sum_{i=1}^{n} x_i y_{i+1} + x_n y_1 - \sum_{i=1}^{n} x_i y_{i+1} - x_n y_1 \right|} \qquad \text{Equation IV-4}$$

Where n is the number of sides of the polygon, and $(x_i y_i)$, i = 1, 2, …, n are the vertices of the polygon.

Results

Phenological trends

The first rains of the wet season began in early December, with two relatively large events of almost 20 mm. Although we did not take the first phenophase observation in early December, these first rains were enough to render a phenological response. By the end of December, when the first phenophase observations were made, both species were at full flush since the intensity of the Fournier Index was 100 % for both species (Figure IV-4).

From January to March, rainfall events were small and intermittent. While *C. pyramidale* maintained almost constant cover, for *C. leptophloeos,* it was greatly reduced at the end of that period. The last sizeable rain event was May 1 (15.2 mm), which marked the end of the wet season. *C. pyramidale* seemed to respond to this event as cover increases slightly, whereas cover did not change for *C. leptophloeos*.

By the end of June, cover decreased significantly for both species. Interestingly, *C. pyramidale* did not flower or fruit at any point during the measurement period. In SDTFs, it is often the elimination of water deficits which produced flowering (Borchert 1994), as has been observed for other high wood density species in the Caatinga (Lima and Rodal 2010). Other multi-year observations report that flowering does not occur every year for *C. pyramidale* (Machado et al. 1997) and can occur at the beginning of the dry season (Griz and Machado 2001). Still, we did note other *C. pyramidale* individuals flowering at the study site. Although rainfall amounts for the 2019 wet season are comparable to the average, this lack of annual flowering may be due to poor distribution of rainfall (Figure IV-3). Instead of a more gradual unimodal distribution of rainfall in the wet season, there was an early peak in December, a dry-down through February, and another peak in May.

Flowering and fruiting were observed in *C. leptophloeos* during the wet season, with substantial seed fall during the transition from wet to dry season.

Previous studies in the Caatinga conclude that for the lowest wood density species such sarcocauls, the initiation of leaf flush has a high degree of intra-specific synchrony and is significantly correlated with photoperiod. Many of these species initiate leaf budding before the start of the rainy season, which would imply utilization of stored stem water (Lima and Rodal 2010; Chapotin et al. 2006a; Borchert 1994). Additionally, we observed that *C. leptophloeos* was also early deciduous compared to *C. pyramidale.* That is, *C. leptophloeos* was ready to take advantage of the first rains, but also quickly dropped its leaves at the first signs of water stress. *C. pyramidale,* on the other hand, was more stable in is phenophase activity—this species was tardily deciduous and exhibited more gradual changes in canopy cover.

Sap flux density and abiotic variables

Net radiation was stable during the measurement (Figure IV-5). Vapor pressure deficit, VPD, is a derived variable which fluctuated based on ambient temperature and relative humidity. Generally, VPD would dip during rainy periods. Soil moisture at 10 cm was more variable than at 50 cm, as a consequence of rainfall evets. Soil moisture at 50 cm only increased after consecutively sizeable rainfall events in April, and then slowly decreased into June. Maximum Js was relatively stable for *C. pyramidale*, ranging from 22.9 to 28.6 cm/h. On the other hand, the maximum Js for *C. leptophloeos* fluctuated, ranging from 4.42 to 17.2 cm/h (Table IV-2), which was almost four times as high on some occasions.

Relationship between sap flux density and vapor pressure deficit

Sap flux density had a diurnal cycle. It increased during early morning (6AM), peaked in the early afternoon (noon to 2PM) and decreased in the evening. On average, *C. pyramidale* peaked an hour earlier than *C. leptophloeos* (Table IV-2). The Js-VPD pattern for *C. pyramidale* had a strong clockwise-hysteresis pattern that was most apparent for the month of January (Figure IV-6). The initial slope (from 6Am to noon) for Js-VPD in *C. pyramidale* didn't change across the 6 months. The hysteresis pattern in *C. pyramidale* shows that maximum Js preceded maximum VPD. This means that *C. pyramidale* exhibited some level of stomatal control to avoid losing water when the atmospheric demand is strongest. This suggest that there is insufficient water in the stem to allow for loss. For *C. leptophloeos* the Js-VPD relationship had a near linear pattern, especially from February through April, and a slight pattern of hysteresis in December. For *C. leptophloeos* on the other hand, Js was linearly related to VPD, with a steeper initial slope during April and May. This suggest that *C. leptophloeos* has a stronger response to VPD (steeper slope) late in the season but seems to be strongly buffering against VPD, particularly in February.

The H_{index} for *C. pyramidale* was largest for the month of January and smallest for the month of April. Monthly rainfall for January was low, at 61 mm, vs. 197 mm in April. The H_{index} was smallest for *C. leptophloeos* was largest in December, and smallest for March. The H_{index} between Js-VPD for *C. pyramidale* was significantly greater than the H_{index} of *C. leptophloeos* (Figure IV-7; $p<0.05$, paired Wilcoxon test), indicating that *C. pyramidale* was less sensitive to VPD and *C. leptophloeos* more closely followed VPD throughout the measurement period.

Comparison between dry and wet conditions

We selected a dry period and wet period of 4 days examine the response of Js to VPD. Although the early pulses of rain began in early December, a dry spell occurred from Dec. 24, 2018 to Jan.9, 2019. Thus, we selected Jan 1-4 to represent "dry" conditions. For wet conditions, we selected March 23-26, as a heavy rain event occurred at midnight on March 25 (56 mm). To highlight time series peaks, Js and VPD were standardized (i.e. the selected time series were divided by their standard deviation) as shown in Figure IV-8. During the dry period, scaled Js leads scaled VPD for *C. pyramidale* but largely aligns for *C. leptophloeos.* In the wet period, for the two days just before the rainfall event, scaled Js seems to mostly align with VPD regardless of species. For the two days after, the Js of *C. pyramidale* just precedes VPD while the Js of *C. leptophloeos* mostly aligns. This seems to indicate that stomatal control of *C. pyramidale* tightens during high water stress and loosens during more favorable conditions. Whereas *C. leptophloeos* continues to follow VPD regardless. Similarly, in the Js-VPD plots of the four-day dry vs. wet periods, the hysteresis pattern of *C. pyramidale* is tightly held during the dry period but oscillates and shape during the wet period. For *C. leptophloeos*, there is little to no lag in the Js-VPD relationship.

Discussion

The ability of *C. pyramidale* to maintain relatively stable Js even during dry conditions indicates that this species is more conservative in its water use. In other words, this species must rely on other water acquisition and use strategies to cope with drought. The strong hysteresis pattern exhibited by *C. pyramidale* is similar to that of other species in the humid tropics (Gimenez et al. 2019; Horna et al. 2011) and has been called a "gs effect"

(Gimenez et al. 2019). This means that Js is greater in the morning than the afternoon and suggests that the partial stomatal closure during the afternoon would allow leaf to recover to less negative water potentials. Thus, a maximum Js that precedes VPD, as in *C. pyramidale* is likely reflecting strategies to reduce water loss and avoid cavitation and embolism. The fluctuation in Js levels for *C. leptophloeos* indicate that this species is more acquisitive in its water use behavior. In other words, this species is concerned with utilizing water as it is made available, but nearly shutting down during water-stress. For this species, we did not find as strong hysteresis pattern. This indicates that *C. leptophloeos* has a lower buffer against atmospheric water demand, but mainly when conditions are favorable. Whether or not this means that *C. leptophloeos* is utilizing stored stem to meet the VPD demands remains to be tested though. Additional evidence shows that *C. leptophloeos* does not tolerate very negative water potentials (see Chapter 2 of this dissertation, range of Ψ_{MD} - Ψ_{PD} *C. leptophloeos* is [-0.6, 0.7] vs.[-11, -0.9] for *C. pyramidale*) which also points to tight control of stomata and isohydric leaf water potentials.

In our study, *C. pyramidale,* which was one-third of the diameter of *C. leptophloeos,* had twice to four times greater maximum Js. This is consistent with observations in other SDTFs (Andrade et al. 2005) but contrast with findings in the humid tropics. In the humid tropics, trees with larger diameter had greater rates of sap flux (Gimenez et al. 2019). Our findings suggest that trees with large diameter have slower rates of water use, meaning there is a greater potential for a large stem water storage capacity. This is corroborated by a labeled water isotope study conducted in a seasonally

dry forest in Ecuador (Graefe et al. 2019) where trees with a large diameter and a low wood density had the longest water residence times.

Some studies suggest that stored stem water is used to meet daily transpiration demands. This was observed for deciduous species in the Brazilian Cerrado (Scholtz et al. 2007; Scholz et al. 2008a; Scholz et al. 2008b), in the desert of inner Mongolia (Yu et al. 2019) and for *Cebia speciosa*, a stem succulent in the Brazilian Atlantic Rainforest (Carrasco et al. 2015). Still, in other regions, studies suggest that this stored stem water is utilized for pre-rain flush, as in the case of the stem succulent baobab tree (*Adansonia spp*). Despite high stem water storage capacity, the baobab tree displayed strict control of stomata as a water conservation strategy and replenish stem water storage during the rainy season when water uptake can exceed daily transpiration demands (Chapotin et al. 2006b).

In our study, fluctuations in Js levels and a Js-VPD slope that varied for *C. leptophloeos* means that this species reduces Js during dry conditions, even as VPD is high. This suggests that stored stem water is not likely utilized to meet daily transpiration needs. Indeed *C. leptophloeos* can produces flower or fruits at the end of the dry season (Machado et al. 1997; Lima et al. 2012), although we did not make phenological observations during this time.

In terms of total water loss, to upscale Js to tree transpiration, estimates of active sapwood area are needed. We observed very wet tree cores taken deep from *C. leptophloeos* during the dry season and believe that the total area of active xylem is probably much larger in the *C. leptophloeos* than *C. pyramidale*. Still, given that *C. leptophloeos* is more sensitive to VPD and rainfall (limits Js during the drier conditions), which species loses a greater volume of water lost to transpiration could be significantly

different and would depend on factors such as the total area of active xylem, seasonality of rainfall, and leaf area.

Conclusion

We have, for the first time, presented data on the sap flux dynamics for species from the Caatinga dry forest. More importantly, we have chosen these two species based on their contrasting wood densities because we wanted to investigate the role of stem water storage on determining these fluxes and sensitivities to water supply and demand. We have shown that the high wood density species, *C. pyramidale*, has a higher, more constant Js generally which generally precedes VPD, meaning it avoids the time of day when atmospheric demand is greatest. That is, the high wood density species tends to show more a conservative water use strategy. *C. leptophloeos* is a stem succulent species with a low wood density and high stem water storage. This species has a near linear response to VPD and tends to exhibit aggressive water use and acquisitions when conditions are more favorable. Our findings indicate that these two specs have very different water uses and potentially difference tolerance to water stress conditions. Future research should consider a more in-depth analysis of drought vulnerability measurements to refine and support our findings. This work support using plant functional types based on wood density and phenology to better understand water use strategies for species in seasonally dry tropical forest.

Figure IV-1. Field site and surrounding area near Serra Talhada, PE, Brazil. Field site image from author. Surrounding area image from Google (2018).

Table IV-1. Selected Caatinga tree species.

UID	Family	Scientific Name	Tree Form	Wood Density (g/cm^3)*	Wood Porosity	Average Height (m)*	Average Diameter (m)*
COLE	Burseraceae	Commiphora leptophloeos (Mart.) Gillett	Stem succulent	0.25 (0.06)	Ring-Diffuse^	5.5	0.30
CEPY	Fabaceae	Cenostigma pyramidale (Tul.) E. Gagnon & G. P. Lewis	Tree Shrub	0.64 (0.02)	Diffuse Porous+	5.8	0.12

+Gasson et al. 2009; Silva et al. 2009
^Godoy-Veiga et al. 2019

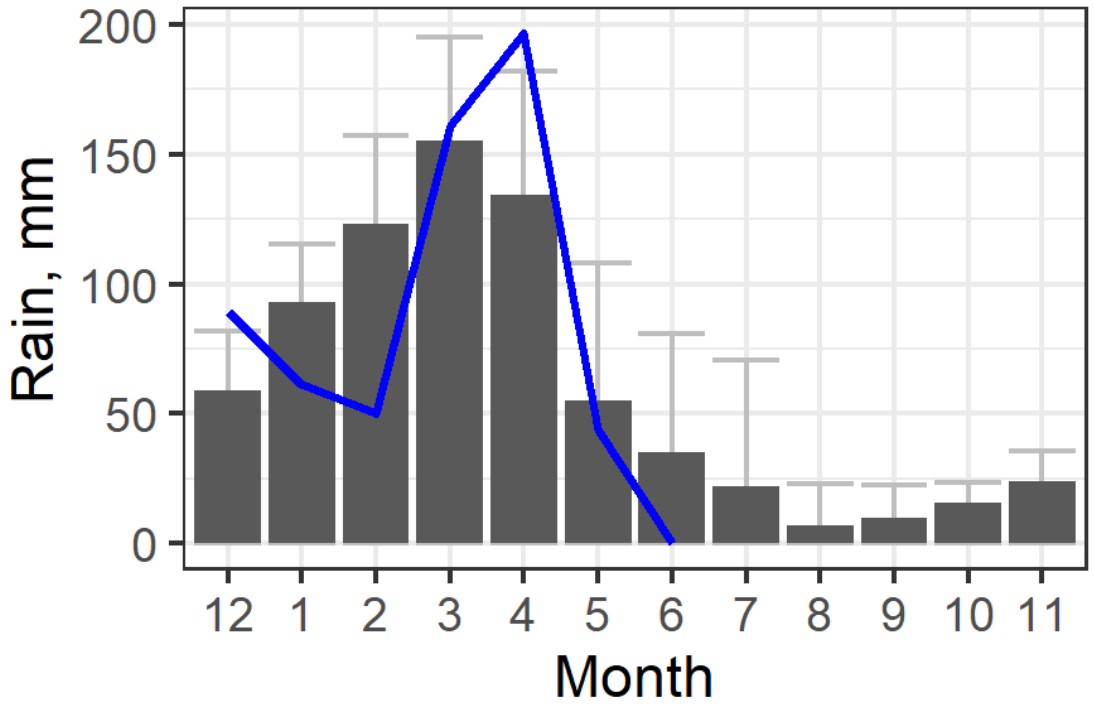

Figure IV-2. Comparison of average (bars, data from Griesser 2006, New LocClim 1.10) and observed (blue line) monthly rainfall at the study site. Error bars are the standard error of average rainfall.

a)

c)

b)

d)

Figure IV-3. The selected species, A-B) Commiphora leptophloeos (Mart.) Gillett. and C-D) Cenostigma pyramidale (Tul.) E. Gagnon & G. P. Lewis. Author's images.

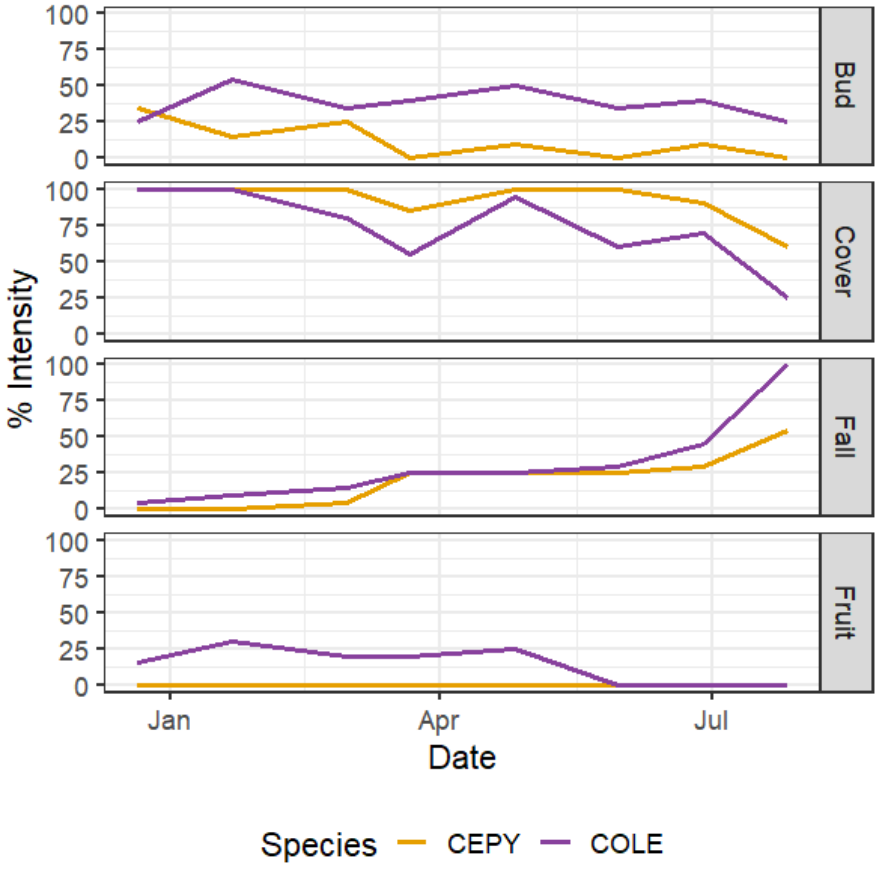

Figure IV-4. Intensity of the Fourier Index by phenological phase, bud flush or cover, leaf fall, or fruit for *C. pyramidale* (CEPY) and *C. leptophloeos* (COLE).

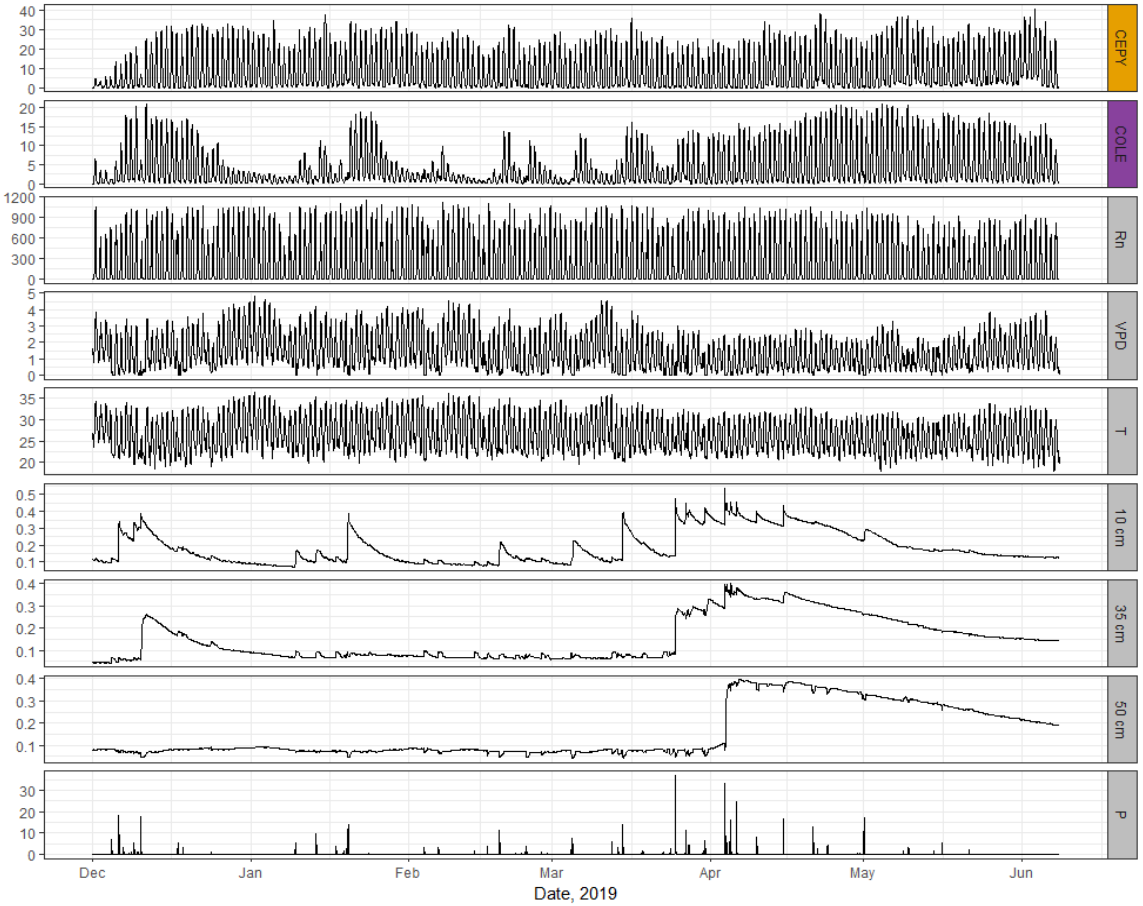

Figure IV-5. Hourly time series of sap flux density for *C. pyramidale* (a; CEPY, cm/h), sap flux density for *C. leptophloeos* (b; COLE, cm/h), net radiation (c; W/m^2), vapor pressure deficit (d; kPa), ambient air temperature (e; °C), volumetric soil water at 10cm (f; m^3/m^3), 35 cm (g; m^3/m^3) and 50cm depth (h; m^3/m^3), and rainfall (i; mm) from December 1, 2018 to June 6, 2019. Note that the y-axes vary to highlight data trends.

Table IV-2. Monthly average peak in sap flux density and corresponding total rainfall.

MONTH	*CENOSTIGMA PYRAMIDALE*		*COMMIPHORA LEPTOPHLOEOS*		VPD	MONTHLY RAINFALL
	Hour	Js, cm/h	Hour	Js, cm/h	Peak Hour	Total, mm
DEC	13:00	22.9	14:00	10.5	16:00	89
JAN	12:00	27.9	14:00	7.0	17:00	61
FEB	13:00	23.3	14:00	4.4	15:00	50
MAR	12:00	24.2	14:00	7.9	15:00	161
APR	13:00	26.5	14:00	16.0	16:00	197
MAY	13:00	28.6	14:00	17.2	15:00	44

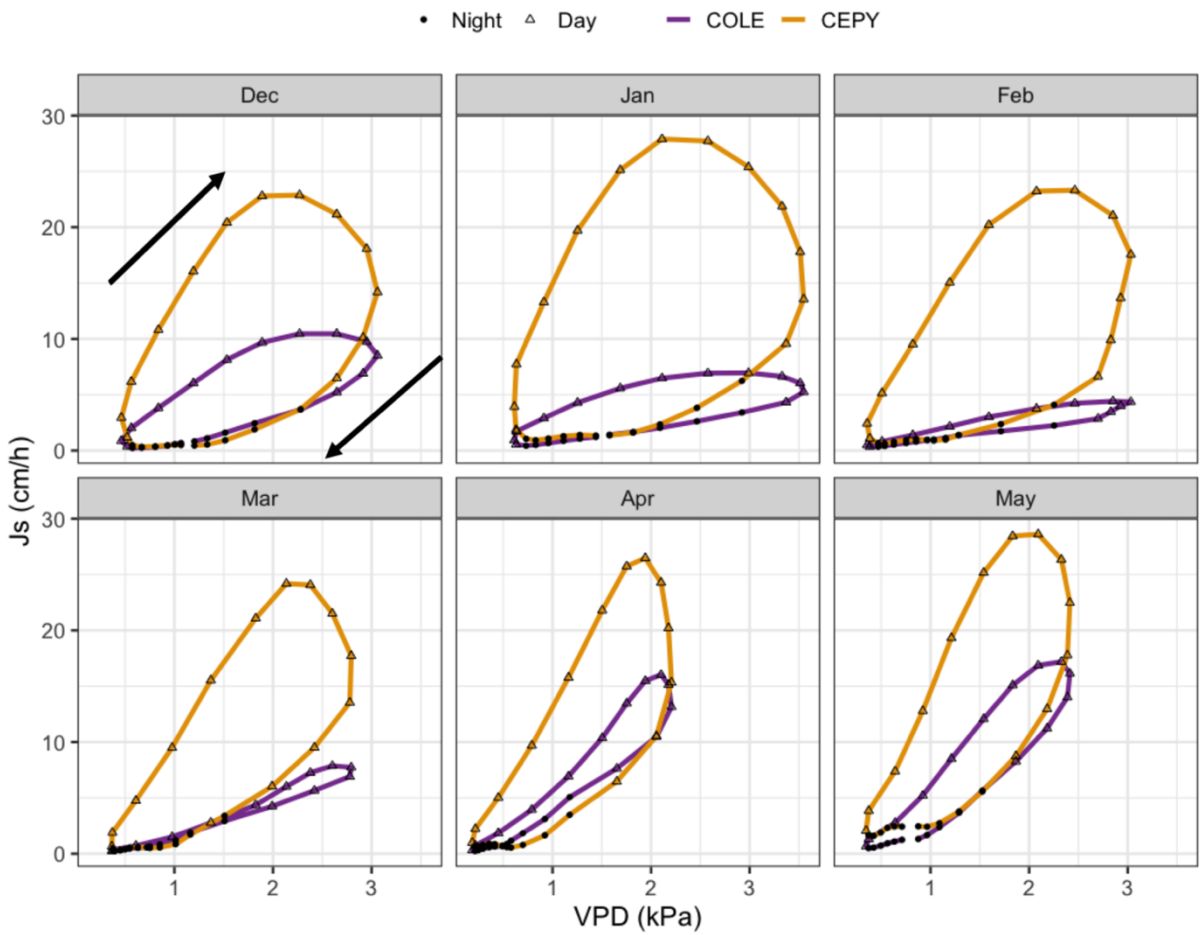

Figure IV-6. Relationship between average hourly sap flux density and vapor pressure deficit by month for *C. pyramidale* (CEPY) and *C. leptophloeos* (COLE). Filled-in points are night-time hours and empty triangles are day-time hours (6AM to 6PM). Arrows represent a clockwise direction for all months.

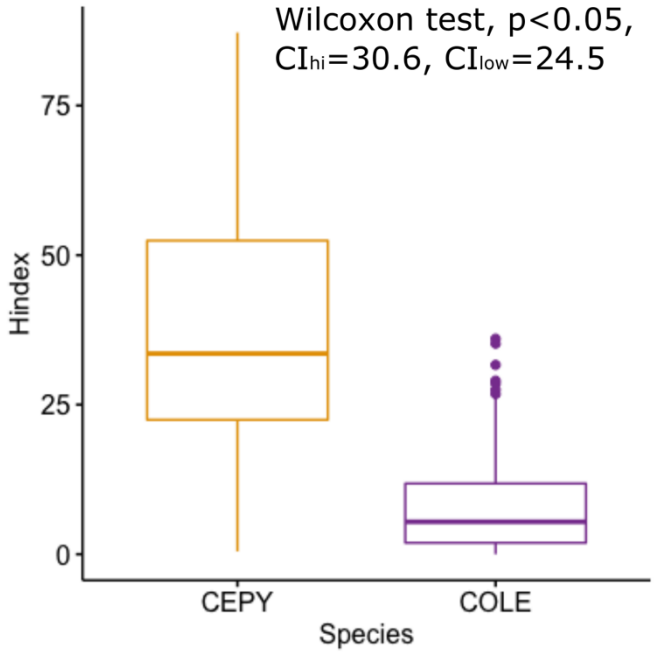

Figure IV-7. Significant difference in daily H_{index} values of *C. pyramidale* vs. *C. leptophloeo* based on two-sided paired Wilcoxon test.

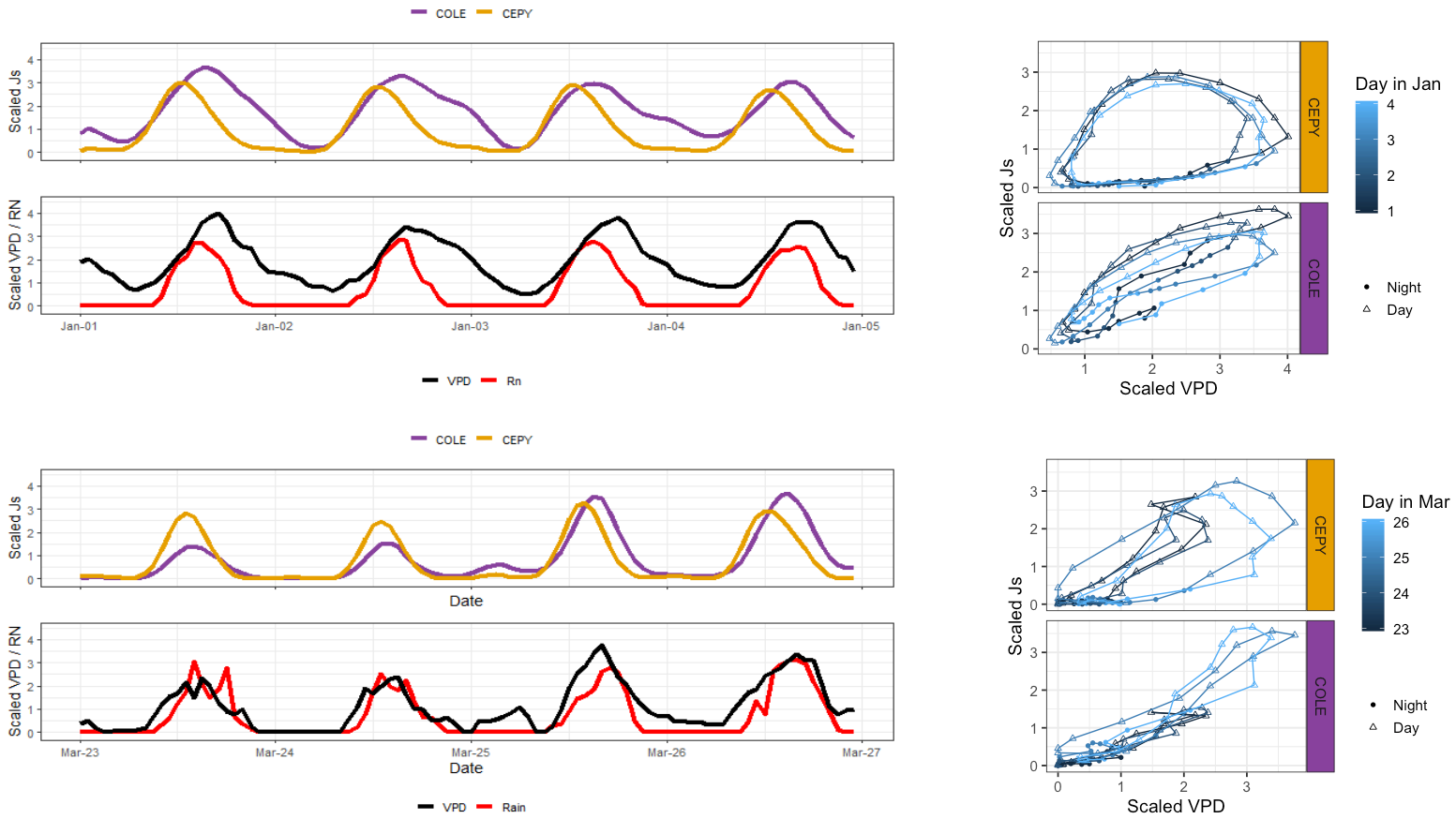

Figure IV-8. Four-day time series plots (left) and corresponding hourly Js vs VPD plots (right), scaled by standard deviation to emphasize and compare trends. Dry conditions are represented in the top plots and wet conditions are represented in the bottom plots.

References

Andrade, J. L., Meinzer, F. C., Goldstein, G., & Schnitzer, S. A. (2005). Water uptake and transport in lianas and co-occurring trees of a seasonally dry tropical forest. *Trees - Structure and Function*, *19*(3), 282–289. https://doi.org/10.1007/s00468-004-0388-x

Ávila-Lovera, E., & Ezcurra, E. (2016). Stem-succulent trees from the Old and New World tropics. In *Tropical Tree Physiology* (pp. 45–65). Springer.

Borchert, R. (1994). Soil and Stem Water Storage Determine Phenology and Distribution of Tropical Dry Forest Trees. *Ecology*, *75*(5), 1437–1449.

Borchert, R., & Pockman, W. T. (2005). Water storage capacitance and xylem tension in isolated branches of temperate and tropical trees. *Tree Physiology*, *25*(4), 457–466. https://doi.org/10.1093/treephys/25.4.457

Braden, B. (1986). The Surveyor's Area Formula. *The College Mathematics Journal*, *17*(4), 326–337. https://doi.org/10.1080/07468342.1986.11972974

Bucci, S. J., Goldstein, G., Meinzer, F. C., Scholz, F. G., Franco, A., & Bustamante, M. (2004). Functional convergence in hydraulic architecture and water relations of tropical savanna trees: From leaf to whole plant. *Tree Physiology*, *24*(8), 891–899. https://doi.org/10.1093/treephys/24.8.891

Chapotin, S. M., Razanameharizaka, J. H., & Holbrook, N. M. (2006). A biomechanical perspective on the role of large stem volume and high water content in baobab trees (Adansonia spp.; Bombacaceae). *American Journal of Botany*, *93*(9), 1251–1264. https://doi.org/10.3732/ajb.93.9.1251

Chapotin, S. M., Razanameharizaka, J. H., & Holbrook, N. M. (2006). Baobab trees (Adansonia) in Madagascar use stored water to flush new leaves but not to support stomatal opening before the rainy season. *New Phytologist*, *169*, 549–559.

Chapotin, S. M., Razanameharizaka, J. H., & Holbrook, N. M. (2006). Water relations of baobab trees (Adansonia spp. L.) during the rainy season: Does stem water buffer daily water deficits? *Plant, Cell and Environment*, *29*(6), 1021–1032. https://doi.org/10.1111/j.1365-3040.2005.01456.x

Christoffersen, B. O., Gloor, M., Fauset, S., Fyllas, N. M., Galbraith, D. R., Baker, T. R., … Binks, O. J. (2016). Linking hydraulic traits to tropical forest function in a size-structured and trait-driven model (TFS v. 1-Hydro). *Geoscientific Model Development*, *9*, 1–29.

D'Odorico, P., & Bhattachan, A. (2012). Hydrologic variability in dryland regions: Impacts on ecosystem dynamics and food security. *Philosophical Transactions of the Royal Society B: Biological Sciences*, *367*(1606), 3145–3157. https://doi.org/10.1098/rstb.2012.0016

Esquivel-Muelbert, A., Galbraith, D., Dexter, K. G., Baker, T. R., Lewis, S. L., Meir, P., … Phillips, O. L. (2017). Biogeographic distributions of neotropical trees reflect their directly measured drought tolerances. *Scientific Reports*, *7*(1), 1–11. https://doi.org/10.1038/s41598-017-08105-8

Flo, V., Martinez-Vilalta, J., Steppe, K., Schuldt, B., & Poyatos, R. (2019). A synthesis of bias and uncertainty in sap flow methods. *Agricultural and Forest Meteorology*, *271*, 362–374.

Fournier, L. A. (1974). Un método cuantitativo para la medición de características fenológicas en árboles. *Turrialba*, *25*, 54–59.

Gao, J., Zhao, P., Shen, W., Niu, J., Zhu, L., & Ni, G. (2015). Biophysical limits to responses of water flux to vapor pressure deficit in seven tree species with contrasting land use regimes. *Agricultural and Forest Meteorology*, *200*, 258–269. https://doi.org/10.1016/j.agrformet.2014.10.007

Gasson, P., Warner, K., & Lewis, G. (2009). Wood anatomy of Caesalpinia s.s., Coulteria, Erythrostemon, Guilandina, Libidibia, Mezoneuron, Poincianella, Pomaria and Tara (Leguminosae, Caesalpinioideae, Caesalpinieae). *IAWA Journal*, *30*(3), 247–276.

Gimenez, B. O., Jardine, K. J., Higuchi, N., Negrón-Juárez, R. I., Sampaio-Filho, I. de J., Cobello, L. O., … Chambers, J. Q. (2019). Species-specific shifts in diurnal sap velocity dynamics and hysteretic behavior of ecophysiological variables during the 2015–2016 el niño event in the amazon forest. *Frontiers in Plant Science*, *10*(June), 1–16. https://doi.org/10.3389/fpls.2019.00830

Godoy-Veiga, M., Slotta, F., Alecio, P. C., Ceccantini, G., Buckeridge, M. S., & Locosselli, G. M. (2019). Improved tree-ring visualization using autofluorescence. *Dendrochronologia*, *55*(January), 33–42. https://doi.org/10.1016/j.dendro.2019.03.003

Google. (2018). [Area near Serra Talhada, PE]. Retrieved July 2019, from Google Earth Pro 7.3. Maxar Technologies 2019.

Graefe, S., Fang, D., & Butz, P. (2019). Water residence times in trees of a neotropical dry forest. *Trees - Structure and Function*, *33*(4), 1225–1231. https://doi.org/10.1007/s00468-019-01849-y

Granier, A. (1985). Une nouvelle méthode pour la mesure du flux de sève brute dans le tronc des arbres. *Annals of Forest Science*, *42*(2), 193–200. Retrieved from https://doi.org/10.1051/forest:19850204

Griesser, J. (2006). New LocClim 1.10. Rome, Italy: Agrometeorology Group, FAO/SDRN.

Griz, L. M. S., & Machado, I. C. S. (2001). Fruiting phenology and seed dispersal syndromes in caatinga, a tropical dry forest in the northeast of Brazil. *Journal of Tropical Ecology*, *17*, 303–321.

Hacke, U. G., Sperry, J. S., Pockman, W. T., Davis, S. D., & McCulloh, K. A. (2001). Trends in wood density and structure are linked to prevention of xylem implosion by negative pressure. *Oecologia*, *126*(4), 457–461. https://doi.org/10.1007/s004420100628

Holbrook, N. M. (1995). Stem water storage. In B. L. Gartner (Ed.) (pp. 151–174). Academic Press.

Horna, V., Schuldt, B., Brix, S., & Leuschner, C. (2011). Environment and tree size controlling stem sap flux in a perhumid tropical forest of Central Sulawesi, Indonesia. *Annals of Forest Science*, *68*(5), 1027–1038. https://doi.org/10.1007/s13595-011-0110-2

Huang, C. W., Domec, J. C., Ward, E. J., Duman, T., Manoli, G., Parolari, A. J., & Katul, G. G. (2017). The effect of plant water storage on water fluxes within the coupled soil–plant system. *New Phytologist*, *213*(3), 1093–1106. https://doi.org/10.1111/nph.14273

Jacobsen, A. L., Ewers, F. W., Pratt, R. B., Paddock, W. A., & Davis, S. D. (2005). Do Xylem Fibers Affect Vessel Cavitation Resistance? *Plant Physiology*, *139*(1), 546–556. https://doi.org/10.1104/pp.104.058404

Kunstler, G., Falster, D., Coomes, D. A., Hui, F., Kooyman, R. M., Laughlin, D. C., … Westoby, M. (2016). Plant functional traits have globally consistent effects on competition. *Nature*, *529*(7585), 204–207. https://doi.org/10.1038/nature16476

Lima, A. L. A. de, & Rodal, M. J. N. (2010). Phenology and wood density of plants growing in the semi-arid region of northeastern Brazil. *Journal of Arid Environments*, *74*(11), 1363–1373. https://doi.org/10.1016/j.jaridenv.2010.05.009

Lima, A. L. A., Sampaio, E. V. S. B., Castro, C. C. de, Rodal, M. J. N., Antonino, A. C. D., Melo, A. L. de, … de Melo, A. L. (2012). Do the phenology and functional stem attributes of woody species allow for the identification of functional groups in the

semiarid region of Brazil? *Trees*, *26*(5), 1605–1616. https://doi.org/10.1007/s00468-012-0735-2

Machado, I. C., Marivando Barros, L., & Sampaio, E. V. de S. B. (1997). Phenology of Caatinga Species at Serra Talhada , PE , Northeastern Brazil Author. *Biotropica*, *29*(1), 57–68.

Maia, N. G. (2012). *Caatinga : árvores e arbustos e suas utilidades.* (2nd ed.). Printcolor Grafica e Editora.

Markesteijn, L., Poorter, L., Paz, H., Sack, L., & Bongers, F. (2011). Ecological differentiation in xylem cavitation resistance is associated with stem and leaf structural traits. *Plant, Cell and Environment*, *34*(1), 137–148. https://doi.org/10.1111/j.1365-3040.2010.02231.x

Matheny, A. M., Bohrer, G., Garrity, S. R., Morin, T. H., Howard, C. J., & Vogel, C. S. (2015). Observations of stem water storage in trees of opposing Hydraulic strategies. *Ecosphere*, *6*(9), 1–13. https://doi.org/10.1890/ES15-00170.1

Méndez-Alonzo, R., Paz, H., Cruz Zuluaga, R., Rosell, J. A., & Olson, M. E. (2012). Coordinated evolution of leaf and stem economics in tropical dry forest trees. *Ecology*, *93*(11), 2397–2406.

Méndez-Alonzo, R., Pineda-García, F., Paz, H., Rosell, J. A., & Olson, M. E. (2013). Leaf phenology is associated with soil water availability and xylem traits in a tropical dry forest. *Trees - Structure and Function*, *27*(3), 745–754. https://doi.org/10.1007/s00468-012-0829-x

Moore, G. W., Adkison, C., Aparecido, L. M. T., Basant, S., Cooper, C. E., Cross, A. J., … Wright, C. (in review). Heat dissipation sensors enter a new age: Navigating frontiers in transpiration and hydrologic function. *Acta Horticulture*.

Morellato, L. P. C., Camargo, M. G. G., Neves, F. F. D., Luize, B. G., Mantovani, A., & Hudson, I. L. (2010). Phenological research: Methods for environmental and climate change analysis. In *Phenological Research: Methods for Environmental and Climate Change Analysis* (pp. 99–121). https://doi.org/10.1007/978-90-481-3335-2_5

Nilsen, E. T., Sharifi, M. R., Rundel, P. W., Forseth, I. N., & Ehleringer, J. R. (1990). Water relations of stem succulent trees in north-central Baja California. *Oecologia*, *82*(3), 299–303. https://doi.org/10.1007/BF00317474

Oliva Carrasco, L., Bucci, S. J., Di Francescantonio, D., Lezcano, O. A., Campanello, P. I., Scholz, F. G., … Goldstein, G. (2015). Water storage dynamics in the main stem of subtropical tree species differing in wood density, growth rate and life history traits. *Tree Physiology*, *35*(4), 354–365. https://doi.org/10.1093/treephys/tpu087

Pasqualotto, G., Carraro, V., Menardi, R., & Anfodillo, T. (2019). Calibration of Granier-Type (TDP) Sap Flow Probes by a High Precision Electronic Potometer. *Sensors (Basel, Switzerland)*, *19*(10). https://doi.org/10.3390/s19102419

Percival, D. B., & Walden, A. T. (2000). *Wavelet methods for time series analysis* (Vol. 4). Cambridge university press.

Poorter, L., Rozendaal, D. M. A. A., Bongers, F., de Almeida-Cortez, J. S., Almeyda Zambrano, A. M., Álvarez, F. S., … Westoby, M. (2019). Wet and dry tropical forests show opposite successional pathways in wood density but converge over time. *Nature Ecology and Evolution*, *3*(6), 928–934. https://doi.org/10.1038/s41559-019-0882-6

Poorter, L., Wright, S. J., Paz, H., Ackerly, D. D., Condit, R., Ibarra-Manríquez, G., … Wright, I. J. (2008). Are functional traits good predictors of demographic rates? Evidence from five neotropical forests. *Ecology*, *89*(7), 1908–1920. Retrieved from http://www.ncbi.nlm.nih.gov/pubmed/18705377

Preston, K. A., Cornwell, W. K., & DeNoyer, J. L. (2006). Wood density and vessel traits as distinct correlates of ecological strategy in 51 California coast range angiosperms. *New Phytologist*, *170*(4), 807–818. https://doi.org/10.1111/j.1469-8137.2006.01712.x

Reich, P. B. (2014). The world-wide "fast-slow" plant economics spectrum: A traits manifesto. *Journal of Ecology*, *102*(2), 275–301. https://doi.org/10.1111/1365-2745.12211

Särkinen, T., Iganci, J. R. V. V, Linares-Palomino, R., Simon, M. F., & Prado, D. E. (2011). Forgotten forests - issues and prospects in biome mapping using Seasonally Dry Tropical Forests as a case study. *BMC Ecology*, *11*(November). https://doi.org/10.1186/1472-6785-11-27

Scholz, F. G., Bucci, S. J., Goldstein, G., Meinzer, F. C., Franco, A. C., & Miralles-Wilhelm, F. (2007). Biophysical properties and functional significance of stem water storage tissues in Neotropical savanna trees. *Plant, Cell and Environment*, *30*(2), 236–248. https://doi.org/10.1111/j.1365-3040.2006.01623.x

Scholz, F. G., Bucci, S. J., Goldstein, G., Meinzer, F. C., Franco, A. C., & Miralles-Wilhelm, F. (2008). Temporal dynamics of stem expansion and contraction in savanna trees: Withdrawal and recharge of stored water. *Tree Physiology*, *28*(3), 469–480. https://doi.org/10.1093/treephys/28.3.469

Scholz, F. G., Bucci, S. J., Goldstein, G., Meinzer, F. C., Franco, A. C., & Salazar, A. (2008). Plant- and stand-level variation in biophysical and physiological traits along tree density gradients in the Cerrado. *Brazilian Journal of Plant Physiology*, *20*(3), 217–232.

Silva, L. B. da, Ribeiro dos Santos, F. de A., Gasson, P., & Cutler, D. (2009). Wood anatomy and basic density of Caesalpinia pyramidalis Tul. (Fabaceae), an endemic species of Northeast Brazil. *Acta Botanica Brasilica*, *23*(2), 436–445.

Steppe, K., De Pauw, D. J. W., Doody, T. M., & Teskey, R. O. (2010). A comparison of sap flux density using thermal dissipation, heat pulse velocity and heat field deformation methods. *Agricultural and Forest Meteorology*, *150*(7–8), 1046–1056. https://doi.org/10.1016/j.agrformet.2010.04.004

United States Department of Agriculture. (1999). Soil taxonomy: A basic system of soil classification for making and interpreting soil surveys. USDA Washington, USA.

Valdez-Hernández, M., Andrade, J. L., Jackson, P. C., & Rebolledo-Vieyra, M. (2010). Phenology of five tree species of a tropical dry forest in Yucatan, Mexico: Effects of environmental and physiological factors. *Plant and Soil*, *329*(1), 155–171. https://doi.org/10.1007/s11104-009-0142-7

Worbes, M., Blanchart, S., & Fichtler, E. (2013). Relations between water balance, wood traits and phenological behavior of tree species from a tropical dry forest in Costa Rica - A multifactorial study. *Tree Physiology*, *33*(5), 527–536. https://doi.org/10.1093/treephys/tpt028

Yu, T., Feng, Q., Si, J., & Pinkard, E. A. (2019). Coordination of stomatal control and stem water storage on plant water use in desert riparian trees. *Trees - Structure and Function*, *33*(3), 787–801. https://doi.org/10.1007/s00468-019-01816-7

Zanne, A. E., Westoby, M., Falster, D. S., Ackerly, D. D., Loarie, S. R., Arnold, S. E. J. J., & Coomes, D. A. (2010). Angiosperm wood structure: Global patterns in vessel anatomy and their relation to wood density and potential conductivity. *American Journal of Botany*, *97*(2), 207–215. https://doi.org/10.3732/ajb.0900178

V SUMMARY AND CONCLUSIONS

The overall aim of this work was to better understand the ecohydrology of seasonally dry tropical forests such as the Caatinga of Northeast Brazil. This work is true to the definition of ecohydrology, which considers the dual regulation between vegetation and water fluxes. Chapter II of this study examined how vegetation cover changes temporal soil water dynamics. A major result of this study was that vegetation cover can change soil physical and hydraulic properties, thereby resulting in contrasting soil water dynamics across soil depths and timescales. A second major result was that soil water dynamics in the forested Caatinga appear to be more variable than the pasture site at short timescales, likely reflecting differences in infiltration and plant water use. A third major result was that the forested Caatinga seems to buffer soil moisture variability at the seasonal timescale. These findings are important considering the accelerated rate of deforestation that many tropical dry forests and shrublands experiences and climate change scenarios which predict more intense rains but also prolonged drought. We would be wise to promote the preservation and restoration of biomes such as the Caatinga.

Chapters III and IV of this work then focused more specifically on tree responses to water availability by distinguishing species according to plant functional types. Chapter III of this study sought to test whether plant functional types can be used to define and predict plant water use strategies in the Caatinga. The first result of this study demonstrated that pre-dawn and mid-day leaf water potential are generally consistent by plant functional type, with some exceptions. The second result of this study showed that plant water source

also tends group by plant functional type. The third result of this study did not show a clear difference in water use efficiency as a function of plant functional type.

Considering that plant functional types are defined by wood density and phenology, Chapter IV of this study the sap flux density of two tree species with contrasting wood densities. The aim was to better understand the how stem water storage capacity influences sap flux patterns. This study found a strong hysteresis pattern between sap flux density and vapor pressure deficit in the high wood density species, but a nearly linear trend in the low wood density species. This difference points to different plant water use strategies between the two species and also indicates that the low wood density species is more sensitive to water demand compared to the high wood density species.

Taken together, this work elucidates upon the ecohydrology of the Caatinga. This work shows that the Caatinga seasonally dry tropical forest is a resilient biome with highly specialized and unique tree species. It is my hope that this work will lead to more research in the Caatinga, so that we can continue to better understand, appreciate, and restore this fascinating system.